POLYTECHNIQUE MONTRÉAL
affiliée à l'Université de Montréal

Demand response for smart homes

MICHAEL DAVID DE SOUZA DUTRA
Département de mathématiques et de génie industriel

Thèse présentée en vue de l'obtention du diplôme de *Philosophiæ Doctor*
Mathématiques de l'ingénieur

AVRIL 2019

POLYTECHNIQUE MONTRÉAL
affiliée à l'Université de Montréal

Cette thèse intitulée:

Demand response for smart homes

présentée par: **Michael David DE SOUZA DUTRA**
en vue de l'obtention du diplôme de Philosophiæ Doctor
a été dûment acceptée par le jury d'examen constitué de:

M. **Charles AUDET**, Ph. D., président
M. **Miguel F. ANJOS**, Ph. D., membre et directeur de recherche
M. **Sébastien LE DIGABEL**, Ph. D., membre et codirecteur de recherche
Mme **Hanane DAGDOUGUI**, Ph. D., membre
M. **Steven WONG**, Ph. D., membre externe

DEDICATION

To my family: Wilma, Miguel, Stephanie, Alan, Erick, Fátima, Geraldo, Lucas and Matheus, to my friends...

ACKNOWLEDGEMENTS

The completion of the work leading up to this project was only possible thanks to the collaboration of a group of people, to whom I address my thanks.

My first words are to my supervisors Mr. Miguel F. Anjos and Mr. Sébastien Le Digabel for the trust placed in me, which gave me the opportunity to participate in this project and to integrate their teams. I'd like to express my gratitude for their great comments, guidance and support.

Thanks also to the members of the Department of Mathématiques appliqueés at Polytechnique Montreal and to the members of GERAD for lessons and support.

I deeply thank the members of the Engineering Department of Production at the Federal University of Minas Gerais, in special Carlos Roberto Venâncio de Carvalho, Gilberto de Miranda Junior, Martín Gómez Ravetti, Maurício Cardoso de Souza and Ricardo Saraiva de Camargo, and also Mr. Philippe Mahey, Christophe Duhamel, Bruno Bachelet and all ISIMA for the hospitality and dedication to the Brafitec 2012-2014 program. Without them, I will not have the basis to start this project.

I did like to thank Ricardo Saraiva de Camargo and Natalia Alguacil Conde by the emails, support and lessons whose knowledge has been used in this thesis.

I would especially like to thank my family. My parents, Wilma and Miguel, merit special thanks for their continued encouragement and support. My wife, Stephanie has been extremely supportive of me throughout this process and has made countless sacrifices to help me get to this point. Without them, I doubt that I would be in this place today.

RÉSUMÉ

Problèmes dans l'opération de la transmission d'électricité, surcharge, émission de carbone sont, entre autres, les préoccupations des gestionnaires de réseaux électriques partout dans le monde. Dans ce contexte, face au besoin de réduire les coûts d'exploitation ainsi que le besoin d'adaptation aux différentes exigences de qualité, de sécurité, de flexibilité et de durabilité, les réseaux intelligents sont considérés comme une révolution technologique dans le secteur de l'énergie électrique. Cette transformation sera nécessaire pour atteindre les objectifs environnementaux, intégrer la participation de la demande, appuyer l'adoption de véhicules électriques et hybrides ainsi que la production distribuée à basse tension.

Chaque partie prenante dans le processus de gestion de l'énergie peut avoir des avantages avec le réseau intelligent, ce qui justifie son importance dans l'actualité. Dans ce travail, on se concentre plutôt sur l'utilisateur final. En plus de l'utilisateur final, nous utilisons également l'agrégateur, qui est une entité qui agrège un ensemble d'utilisateurs de sorte que l'union de leurs participations individuelles devienne plus représentative pour les décisions relatives au système d'énergie. La fonction de l'agrégateur est d'établir un engagement d'intérêts entre les utilisateurs finaux et l'entreprise de génération afin de satisfaire les deux parties.

L'une des contributions principales de cette thèse est la mise au point d'une méthode qui donne à un agrégateur la possibilité de coordonner la consommation d'un ensemble d'utilisateurs, en maintenant le niveau de confort souhaité pour chacun d'entre eux et en les encourageant via des incitations monétaires à changer ses consommations, de sorte que la charge globale ait le coût minimal pour le producteur.

Dans la première contribution (chapitre 4), ce travail se concentre sur le développement d'un modèle mathématique représentatif pour la planification des équipements d'un utilisateur. Le modèle intègre des modèles détaillés et fiables pour des équipements spécifiques tout en conservant une complexité telle que les solveurs commerciaux puissent résoudre le problème en quelques secondes. Notre modèle peut donner des résultats qui, comparés aux modèles les plus proches de la littérature, permettent des économies de coûts allant de 8% à 389% sur un horizon de 24 heures.

Dans la deuxième contribution (chapitre 5), l'accent a été mis sur la création d'un cadre algorithimique destiné à aider un utilisateur final particulier dans son processus de décision lié à la récupération d'investissement sur l'acquisition d'appareils ou d'équipements (composants) intelligents. Pour un utilisateur spécifique, le cadre analyse différentes combinaisons de composants intelligents afin de déterminer lequel est le plus rentable et à quel moment il convient

de l'installer. Ce cadre peut être utilisé pour encourager un utilisateur à adopter un concept de maison intelligente réduisant les risques liés à son investissement.

La troisième contribution(chapitre 6) regroupe plusieurs maisons intelligentes. Un cadre algorithimique basé sur les programmes de réponse à la demande est proposé. Il utilise les résultats des deux contributions précédentes pour représenter plusieurs utilisateurs, et son objectif est de maximiser le bien-être social, en tenant compte de la réduction des coûts pour un producteur donné ainsi que de la satisfaction de chaque consommateur. Les résultats montrent que, du point de vue du producteur, la courbe de charge globale est aplatie sans que cela ait un impact négatif sur le confort des utilisateurs ou sur leurs coûts.

Enfin, les expériences rapportées dans chaque contribution valident théoriquement l'efficacité des approches proposées.

ABSTRACT

Transmission operation issues, overload, carbon emissions are, among others, the concerns of power system operators worldwide. In this context, faced with the need to reduce operating costs and the need to adapt to the different requirements of quality, security, flexibility and sustainability, smart grids are seen as a technological revolution in the field of power system. This transformation will be necessary to achieve environmental objectives, support the adoption of electric and hybrid vehicles, improve distributed low-voltage generation and integrate demand participation.

Each stakeholder in the energy management process can have advantages with the smart grid, which justifies its current importance. The focus of this thesis is rather on the end user. In addition to the end-user, this work also uses the aggregator that is an entity that aggregates a set of users such that the union of the individual participation of each user becomes more representative for power system decisions. The function of the aggregator is to establish an engagement of interests between the end users and the generator company in order to satisfy both parties.

One of the main contributions of this thesis is the development of a method that gives an aggregator the possibility to coordinate the consumption of a set of users, keeping the desired comfort level for each of them and encouraging them via monetary incentives to change their consumption such that their aggregated load has the minimal cost for the generator company.

In the first contribution (Chapter 4), this work focuses on developing a representative mathematical model for user appliances scheduling. The model integrates detailed and reliable models for specific appliances while keeping a complexity such that commercial solvers are able to solve the problem in seconds. Our model can give results that, compared to the closest models in the literature, provide a cost savings in the range of 8% and 389% over a scheduling horizon of 24 hours.

In the second contribution (Chapter 5), the focus was given in making a framework to help a specific end-user in their decision process related to the payback for an acquisition of smart appliances or equipment (components). For a specific user, the framework analyses various combinations of smart components to discover which one is the most profitable and when it should be installed. This framework can be used to encourage users towards a smart home concept decreasing the risks about their investment.

The third contribution (Chapter 6) aggregates several smart homes. A framework based on

demand response programs is proposed. It uses outputs from the two previous contributions to represent multiple users, and its goal is to maximize the social welfare, considering the reduction of costs for a given generator company as well the satisfaction of every user. Results show that, from the generator company perspective, the aggregate load consumption is flattened without impacting negatively the users' comfort or their costs.

Finally, the experiments reported in each contribution validate, in theory, the efficiency of the proposed approaches.

TABLE OF CONTENTS

LIST OF TABLES

LIST OF FIGURES

LIST OF SYMBOLS AND ACRONYMS

APF	Approximate Pareto Front
BH	Belo Horizonte
CA	Centralized formulation
C&CG	Column-and-Constraint Generation
CHP	Combined Heating Power
CL	Curtailable Load
CPI	Consumer Price Index
DH	Decentralized Heuristic
DLC	Direct Load Control
DR	Demand Response
ESS	Energy Storage System
EV	Electric Vehicles
FIT	Feed-in Tariffs
GENCO	Generator Company
GHG	Greenhouse Gas
HEMS	Home Energy Management System
HVAC	Heating, Ventilation, and Air Conditioning
IBR	Inclining Block Rates
ICE	Internal Combustion Engine
IR	Investment Return
IRR	Internal Rate of Return
KKT	Karush-Kunh-Tucker
LB	Lower Bound
MILP	Mixed-Integer Linear Program
MIP	Mixed Integer Programming
MOO	Multi-objective Optimization
MPC	Model Predictive Control
NPV	Net Present Value
PAR	Peak to Average Ratio
PV	Photovoltaic Panels
PVT	Photovoltaic and Thermal Panels
RTP	Real-Time Pricing
SC	Solar Collector

SHC	Smart Home Component
SOC	State of Charge
SWMP	Social Welfare Maximization Problem
TOU	Time of Use
TUS	Time-Use Survey
TW	Time Window
UB	Upper Bound
WH	Water Heater
WS	Waste the Surplus
WT	Wind Turbine

CHAPTER 1 INTRODUCTION

1.1 Context: Smart grids and smart homes

Electricity is a fundamental product in our society. Political and social factors are affected by this topic at the global level. Population growth, energy dependence, greenhouse gas emissions and environmental issues are well under consideration when discussing power generation.

Today, there exist several types of non-renewable energy sources. A trend towards a more environmental approach is to, progressively, replace these sources with renewable production sources such as photovoltaic panels. To encourage behavioral changes, several countries offer the opportunity for customers to generate their own electricity and sell their surplus such as Germany, United Kingdom, United States and Canada. This implies a challenge for the network administrator that have control over the amount of electricity being transported from and for each customer. Therefore, the current power grid system will progressively become a "smart grid".

The European Technology Platform Smart Grid defined a smart grid to be "*an electricity network integrating users, consumers, and generators in order to produce and deliver economic, secure and sustainable electricity supplies*".

The literature presents many benefits [11,29,61,68,125] for smart grid. Overall, it is expected that the smart grids can facilitate the linking and operation of all generators of any size and technology [125], or more broadly, that it can monitor and manage all the components of the power supply system [72]. Each stakeholder in the energy management process can have advantages with the smart grid, which justifies its importance nowadays.

From the end-user perspective, beyond selling electricity surplus, there is a tendency for home appliances to be connected and controlled by a Home Energy Management System (HEMS), which is designed to promote comfort, convenience, security and entertainment for users. Houses with these equipment are called "smart homes". In this context, consumers can optimize their electricity usage for saving, or even profit from it. To do so, users need to know the right moment to activate their heaters, to buy electricity or to charge the batteries of their cars, or in other words, to schedule the times when these machines activate considering the comfort and the cost associated with their usage. This is not an easy task, given the amount of equipment that one can have at home. The first step to address the problem is building its representation. A second characteristic is that users are facing two conflicting

objectives: discomfort level and cost. Therefore, there is not only one optimal solution, but a Pareto front to be found with the efficient solutions.

Although smart homes seem to be the future for homes, customers are not sure about the profitability of the transition from current homes to smart ones. Thus, a question in the context is *for a specific household, when and/or what set of home appliances should be acquired so that the householder has a positive return on investment?* An answer to that question can encourage the aforementioned transition.

In order to make the smart home transition profitable, each customer is supposed to use its own HEMS to maximize its comfort level or/and minimizes its cost. If the same tariffs are used for every user, they will try to consume more electricity in cheaper periods rather than expensive ones. With the increase in the number of smart homes, a new problem for the generator company (GENCO) appears: a high-peak load consumption in cheaper periods. Hence, the coordination of the users' consumption can attenuate this problem. One coordination approach is Demand Response (DR) programs, which expects that customers change their electricity consumption in response to incentive: payments or different tariffs.

Comparing with industries, individual residences have little contribution to the DR strategies output due to the scale of consumption. Aggregators, entities that aggregates the consumption of many users, are used to compromise interests of a group of users and a GENCO, which are keeping comfort level and minimizing electricity bills for users, and minimizing costs for the GENCO.

1.2 Objectives

From a consumer's point of view, a first problem can be the lack of personalized information about the profitability of acquiring new technologies to transform its home in a smart one.

A second problem is the management of energy. Assuming there are available resources for generating energy and also smart appliances, a question arises is how to plan the use of these components while maintaining comfort and reducing the consumption cost. Beyond the plan, it is desired that customers to have a range of solutions so that they can choose a solution that provides a satisfactory compromise between comfort and cost.

Another important problem is the effect of individualized customer optimization on the network. By having a known price mechanism, there may be a period of the day in which the price is the cheapest. This pricing policy can provoke a scenario in which several customers prefer to focus their consumption in this cheapest period. However, there will be a high-peak demand in this period, which is a problem for the network manager. If there is an increase

in prices in these periods, this does not prevent a shift in consumption towards the new cheapest period. So, a solution that is holistic for a set of clients under the administration of an aggregator is desirable.

Considering these problems, the general objective of this thesis is to provide a method to maximize the social welfare considering users and an aggregator. This general objective is divided into three specific objectives which correspond to three contributions of this research:

- Construct a planning tool to represent and to schedule the consumption of a given user.
- Build a tool to answer the following question: for a specific household, when and/or what set of home appliances should be acquired such that the householder has a positive return on investment?
- Construct a method to coordinate a set of users in such way the users minimizes its cots while keeping the desired comfort level, and the GENCO minimizes its costs by flattening the aggregated load profile of users.

This thesis proposes a bottom-up approach. The first two objectives treat the user individually while the last objective considers multiple users interacting with each other via an aggregator to improve the grid performance.

1.3 Thesis organization

The organization of this thesis is as follows. Chapter 2 presents definitions, the most relevant literature and the scope of this research. Chapter 4 proposes a representative optimization model for scheduling electricity consumption in an individual smart home. The complexity of the model is low enough to be solved in reasonable time by commercial solvers. In Chapter 5 a framework is proposed to guide the transition from current houses to smart homes considering customized electricity usage. The framework is based on the results of Chapter 4 and gives a payback analysis of each possible acquisition combination of smart appliances or equipment for a specific user. In Chapter 6, a framework is proposed that makes a trade-off based on interests of two sides: generator companies and end-users. This framework minimizes costs for both sides, by shaving aggregated peak loads and keeping desired comfort level for users. Concluding remarks are provided in Chapter 8.

CHAPTER 2 LITERATURE REVIEW

This chapter presents an overview of the most relevant literature. Firstly, works related to the payback and return on investment are presented. Then, works that directly contribute to the consumption optimization on smart homes are reviewed.

2.1 Payback and return on investment

Many studies have investigated the payback and/or the return on investment of some combination of appliances/equipment. Some studies focused in a specific component. For example, in [6], they considered energy storage technologies; in [7, 129], energy storage batteries and photovoltaic panels (PV); in [16,19,20,177], micro Combined Heating Power (CHP) systems; in [40, 122] μ-CHP systems and thermal storage; in [57], Wind Turbine (WT) and batteries; in [37,148], PV; in [1], combinations of PV, WT and batteries systems; in [94], Solar Collector (SC) systems.

Few studies consider a set of components focusing in selecting the best promising combination of appliances. Example of studies in this category are: a) [202], which considers PVs, SC, hybrid of PV and thermal panels, heat pumps, phase changing materials, and μ-CHP systems for house design; b) [203] that finds for a given building the best economical combination and optimal capacities of batteries, water tanks and ice/heat storage units under time of use electricity prices considering also PV, SC, Water Heater (WH), CHP, HVAC; and c) [192] that proposes an economic analysis of a community energy storage considering individual householder batteries and smart appliances.

The main difference between this work and the aforementioned ones is that this thesis proposes a framework that can be used for any householder to analyze economically every combination of smart appliances/equipment acquisition in the context of a transition towards smart homes. More details are given in Chapter 5.

2.2 Optimization on smart homes

2.2.1 Single user

According to [110, 163], existing models for the scheduling of appliances often do not account for the accuracy of operational and energy-consumption characteristics of each device. From now on, let consider the expression “less accurate model” as simplified model.

An example of a simplified model is used in [128]. Considering the set of devices A, each device $a \in A$ has a time window $[\alpha_a, \beta_a]$ defined by the user in which the appliance must be operated. The horizon plan is H discretized in time periods $h \in H$. Let define γ_a^{min} and γ_a^{max} as bounds for the consumption of appliance $a \in A$, E_a as the amount of electricity needed by appliance $a \in A$, E^{max} as the grid electricity capacity and x_a^h as the only decision variable for the amount of electricity consumption for the device $a \in A$ at the period $h \in H$. According to this reference, all smart devices can be represented by Model (2.1)-(2.5).

$$\sum_{h=\alpha_a}^{\beta_a} x_a^h = E_a \quad \forall\, a \in A \tag{2.1}$$

$$\gamma_a^{min} \leq x_a^h \quad \forall\, a \in A, h \in [\alpha_a, \beta_a] \tag{2.2}$$

$$\gamma_a^{max} \geq x_a^h \quad \forall\, a \in A, h \in [\alpha_a, \beta_a] \tag{2.3}$$

$$x_a^h = 0 \quad \forall\, a \in A, h \in H \backslash [\alpha_a, \beta_a] \tag{2.4}$$

$$\sum_{a \in A} x_a^h \leq E^{max} \quad \forall\, h \in H \tag{2.5}$$

Constraints (2.1) establish that a device $a \in A$ must consume the amount E_a of electrical energy in its time window. Constraints (2.2), (2.3) and (2.4) set consumption limits by each device $a \in A$ for each period of time. Finally, Constraints (2.5) limit the total consumption of the devices per period of time with the aim of, for example, protecting circuit-breakers. Note that the model is linear.

A model is considered representative when it is more accurate from a reality perspective; able to validate more details in the reality. For instance, in order to represent a refrigerator, a transient model was developed in [24, 25] for the temperatures of refrigerated compartments that is able to predict energy consumption with a maximum deviation of $\pm 2\%$. However the model is nonlinear, discrete and nonconvex even with linear relaxation.

In the context of smart homes, agreeing with the work of [43] and [127], the authors of [69] affirms that *"Solving an optimization-based HEMS model with high levels of accuracy based on a not enough accurate model for the controllable appliances is useless."*

Representative appliance models give more accurate information and can better predict consumption, which is important for the cost evaluation in a scheduling energy model for a smart home. However, if these models are used in the context of optimization, an optimal solution cannot be found in a reasonable time from the reality perspective.

There are studies to represent a scheduling problem for smart home consumption, see for

example [164] and [22] for surveys of modeling approaches. However, beyond the representativeness of appliance models, the literature has no specific model for each device to be inserted into a scheduling model.

For instance, the authors of [163] claims that "*the optimal electricity load scheduling with considering appropriate models for operation and energy consumption characteristics of various appliances has not been well investigated yet*". Then, they classify residential appliances into five groups by giving them specific mathematical models. The work in this reference therefore makes a multiobjective formulation with the aim of maximizing the trade-off between the utility of the devices which gives a measure of comfort and the cost with the weighted sum approach. This work considers constraints of energy availability and budget. It uses as a method the generalized Benders decomposition. This decomposition is done so that each device group has a subproblem. For the analysis of the results, first, the work considered only one appliance of each group with the aim of illustrating the progress of the method. Afterwards, this work took into consideration a total of 25 appliances. Although a classification is done, models are simplified which constitute a drawback related to the representativity. Moreover, it does not consider PV.

Some studies neglected characteristics that is considered important from a DR perspective. For instance, the reference [214] makes a multiobjective formulation to optimize the cost in compromise with the issue of CO_2. The work in this reference uses the *ε-constrained* algorithm to find an approximation of the Pareto front. However, the energy that is produced by the consumer cannot be sold.

In summary, beyond the refrigerator model, representative mathematical models for appliances are available in the literature; see [97] for EV, [215] for PV, [2] for PV/EV. However, the integration of these models in a unique scheduling model to represent a smart home consumption in a DR context is a gap to be filled.

2.2.2 Multiple users

Many studies has already considered the coordination of multiple users via an aggregator. In the context of DR programs, the literature can be divided into two categories depending on the mode that the problem if formulated. In the first category, there are studies that used multiobjective methods [117, 123, 130, 152, 166, 171, 214] while in the second category studies that preferred bilevel formulations or game theory algorithms linking players via their corresponding formulation [33, 151, 165]. The work in [130] extends the model from [163] to multiple users. Thus, the representativity drawback is also extended.

The work in [123] proposes a coordinated scheduling for 2560 houses via an aggregator. For the client side, each house has 10 appliances on average, PVs and batteries. They used simplified models for each device type, following [163]. For the aggregator side, they define a quadratic cost function. The goal is to minimize the trade-off between the cost of the aggregator and customer dissatisfaction. They used a multiobjective formulation with Pareto front approach. This work uses the strategy from [169], but with Lagrangian relaxation. The difference is that the subproblems are divided by a stakeholder. Each client will have a subproblem and the aggregator another. The Lagrangian relaxation takes advantage of GAP's relaxation when adding appliances whose operation can be interrupted. However, the dual Lagrangian function is non differentiable and this leaves the convergence of the gradient method slow. So, the authors of [123] use a two-phase method, but algorithm was stooped after 60 iterations to make it practically feasible.

Focusing in a reduction of the peak-to-average load ratio, and in the maximization of each user's payoff and the retailer's profit, a scheme is proposed by [151] through a two-stage optimization problem. For the users, a scheduling linear problem is formulated with a payoff objective function. For the utility, a nonlinear problem is used. The retailer's cost is considered as a cubic function of demand. The resolution method uses heuristics to solve the utility problem. It was found that the real-time pricing scheme reduces the peak-to-average load ratio by about 20% compared to the flat rate pricing schemes.

Using heuristics over simplified models, the work in [33] proposes a distributed algorithm in which each user minimizes electricity cost, which depends on the aggregated load of other users. Each user schedules its energy consumption that will be communicated to the generator company. The utility company will then adjust the price depending on the overall system load and broadcast the price to all the users. The users will then update their energy consumption based on the new price. This mechanism is done until convergence. The goal is to reduce costs for the consumers, to increase the profit for the utility company, to decrease peak load, and load variance.

In [198], a multi-agent framework that considers an aggregator and multiple homes is proposed. Householders have an explicit optimization problem, but not the aggregator. Peak to average power ratio is reduced indirectly in the results.

The work in [206] proposes a model to minimize generator company costs, user dissatisfaction and battery cost. Similar approach of [123] is applied. In the results, they show that the users avoid the peak-demand period in order to save the cost of micro-grid. However, peak-shaving was not investigated.

A decentralized method is proposed in [119]. A Dantzig-Wolfe decomposition method is

used to minimize the peak load consumption. Many aggregators are considered with their respective user groups. Direct load control is applied, so each aggregator has a set of must-run appliances and a set of shiftable appliances under their command. The objective function is modeled as the minimal maximum peak load. Time windows are used to measure a quality of service that was penalized at the objective function. In the work [119], there is no specific models for appliances.

The work in [171] proposes a biobjective mixed integer nonlinear programming model to minimize peak load and electricity cost considering multiples homes. Appliances in [171] are represented by load profiles. Results show a reduction in peak load. However, users could not be interested in having peak load as objective function without incentives.

In [115], a game considering two generating units and five aggregators is proposed. Each aggregator has 400 houses, which are represented by simplified models. Each home considers, in the objective function, the load of all the houses connected to the same aggregator. The aggregator have an optimization problem connected to the generation utility. The solution to the aggregator problem that appears to be optimal and balanced. Each level is solved separately. The results show a perfect quasi leveling of the generation curve. According to the results, in average, customers' hourly costs have reduced.

The work in [109] proposes a bilevel problem to find day-ahead prices that induce a desired load profile for WH from a leader perspective, while minimizing user costs. Results show that there are multiple solutions for lower levels given a fixed electricity price. As optimistic bilevel approach is used, the optimization procedure chooses, among the multiple solutions, the one that is better for the upper level's objective function. However, in practice, the user could not apply that solution, which implies in a different load profile from the one desired by the upper level, which could be, according to the authors, a drawback of the bilevel optimistic approach. Then, the authors found that prices in combination with thermostat control can be used to set the time slot in which the WH will draw more energy. Changing prices for various WHs can make each of them draw more energy at different time slots, approximating the total load to a desired load profile, but the customer's comfort can be impacted.

The work in [204] considers a small number of households linked by a residential energy local network: a controller for all the houses. Mixed Integer Programming (MIP) is used to minimize total costs. Pricing is based on Inclining Block Rates (IBR) and on day-ahead Real Time Pricing (RTP). The RTP cost is represented by a quadratic function. The objective function considers also maintenance cost. Four houses are considered sharing the PV and WT. They consider deterministic and stochastic scenarios. Results show that having the freedom to schedule appliances reduces the peak load. For the deterministic case, using

Model Predictive Control (MPC) is useless. On the one hand, MPC decreases costs in the stochastic scenario.

In [106], a framework with a Stackelberg model that considers the profits' maximization for an aggregator and the minimization of cost versus comfort for users. The results show the Peak to Average Ratio (PAR) and users bill were reduced, but the computational time reported in the paper can be 10^4 seconds for a case with 500 houses.

In [114], a model to minimize costs of multiples households is proposed. It considers that prices vary with the overall load of the entire grid in real-time and that the renewable power generation is uncertain. The cost for each house is proportional to its consumption. The sum of cost of all houses is minimized. A centralized approach, which is solved by two methods: Column-and-Constraint Generation (C&CG) and for small size problems and heuristic for big size problems. They conclude that the heuristic is scalable and efficient compared to C&CG.

In [85], a distributed real-time algorithm is proposed to find the optimal energy management scheduling scheme for each user and for the utility company. The target is the maximization of the social welfare. Its novelty is the consideration of temporally coupled constraints (constraints liking time, for instance, the batteries' state of charge in time step t depends on time step $t-1$); the consideration of space coupled constraints that is related to the pricing being dependent of many users' consumption at the same time; and the consideration of batteries. A weighted sum approach is used to represent the objective function. The resolution method used is a dual decomposition via Lagrangian relaxation. However, it does not consider thermal loads as a specific model, which complicates temporally and spacial coupled constraints.

Considering multiple householders, this thesis faces the problem of coordinating multiples houses via an aggregator as the works referenced above. The novelties of the present work rests on the combination of characteristics used for users and DR options integrated in a new formulation.

CHAPTER 3 SYNTHESIS OF WORK AS A WHOLE

The synthesis of the PhD project as a whole is represented by Figure 3.1. The first step, which is linked to the first objective (Obj.1) has as input the data of appliance specification, the data for costs and the user comfort information. Using this input, a planning tool is designed to represent and to schedule the consumption of a given user. The output of this step is a solution that compromises comfort level and cost, which is taken as input for the second step. The analysis is conducted in Chapter 4.

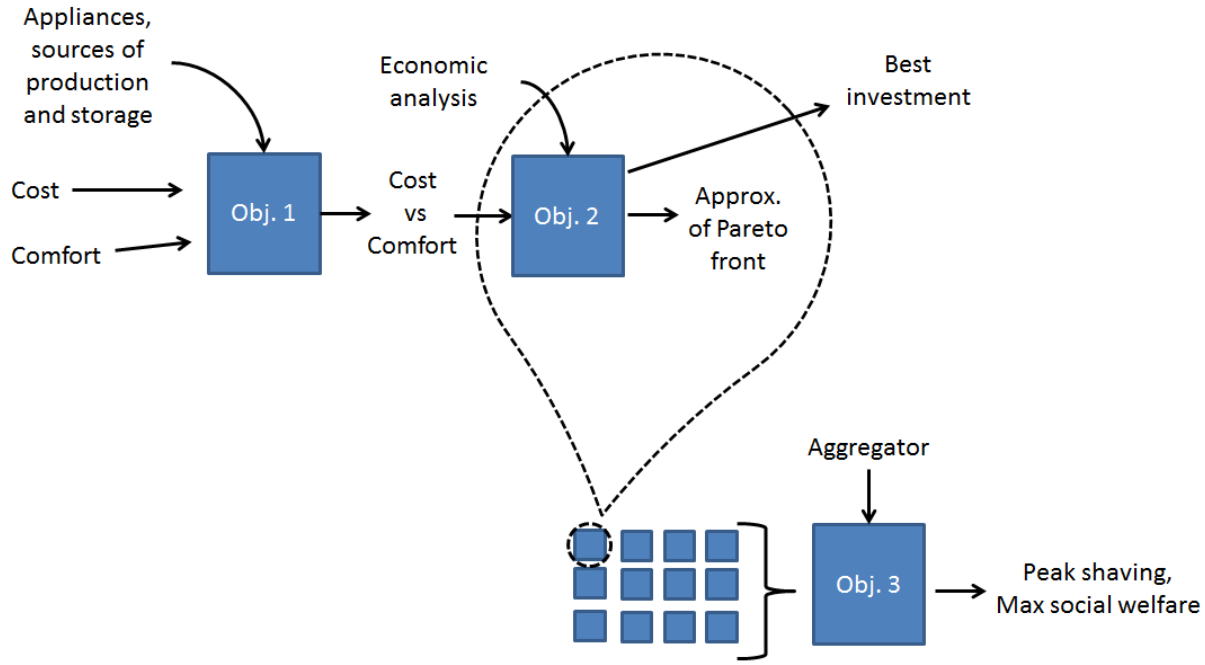

Figure 3.1 Synthesis of the PhD project.

The second step corresponds to the second objective (Obj. 2). In addition to the input from step 1, this step also receives economic information such as inflation rates, lifespan and acquisition cost for appliances, machines and technologies linked to smart homes. A framework is proposed to answer the following question: *for a specific household, when and/or what set of home appliances should be acquired so that the householder has a positive return on investment?* The output of this step is an approximation of the Pareto front and the best investment to be done for a given user. The analysis is conducted in Chapter 5.

Finally, in the third step, many users with their own Pareto front approximation are considered as input as well an aggregator. This corresponds to the third objective of this thesis. Hence, this work proposes a framework to coordinate a set of users in such a way that the

users minimize their costs while keeping the desired comfort level, and the GENCO minimizes its costs by flattening the aggregated load profile of users. The results reported a production curve flatten than the one without coordination, which improves the social welfare for the energy market. The analysis is conducted in Chapter 6.

CHAPTER 4 ARTICLE 1: A REALISTIC ENERGY OPTIMIZATION MODEL FOR SMART-HOME APPLIANCES

Authors: Michael David de Souza Dutra, Miguel F. Anjos and Sébastien Le Digabel.
International Journal of Energy Research, 2019[1].

Abstract: Smart homes have the potential to achieve optimal energy consumption with appropriate scheduling. The control of smart appliances can be based on optimization models, which should be realistic and efficient. However, increased realism also implies an increase in solution time. Many of the optimization models in the literature have limitations on the types of appliances considered and/or their reliability. This paper proposes a home energy management scheduling model that is more realistic and efficient. We develop a mixed integer linear optimization model that minimizes the energy cost while maintaining a given level of user comfort. Our main contribution is the variety of specific appliance models considered and their integration into a single model. We consider the use of energy in appliances and electric vehicles (EVs) and take into account renewable local generation, batteries, and demand-response. Our models of a shower, a fridge, and a hybrid EV consider both the electricity consumption and the conventional fuel cost. We present computational results to validate the model and indicate how it overcomes the limitations of other models. Our results, compared to the best competitors, provide cost savings ranging from 8% to 389% over a horizon of 24 hours.

Keywords: Smart home, Energy management system, Power demand, Residential load, Multi-class appliance.

4.1 Introduction and Related Work

In 2006, the European Technology Platform Smart Grid defined a smart grid to be "an electricity network integrating users, consumers, and generators in order to produce and deliver economic, secure and sustainable electricity supplies". Smart grids are used worldwide [59,65], and many distribution companies use demand-response pricing mechanisms in the residential sector.

A smart home is a home where the appliances and devices can be controlled remotely, and

[1]Available in [47]

the number of such homes has increased considerably in recent years. In North America the number is expected to reach 46.2M by 2020 [98], corresponding to 35% of households. In Europe, 44.9M are expected by 2020, corresponding to 20% of households. Governments are supportive because smart homes allow investment in the grid infrastructure to be postponed. Moreover, if the local generation comes from renewables, the environmental impact of coal/oil-based generation is reduced. The advantage for the users are that they can optimize energy usage to reduce costs while maintaining a desired comfort level; sell electricity back to the utility; or obtain financial incentives from demand-response programs.

We define smart home components (SHCs) to be the appliances, machines, and technologies available for use in smart homes. Examples of SHCs include photovoltaic solar panels (PVs), wind turbines (WTs), combined heating power (CHP), energy storage systems (ESSs), heating, ventilation, and air-conditioning (HVAC), and water heating (WH). SHCs are controlled by a home energy management system (HEMS), which also respects the power capacity (maximum amount of electric power that the house can use at any given time), ensures an adequate level for the air/water temperature, and makes decisions about when to buy and sell electricity. In essence, the HEMS solves a scheduling problem; for more details see [216].

See [164] and [22] for surveys of modeling approaches for this scheduling problem. However, existing models for appliance scheduling [110, 163] often do not accurately account for the operational and energy-consumption characteristics of each device. Table 4.1 summarizes the EMS models in the literature: columns 2 to 16 indicate the features included. The column *IBR constraints* indicates the use of inclining blocking rates (IBR), a pricing scheme where the prices increase for each incremental block of consumption. The column *Fraction of step* indicates that the appliances can be used for brief cycles. This occurs when, for example, a model uses a fixed interval of 10 min but allows the A/C to operate in cycles of 2.5 min. The column *Comfort* indicates the model used for the comfort function, and *Pricing* indicates the pricing policy, where TOU is time-of-use and RTP is real-time pricing. Finally, the column *Objective* indicates the optimization objective(s).

Table 4.1 shows that no article uses a detailed model for every appliance. Detailed appliance models give more accurate information and can better predict consumption, which is important for the evaluation of expansion strategies in the medium- and long-term [126]. Such models are available in the literature: see [97] for electric vehicles (EVs), [215] for PV, and [2] for PV/EV. However, the resulting optimization models may be computationally expensive to solve. Several authors [43, 69, 127] have emphasized the importance of a realistic model for the controllable appliances and the need for a trade-off between realism and computational difficulty. Realistic approaches to smart home scheduling require appropriate appliance mod-

els [127], and this is the motivation for this paper. Our specific goal is to create a realistic optimization model that can be solved in a reasonable time. Our main contribution is that we combine all of the SHCs of Table 4.1 into a single HEMS, formulated as a mixed integer linear optimization problem. In summary, we develop a model that finds the optimal cost while maintaining a high level of user comfort. The secondary contributions are:

1. Fridge model: We develop a realistic fridge model by linearizing a nonlinear model.
2. Shower model: In some countries, such as Brazil, the electric shower is one of the largest components of the electricity bill.
3. New EV model: To the best of our knowledge, no previous work has considered the additional costs of fuel or recharging outside the house.

This paper is organized as follows. In Section 4.2, we introduce the appliance models, IBR pricing, thermal machines, and other components. Section 4.3 describes our instances, and Section 4.4 presents the results. Section 4.5 provides concluding remarks.

4.2 Mathematical Models

In this section, we describe the models for the SHCs and the integrated optimization model. We consider only power consumption, and we retain the units used by the corresponding references. The nomenclature is provided before references.

4.2.1 Photovoltaic solar panels (PV) and Solar Collector Models

The PV and solar collector models calculate the values of the parameters E_{pv}^t and T_{in}^t. We first need to estimate T_o^t so that we can use the formulas from [9, Example 9, Section 14.12]. We also need to know the quantity of solar radiation available at the surfaces of the panels and collectors. We used the equations from [56, Chapters 1 and 2] (without shading and "track moving" but with "clear sky"). We implemented four models: the isotropic diffuse model, the HDRK model, the Perez model, and the ASHRAE revised clear sky model ("Tau Model") from [9, Chapter 14] and [10, Chapter 35]. From these we selected the Perez model. We also considered the absorptance effect.

We must convert the solar radiation into power for the PV and heat for the solar collector. For the PV, we use the approach from [135] with $V = V_{mp}$; we replace Equation 3 of [135] by Equation 9 of [44]. For the cell temperature, we use the approach from [56, Section 23.3]. For the solar collector, we use the collector-efficiency equations from [56, Chapters 3–6] with

Table 4.1 Summary of features of EMS models

Reference	WT	PV	Solar Collector	ESS	WH	Shower	Freezer/Fridge	HVAC	Phase Machines	A_{IEUI}	EV	CHP	Lighting	IBR Constraints	Fraction of Step	Comfort	Pricing	Objective
Our	x	x	x	x	x	x	x	x	x	x	x	x		x	x	L	TOU	↓ D vs C
[178]	x	x						x			x	x					NC	↓ C
[102]									x	x				x		NL	RTP	many
[211]								x							x	Q	NC	↓ TD
[207]													x			L		↓ IL
[205]				x					x	x						Q	NC	↓ C vs D vs B
[51]								x	x	x						Q	DA RTP	↓ D vs C
[103]									x	x							DA RTP	↓ C
[55]					x											L	DA TOU	↓ B
[84]								x								L	DA NC	↓ B vs D
[151]									x	x						CF	NC RTP	↑ -D vs C
[87]				x				x	x	x		x				L	DA NC	↓ C
[218]									x	x				x		L	NC	↓ C vs W
[15]	x	x		x												L		↓ C
[144]					x			x								L	NC	↑ -D vs C
[145]					x			x								L	NC	↑ -D vs C
[128]									x	x				x		L	RTP	↓ C vs W
[64]									x	x							RTP TOU	↓ C
[154]				x						x	x					L	TOU	↓ C / ↓ C vs D
[35]				x										x			NC	↓ C
[77]										x							DA TOU	↓ C
[3]									x	x						L	NC	↓ C / ↓ C vs PL
[4]				x					x	x							DA RTP	↓ C
[13]	x	x		x	x			x	x	x		x				NL	RTP	many
[14]				x	x			x	x	x		x				NL	RTP	many
[5]				x				x	x	x						L	NC	↓ C vs D
[36]					x			x	x	x	x						RTP	↓ B
[217]				x	x			x		x	x						RTP	↓ C
[196]					x					x							NC	↓ C
[134]			x		x			x	x	x	x					L	RTP	↓ C
[162]					x		x	x									TOU	↓ C
[34]								x	x	x						L	NC	↓ C
[163]					x		x	x		x						NL	TOU	↑ -D vs C
[120]		x		x							x							↓ C
[129]		x		x													Flat	↓ C vs CO_2
[186]		x		x							x							↓ E[C]
[76]		x		x						x	x							↓ C
[176]	x			x					x	x						L	RTP	↓ C

Table 4.1 *Continuation and end*: Summary of features of EMS models

[69]		x		x	x					x		x	–	TOU,RTP	↓ C
[170]		x		x		x	x							TOU	↓ C vs D
[127]		x		x				x	x	x				NC	↓ C
[168]	x	x		x			x		x	x				NC	↑ Profit
[131]				x			x		x					NC	↓ C
[63]		x		x						x				NC	↓ C
[143]		x		x	x			x	x					NC	↓ C
[174]	x	x		x	x	x	x		x		x	x	L	RTP	↓ C
[173]	x	x		x	x	x	x		x		x	x	L	RTP	↓ C / ↓ C vs PL
[104]				x	x	x	x		x	x	x			TOU	↓ C

Legend: ↓: Minimize ↑: Maximize IL: Illumination level D: Discomfort -D: Comfort C: Cost L: Linear Q: Quadratic NC: Not constant TD: Thermal discomfort B: Electricity bill BL: Battery loss DA: Day ahead CF: concave function W: Waiting time NL: Nonlinear PL: Peak load

the factor F' = 0.8, the temperature of the plates equal to the outside temperature, and the difference of temperature between the plates and glass set to 20^{o}C. All the layers of glass have the same temperature, and the inlet water comes from the street.

4.2.2 Wind Turbines (WT) Model

The WT model forecasts the value of E^t_{wt}. Villaneuva & Feijóo [195] propose a relationship between wind speed and WT power produced. They consider operation at maximum capacity and specify cut-in and cut-out inequalities:

$$\begin{array}{cc} \text{Wind speed interval (m/s)} & \text{Output power (W)} \\ U < U_{CutIn} & 0 \\ U_{CutIn} \leq U < U_{Pmax} & 0.5A\rho U^3 C_{p2} \\ U_{Pmax} \leq U \leq U_{CutOut} & Pmax \\ U > U_{CutOut} & 0 \end{array} \tag{4.1}$$

where U is the wind speed (m/s); U_{CutIn} is the lowest wind speed (m/s) at which it is possible to obtain power from the wind; U_{Pmax} is the wind turbine power speed rate (m/s); A is the area of the air-stream, measured in a perpendicular plane to the direction of the wind speed (m^2); ρ is the air density (kg.m^{-3}); C_{p2} is the power coefficient, which is the ratio between the power produced by the WT and the power carried by the free air-stream; U_{CutOut} is the upper limit (m/s) at which it is possible to get power from the wind; and $Pmax$ is the rated power (W).

We can find ρ using the ideal gas law for dry air, Equation 1.18 from [181].

4.2.3 Heating, Ventilation, and Air Conditioning (HVAC) Model

The HVAC model is outlined in this subsection. We discuss also assumptions and flexibility strategies. With $\Upsilon = \Delta t_2 / V_{house} \rho_{air} c_{air}$, the HVAC model is

$$T_{room}^{t+1} = T_{room}^{t} + \Upsilon[3600(P_{heating} z_{HVAC}^{t} - P_{cool} z_{air}^{t})] + \Upsilon(G^t) \ \forall \ t \in T \backslash \{|T|\} \tag{4.2}$$

$$G^t = \left[\frac{A_{ceiling}}{R_{ceiling}} + \frac{A_{wall}}{R_{wall}} + \frac{A_{window}}{R_{window}}\right](T_o^t - T_{room}^t) + [n_{ac} V_{house} \rho_{air} c_{air}](T_o^t - T_{room}^t) + 3600 H_p^t + 3600(SHGC) A_{window} H_{sun}^t \ \forall \ t \in T \backslash \{|T|\} \tag{4.3}$$

$$T_{room}^1 = T_o^1 \tag{4.4}$$
$$x_{HVAC}^t = P_{heating} z_{HVAC}^t + P_{cool} z_{air}^t \ \forall \ t \in T$$

$$\begin{aligned} y_{HVAC}^t &\in \{0,1\} \ \forall \ t \in T \\ y_{air}^t &\in \{0,1\} \ \forall \ t \in T \\ 1 &\geq y_{HVAC}^t + y_{air}^t \ \forall \ t \in T \end{aligned} \tag{4.5}$$

$$\begin{aligned} z_{HVAC}^t &\leq y_{HVAC}^t \ \forall \ t \in T \\ z_{air}^t &\leq y_{air}^t \ \forall \ t \in T \end{aligned} \tag{4.6}$$

$$\begin{aligned} z_{HVAC}^t &\geq 0 \ \forall \ t \in T \\ z_{air}^t &\geq 0 \ \forall \ t \in T \end{aligned} \tag{4.7}$$

$$\begin{aligned} V_{HVAC}^t &\geq T_{room}^t - T_f^t \ \forall \ t \in D_{air} \\ V_{HVAC}^t &\geq -T_{room}^t + T_f^t \ \forall \ t \in D_{air} \end{aligned} \tag{4.8}$$

Constraints (4.2) to (4.7) represent the room temperature, and (4.8) permit deviation from the target temperature and measure the discomfort during the intervals when HVAC is used. Constraints (4.2) and (4.3) are based on Shao et al. [172]. They propose a model with a 1.2% total daily energy difference. The differences between our model and their model are explained below.

Assumptions: A_{wall} in [172] is derived from the floor area, assuming that the height of the house is 10 ft. If A_{wall} is not given by the user, we assume that the floor is square and calculate

A_{wall} accordingly. In [172] the authors consider a specific window turned to the south. In our model, we consider every window of the same type. The values for H_p^t, SHCG, and n_{ac} are not available in [172]. H_p can be found ([13], [212, pp. 41–43]) via $H_p = P_{activity} A_{body}$, where $P_{activity}$ is the metabolic rate and $A_{body} = 0.202 m^{0.425} h^{0.725}$, where h is the height (m) and m is the mass of the body (kg). We define np^t to be the number of occupants at time t. We then have $H_p^t = \sum_{i=1}^{np^t} P_{activity,i}^t A_{body,i}^t \ \forall\ t \in T$.

For SHCG, we used the average of the values of [9, p. 353], and H_{solar} is calculated from our PV model. We have $\rho C_{air} = \frac{1214.4J}{^oC \times m^3} \approx \frac{0.018Btu}{^oF \times ft^3}$ from [9, Chapter 17]: $n_{ac} = ACH = 3.6 Q_i / V$, $Q_i = A_L IDF$, $A_L = A_{es} A_{ul}$, where ACH is the hourly air change; Q_i is the infiltration airflow rate (L/s); V is the building volume (m^3); A_L is the effective leakage area (cm^2) (including the flue) at a reference pressure difference of 4 Pa, assuming a discharge coefficient CD of 1; IDF is the infiltration driving force ($L/(s.cm^2)$); A_{es} is the exposed surface area of the building (m^2); and A_{ul} is the unit leakage area (cm^2/m^2). This gives $ACH = 3.6 A_{es} A_{ul} IDF / V$. With the values given for IDF [9, Table 5 of Chapter 17] and A_{ul} [9, Table 3 of Chapter 17], n_{ac} has an acceptable value.

Our other assumptions are as follows: i) there is a single conditioned space; ii) no independent thermal storage is linked to the main HVAC equipment; iii) the humidity control is neglected; iv) the internal heat sources of the equipment are neglected; v) the temperature is constant throughout the space.

We have rewritten the model from [172] given the considerations above to arrive at an on-off model composed of Constraints (4.2) to (4.5), (4.8).

Flexibility: (4.2) introduces the on-off feature, since y_{HVAC}^t and y_{air}^t are binary variables. Thus, we are working with fixed power in a fixed time interval. However, forcing a machine to operate for a full interval could generate an overcharge. Let the variable z_a^t be the fraction of Δt during which appliance a is on. We have $z_a^t y_a^t = z_a^t$. We can model the implications with inequalities such as (4.6). Therefore, with the new variable, we can build a single model that is represented by Constraints (4.2) to (4.8). With the objective function (4.76), we can, without any impact on the results, drop the variables y_{HVAC}^t and y_{air}^t and the restrictions (4.5) to (4.6). We refer to this as the *Fraction of step*.

The strategy above does not indicate when the machine is on/off in the fixed time interval. Given x_{HVAC}^t for each $t \in T$, we can find whether the machine is on or off at each second.

The temperature at the end of the period depends on exactly when it is used. If it is used at the end of the period, the results are closer to the results for the complete optimization model. However, the difference is not as large. With nomimal power of 25 kW, the difference

in temperature will be around 0.12^oC at some point in the time interval.

Note that the addition of z_a^t does not violate energy conservation. For example, suppose an appliance has a power of 5000 W and it operates for 50% of the time, giving a consumption of $5000\,W \times 0.5\Delta t$. It will contribute $2500\,W \times \Delta t$ to the conservation constraint.

4.2.4 Water Heaters (WH) Model

The Water Heaters model is outlined in this subsection. A comparison with reference model is done for validation purposes. With $\Psi = \Delta t_2/(v_{tank}C_p)$, the HVAC model is

$$T_{out,wh}^{t+1} = T_{out,wh}^t + \Psi[-227.4 fr_{wh}^t C_p(T_{out,wh}^t - T_{in}^t)] + \Psi[3600(x_{wh}^t + 1000P_{CHPt}^t)] - \Psi[3600(UA)_{wh}(T_{out,wh}^t - T_{room}^t)] \;\forall\; t \in T\backslash\{|T|\} \quad (4.9)$$

$$T_{out,wh}^1 = T_{in}^1 \quad (4.10)$$
$$x_{wh}^t = P_{wh} y_{wh}^t \;\forall\; t \in T$$

$$y_{wh}^t \in \{0,1\} \;\forall\; t \in T \quad (4.11)$$

$$V_{wh}^t \geq T_f^{wh} - T_{out,wh}^t \;\forall\; t \in D_{wh} \quad (4.12)$$
$$V_{wh}^t \geq -T_f^{wh} + T_{out,wh}^t \;\forall\; t \in D_{wh}$$

$$y_{wh}^t \leq E_{wh} \;\forall\; t \in T \quad (4.13)$$

Constraints (4.9) to (4.11) represent the WH temperature, and (4.12) permit deviation from the target temperature and measure the discomfort during the intervals when hot water is used. If $E_{wh} = 0$, there is no WH, and $T_{out,wh}^t$ is at most the street water temperature or the water temperature from SC if it exists. In this case, we need Constraint (4.13), which also imposes an upper bound on the temperature. Note that T_{room}^t in (4.9) comes from the HVAC model.

We assume that all the water inside the WH is at the same temperature. The model was constructed from [56, Equation 8.3.3] and validated by comparisons with the model from [172], which was validated experimentally.

For a validation example, we convert units where necessary and use the following data: the room temperature is given in Figure 4.1, $T_{out,wh}^1 = 77^oF$, $x_{wh}^t = 5\,\text{kW} \;\forall\; t \in T$, the surface area of the WH equals $5\,\text{ft}^2$, the tank heat resistance equals $25^oF \cdot ft^2 \cdot h/Btu$, $\Delta t = 10\,\text{min}$, $T_{in}^t = 104^oF \;\forall\; t \in T$, $v_{tank} = 80\,\text{gallons}$, $fr_{wh}^t = \ddot{f} \;\forall\; t \in T\,(\text{gallons/min})$ for $\ddot{f} \in \{0,1,5,10\} \;\forall\; i$. If we assume that the WH is always on, we obtain the results of [172]

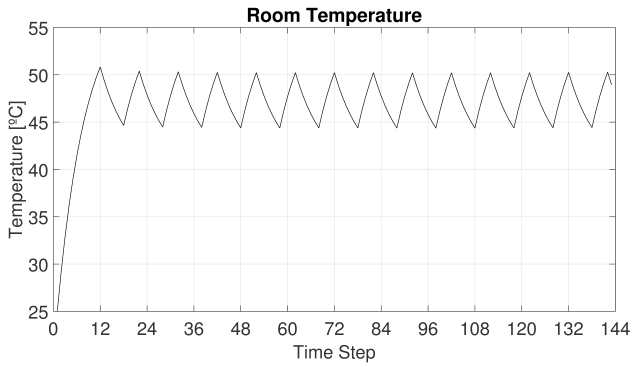

Figure 4.1 Room temperature for validation example.

when $fr^t_{wh} > 0 \; \forall \; t \in T$, as shown in Figures 4.2 and 4.3. When $fr^t_{wh} = 0 \; \forall \; t \in T$, the model deviates after about 150^{o}C, but in practice there are mechanisms to avoid water evaporation. Thus, our model is faithful to the results of [172].

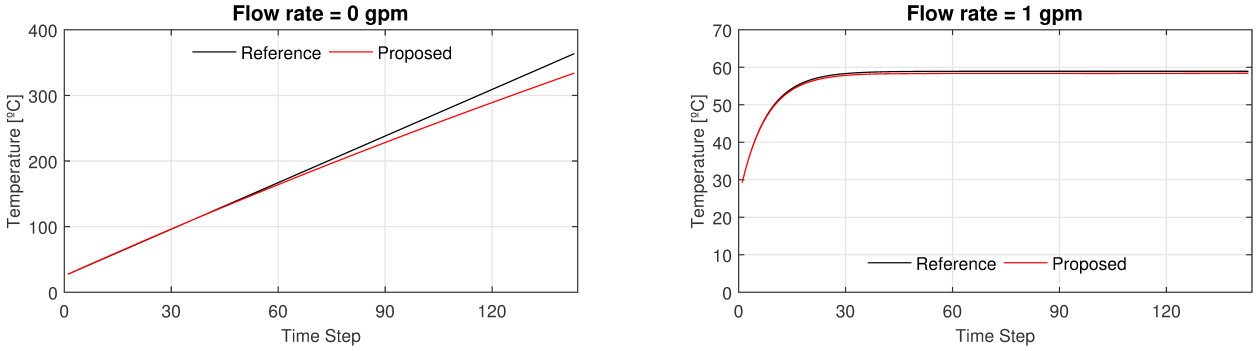

Figure 4.2 Comparison of our model and reference model from [172]: WH always on and low flow rate.

4.2.5 Shower Model

In this subsection, the shower model is outlined and thermodynamics explanations are given. The shower is modeled by:

$$\begin{aligned} T^t_{chu\_hand} &\leq T^t_{out,wh} \; \forall \; t \in D_{chu} \\ T^t_{chu\_hand} &\geq T^t_{inlet} \; \forall \; t \in D_{chu} \end{aligned} \tag{4.14}$$

$$\begin{aligned} T^t_{out,chu} = T^t_{chu\_hand} + 60x^t_{chu}/(C_e fr^t_{chu}) \; \forall \; t \in D_{chu} \\ x^t_{chu} = P_{chu} y^t_{chu,hot} \; \forall \; t \in D_{chu} \end{aligned} \tag{4.15}$$

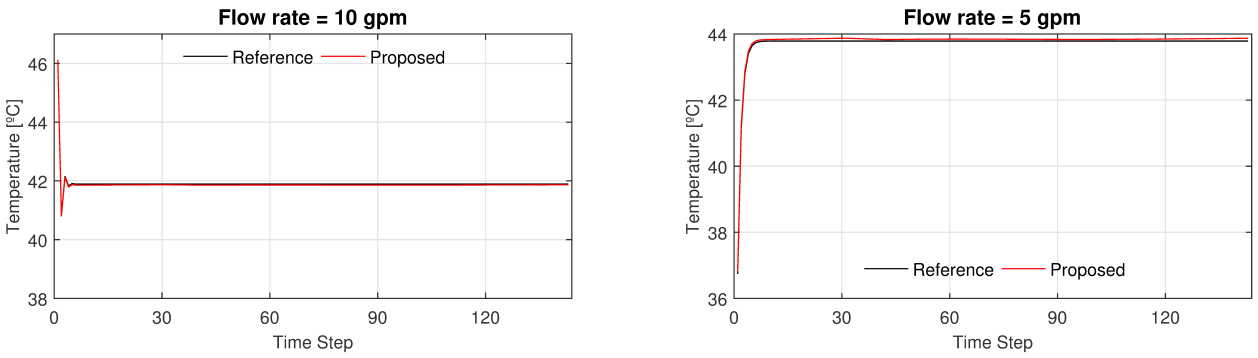

Figure 4.3 Comparison of our model and reference model from [172]: WH always on and high flow rate.

$$x^t_{chu} = 0 \; \forall \; t \notin D_{chu} \tag{4.16}$$

$$\begin{aligned} V^t_{chu} &\geq T^{chu}_f - T^t_{out,chu} \; \forall \; t \in D_{chu} \\ V^t_{chu} &\geq -T^{chu}_f + T^t_{out,chu} \; \forall \; t \in D_{chu} \end{aligned} \tag{4.17}$$

$$y^t_{chu,hot} \in \{0, 1\} \; \forall \; t \in D_{chu} \tag{4.18}$$

Constraints (4.14) place bounds on the shower temperature without using the shower resistance. Constraints (4.15) to (4.16) represent the shower temperature, and (4.17) permit deviation from the target temperature and measure the discomfort during the intervals when the shower is used. Constraints (4.18) are the binary restrictions.

We obtain Constraints (4.14) to (4.18) from [212, Chapter 1] through the thermodynamics formula $\dot{Q} = \dot{m} C_p \Delta T$ where $\dot{m}$ is the mass flow rate of a fluid flowing in a pipe (kg/s); C_p is the specific heat of the fluid (J/kg·^oC); ΔT is the temperature difference (^oC); and $\dot{Q}$ is the rate of net heat transfer of the control volume (W). Moreover, $\dot{m} = \rho V A_c$ where ρ is the fluid density; V is the average fluid velocity in the flow direction; and A_c is the duct cross-sectional area. This gives $\dot{Q} = \rho \dot{V} C_p \Delta T$, where $\dot{V}$ is the volumetric flow rate (m^3/s). We write $P = \rho \dot{V} C_p \Delta T$ where P is the power (W) lost or injected.

For each step $t \in D_{chu}$, $P_{chu} = P$, f_r is the equivalent measure of $\dot{V}$ (gpm) and $\Delta T = T_{out,chu} - T_{chu\_hand}$. This gives (4.15).

4.2.6 Batteries (ESS) Model

The ESS model is outlined in this subsection. A comparison with reference models is done

to demonstrate our differences. The ESS is modeled by

$$SOC^{t+1} = SOC^t + \frac{100\Delta t_2}{E_{bat}}\left(P_{bat}^{ch,t}\eta^{ch}\mu - \frac{P_{bat}^{dch,t}}{\eta^{dch}\mu} - p_{loss}y_{float}^t\right) \forall\ t \in T\backslash\{|T|\} \tag{4.19}$$

$$SOC^t \geq SOC_{min} \forall\ t \in T \tag{4.20}$$

$$SOC^t \leq SOC_{max} + (100 - SOC_{max})y_{float}^t \forall\ t \in T \tag{4.21}$$

$$SOC^1 = SOC_{min} \tag{4.22}$$

$$\begin{aligned} P_{bat}^{ch,t} &\leq \tfrac{P_{max}^{ch}}{\eta^{ch}\mu} y_{bat}^{ch,t} \forall\ t \in T \\ P_{bat}^{ch,t} &\geq \tfrac{P_{min}^{ch}}{\eta^{ch}\mu} y_{bat}^{ch,t} \forall\ t \in T \\ P_{bat}^{dch,t} &\leq P_{max}^{dch}\eta^{dch}\mu y_{bat}^{dch,t} \forall\ t \in T \\ P_{bat}^{dch,t} &\geq P_{min}^{dch}\eta^{dch}\mu y_{bat}^{dch,t} \forall\ t \in T \end{aligned} \tag{4.23}$$

$$1 \geq y_{bat}^{dch,t} + y_{bat}^{ch,t} \forall\ t \in T \tag{4.24}$$

$$\begin{aligned} y_{bat}^{dch,t} &\in \{0,1\} \forall\ t \in T \\ y_{bat}^{ch,t} &\in \{0,1\} \forall\ t \in T \\ y_{float}^t &\geq 0 \forall\ t \in T \end{aligned} \tag{4.25}$$

Constraints (4.19) establish the relationships between the state of charge (SOC), discharging and charging powers, and battery float losses. Constraints (4.20) place a lower bound on the SOC. Constraints (4.21) place an upper bound on the float losses that is activated when a threshold is reached. Constraint (4.22) sets an initial value for the SOC. Constraints (4.23) set bounds on the discharging and charging power. Constraints (4.24) ensure that at each $t \in T$ the battery either charges or discharges. Constraints (4.25) are the domain restrictions.

We based our model on [13], [14], and [217]. The differences between these models will be explained using the following data: $|T| = 144$, $E_{bat} = 24\,\text{kWh}$, $SOC_{max} = 80\%$, $SOC_{min} = 20\%$, $P_{max}^{ch} = P_{max}^{dch} = 3.3\,\text{kW}$, $P_{min}^{ch} = P_{min}^{dch} = 0.3\,\text{kW}$, $\eta^{ch} = \eta^{dch} = 0.91$, and $\mu = 1$. We define the objective function as $\max 30SOC^2 - \sum_{t\in T} SOC^t$. Thus, in Interval 1, the battery will charge at a maximal power and in Interval 2 it will discharge at a maximal power.

The solution to the models of [13] and [14] is $SOC^2 = 22.0854$, $SOC^t = 20\ \forall\ t \in T\backslash\{2\}$, $P_{batt}^{ch,1} = P_{batt}^{dch,2} = 3.003$, and the other power variables are null. Thus, the charging consumption was 3.003 KW instead of 3.3 KW. For the discharging, $P_{batt}^{dch,2}$ takes the value of the power inside the battery instead of the power sent to the house. Thus, when we put these variables into the energy conservation constraints, they use different values than the values sent to or

consumed in the battery model. Therefore, there is an energy construction if we take the home as the reference point.

The model from [217] gives the same objective value, but we could have maximal power charging in the battery.

Constraints (4.21) implement the battery float charge loss, which results from the energy used to maintain the battery charge when SOC $\approx 100\%$ [30].

4.2.7 Fridge Model

The fridge model is outlined in this subsection. A comparison with reference model is done for validation purposes. The fridge is modeled by

$$\begin{aligned} T^{t+1}_{freezer} &= T^{t}_{freezer} - (7/25)\Delta t y^{t}_{comp} + (15/67)\Delta t \left(1 - y^{t}_{comp}\right) \ \forall\ t \in T\backslash\{|T|\} \\ T^{t+1}_{refri} &= T^{t}_{refri} - 0.1467\Delta t y^{t}_{comp} + 0.1196\Delta t(1 - y^{t}_{comp}) \ \forall\ t \in T\backslash\{|T|\} \end{aligned} \tag{4.26}$$

$$T^{1}_{freezer} = T^{start}_{freezer} \tag{4.27}$$

$$T^{1}_{refri} = T^{start}_{refri} \tag{4.28}$$

$$x^{t}_{refri} = P_{comp} y^{t}_{comp} \ \forall\ t \in T \tag{4.29}$$

$$\begin{aligned} V^{t}_{freezer} &\geq T^{freezer}_{f} - T^{t}_{freezer} \ \forall\ t \in T \\ V^{t}_{freezer} &\geq 0 \ \forall\ t \in T \\ V^{t}_{refri} &\geq T^{refri}_{f} - T^{t}_{refri} \ \forall\ t \in T \\ V^{t}_{refri} &\geq 0 \ \forall\ t \in T \end{aligned} \tag{4.30}$$

$$y^{t}_{comp} \in \{0, 1\} \ \forall\ t \in T \tag{4.31}$$

We consider a frost-free top-mount refrigerator. Constraints (4.26) represent the freezer temperature and fridge temperature, respectively. Constraint (4.27) establishes the initial freezer temperature, and Constraint (4.28) establishes the initial fridge temperature. Constraints (4.29) initialize the x^{t}_{refri} values for the link with the complete model. Constraints (4.30) permit deviation from the target temperature and measure the discomfort, and Constraints (4.31) are the binary restrictions.

A transient model has been developed [24, 25] for the temperatures of refrigerated compartments; the predicted energy consumption has a maximum deviation of $\pm 2\%$. Our model is based on this, with some adjustments. We observe a correlation between the power consump-

tion and the air temperature at the evaporator outlet [24, Figures 2.15 and 2.16]. We apply Newton's law of cooling to find the temperature at the evaporator outlet when the compressor is operating. When it is off, we have a choice of two approaches. In the first, suggested by the author of [25] via email, we assume that the temperature at the evaporator outlet is the same as the air temperature at the evaporator inlet. In the second, we use Newton's law of cooling for the temperature increase around the evaporator outlet. We selected approach 2.

We can rewrite Equation 3.71 from [24] as $(T^t_{o,e})' = T^t_{o,e} + (3600 w_{fan})/(\dot{m}_a C_{p,a}) y^t_{comp}$, where $(T^t_{o,e})'$ is the air temperature of the fan discharge (^oC); w_{fan} is the rated fan power (W); $\dot{m}_a$ is the total mass flow rate of air (kg/h); and $C_{p,a}$ is the specific heat at a constant pressure (J/kg^oC). The fan is on only when the compressor is on.

With $\kappa \in \{T_{newton_2}, rT^{t-1}_{freezer} + (1-r)T^{t-1}_{refri}\}$ and following [24], we obtain $\forall\, t \in T\backslash\{|T|\},\ \forall * \in \{r, f\}$: $T^{t+1}_* = T^t_{eq,*} - (T^t_{eq,*} - T^t_*)\exp\left(-\frac{60\Delta t\left(Ua_* + UA_m + \frac{\dot{m}_* C_{air}}{3600} y^t_{comp}\right)}{C_*}\right)$ where $T^t_{eq,f}$ ($T^t_{eq,r}$) is associated with the steady-state temperature of the freezer (fridge) if constant conditions are maintained at time t (^oC); UA_f (UA_r) is the global freezer (fridge) thermal conductance (W/^oC); $\dot{m}_{d,f}$ ($\dot{m}_{d,r}$) is the air flow leaving the freezer (fridge) when the door is open; T^t_a is the exterior temperature around the fridge at time t (^oC); UA_m is the global mullion thermal conductance (W/^oC); $T^t_f = T^t_{freezer}\ \forall\, t \in T$; and $T^t_r = T^t_{refri}\ \forall\, t \in T$. Note that T^t_a is T^t_{room} from the HVAC model.

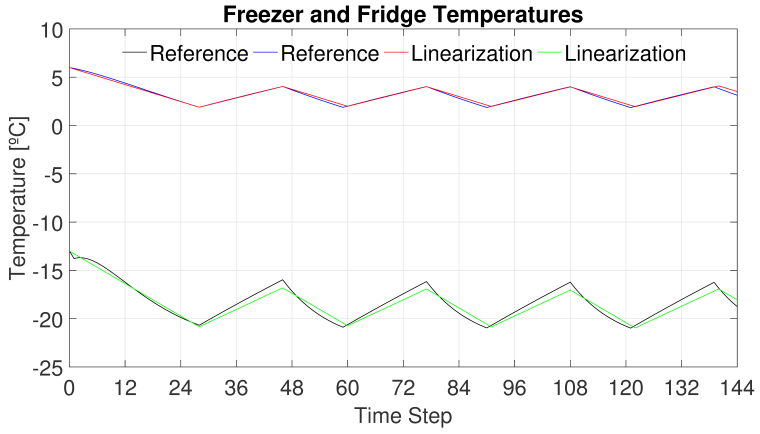

Figure 4.4 Comparison of simulation results for fridge from linearization and reference model.

To simplify this nonlinear model, we perform a linear regression, obtaining: $T^{t+1}_f = T^t_f - (7/25)\Delta t y^t_{comp} + (15/67)\Delta t(1 - y^t_{comp})$ for the freezer and $T^{t+1}_r = T^t_r - 3.5/25\Delta t y^t_{comp} + 7.25/67\Delta t(1 - y^t_{comp})$ for the fridge. Figure 4.4 presents simulation results for the linearizations, and they agree well with the reference model [24]. We thus obtain (4.26) to (4.31).

4.2.8 Plug-in Hybrid Electric Vehicle (EV) Model

In this subsection, the EV model is outlined. We explain also considerations used in the formulation. Let ϱ^t be the vector $\left(y^{dch,t}_{EVbat}, y^{ch,t}_{EVbat}, y^t_{EVfloat}\right)\ \forall\ t \in T$. The EV is modeled by

$$EVSOC^{t+1} = EVSOC^t + \frac{100\Delta t_2}{EEV_{bat}}\left(P^{ch,t}_{EVbat}\eta^{ch}_{Ev}\mu_{Ev} - \frac{P^{dch,t}_{EVbat}}{\eta^{dch}_{Ev}\mu_{Ev}} - EVp_{loss}y^t_{EVfloat}\right)$$
$$\forall\ t \in T\backslash\{|T|\}, s \in \{1,2,\ldots,n_{trips}\} : t^s_{start} \leq i < t^s_{end}, t^1_{start} \leq t < t^1_{end}$$

$$EVSOC^{t+1} = EVSOC^t + \frac{100\Delta t}{EEV_{bat}}\left(P^{ch,t}_{EVbat}\eta^{ch}_{Ev}\mu_{Ev} - \frac{P^{dch,t}_{EVbat}}{\eta^{dch}_{Ev}\mu_{Ev}} - EVp_{loss}y^t_{EVfloat}\right)$$
$$\forall\ s \in \{1,2,\ldots,n_{trips}\}, t \in \{1,2,\ldots,t^1_{end}-1\} \cup \left\{t^s_{start}, t^s_{start}+1,\ldots,t^{s+1}_{end}-1\right\} : t^1_{start} > t^1_{end} \tag{4.32}$$

$$EVSOC^t \geq 0\ \forall\ t \in T \tag{4.33}$$
$$EVSOC^t \leq EVSOC_{max} + (100 - EVSOC_{max})y^t_{EVfloat}\ \forall\ t \in T \tag{4.34}$$

$$EVSOC^1 = EVSOC\_last\_day :\ t^1_{start} > t^1_{end} \tag{4.35}$$
$$EVSOC^{t^1_{start}} = EVSOC_{ret} :\ t^1_{start} < t^1_{end}$$

$$EVSOC^{t^s_{start}} = EVSOC^{t^s_{end}} - 100\frac{Km^s_{next} - Km^s_{fuel}}{Km^{100}}\ \forall\ s \in \{1,2,\ldots,n_{trips}\} : t^1_{start} > t^1_{end}$$

$$EVSOC^{t^{s+1}_{start}} = EVSOC^{t^s_{end}} - 100\frac{Km^s_{next} - Km^s_{fuel}}{Km^{100}}\ \forall\ s \in \{1,2,\ldots,n_{trips}-1\} : t^1_{start} < t^1_{end} \tag{4.36}$$

$$EVSOC^{t^s_{end}} \geq EVSOC^{end}_{min}\ \forall\ s \in \{1,2,\ldots,n_{trips}\} \tag{4.37}$$
$$EVSOC^{t^{n_{trips}+1}_{end}} \geq EVSOC^{end}_{min} : t^1_{start} > t^1_{end}$$

$$\begin{aligned} P^{ch,t}_{EVbat} &\leq \frac{EVP^{ch}_{max}}{\eta^{ch}_{Ev}\mu_{Ev}} y^{ch,t}_{EVbat}\ \forall\ t \in T \\ P^{ch,t}_{EVbat} &\geq \frac{EVP^{ch}_{min}}{\eta^{ch}_{Ev}\mu_{Ev}} y^{ch,t}_{EVbat}\ \forall\ t \in T \\ P^{dch,t}_{EVbat} &\leq EVP^{dch}_{max}\eta^{dch}_{Ev}\mu_{Ev}y^{dch,t}_{EVbat}\ \forall\ t \in T \\ P^{dch,t}_{EVbat} &\geq EVP^{dch}_{min}\eta^{dch}_{Ev}\mu_{Ev}y^{dch,t}_{EVbat}\ \forall\ t \in T \end{aligned} \tag{4.38}$$

$$y^{dch,t}_{EVbat} + y^{ch,t}_{EVbat} \leq 1\ \forall\ t \in T \tag{4.39}$$

$$
\begin{aligned}
\varrho^t = 0 \ \forall \ s \in \{1,2,\ldots,n_{trips}\}, t \in \{t^s_{end}, t^s_{end}+1, \ldots, t^s_{start}-1\} : \ t^1_{start} > t^1_{end} \\
EVSOC^t = 0 \ \forall \ s \in \{1,2,\ldots,n_{trips}\}, t \in \{t^s_{end}+1, t^s_{end}+2, \ldots, t^s_{start}-1\} : \ t^1_{start} > t^1_{end} \\
\varrho^t = 0 \ \forall \ t \in \left\{t^{n_{trips}+1}_{end}, t^{n_{trips}+1}_{end}+1, \ldots, |T|\right\} \ : t^1_{start} > t^1_{end} \\
EVSOC^t = 0 \ \forall \ t \in \left\{t^{n_{trips}+1}_{end}+1, t^{n_{trips}+1}_{end}+2, \ldots, |T|\right\} \ : t^1_{start} > t^1_{end} \\
\varrho^t, EVSOC^t = 0 \ \forall \ t \in \{1,2,\ldots,t^1_{start}-1\} : t^1_{start} < t^1_{end} \\
\varrho^t = 0 \ \forall \ s \in \{1,2,\ldots,n_{trips}-1\}, t \in \{t^s_{end}, t^s_{end}+1, \ldots, t^{s+1}_{start}-1\} : t^1_{start} < t^1_{end} \\
EVSOC^t = 0 \ \forall \ s \in \{1,2,\ldots,n_{trips}-1\}, t \in \left\{t^s_{end}+1, t^s_{end}+2, \ldots, t^{s+1}_{start}-1\right\} : t^1_{start} < t^1_{end} \\
\varrho^t = 0 \ \forall \ t \in \left\{t^{n_{trips}}_{end}, t^{n_{trips}}_{end}+1, \ldots, |T|\right\} : t^1_{start} < t^1_{end} \\
EVSOC^t = 0 \ \forall \ t \in \left\{t^{n_{trips}}_{end}+1, t^{n_{trips}}_{end}+2, \ldots, |T|\right\} : t^1_{start} < t^1_{end}
\end{aligned}
\tag{4.40}
$$

$$
C^s_{ev} \geq Km^s_{fuel} P_{gas} \ \forall \ s \in \{1,2,\ldots,n_{trips}\} \tag{4.41}
$$

$$
C_{ev} \geq \sum_{s=1}^{n_{trips}} C^s_{ev} \tag{4.42}
$$

$$
\begin{aligned}
y^{dch,t}_{EVbat} \in \{0,1\} \ \forall \ t \in T \\
y^{ch,t}_{EVbat} \in \{0,1\} \ \forall \ t \in T \\
y^t_{EVfloat} \in \{0,1\} \ \forall \ t \in T \\
C^s_{ev} \geq 0 \ \forall \ s \in \{1,2,\ldots,n_{trips}\} \\
Km^s_{fuel} \geq 0 \ \forall \ s \in \{1,2,\ldots,n_{trips}\} \\
C_{ev} \geq 0
\end{aligned}
\tag{4.43}
$$

Constraints (4.32) establish the relationships between the SOC, the discharging and charging powers, and the float loss. The vehicle could arrive without energy, so Constraints (4.33) place a lower bound of zero on the SOC. Constraints (4.34) place an upper bound on the float losses that is activated when a threshold is reached. Constraints (4.35) establish an initial value for the SOC. The former is activated when the first event is a departure, and the latter is activated when the first event is an arrival. Constraints (4.36) create a link between consecutive trips to ensure energy conservation. Constraints (4.37) place a lower bound on the SOC (sufficient to reach the nearest gas station) in intervals when travel is necessary. Constraints (4.38) establish bounds on the discharging and charging power. Constraints (4.39) ensure that at each $t \in T$ the battery either charges or discharges. Constraints (4.40) ensure null values for the intervals when the EV battery cannot be used. Constraints (4.41) calculate the fuel cost for each trip s. Constraint (4.42) gives the total cost of the fuel consumption.

Constraints (4.43) are the binary and nonnegative restrictions.

An EV model is essentially the same as a battery model [14], but there are more constraints, including minimal SOC constraints and trip-signal constraints to ensure that the EV charges and discharges only when at home. Sousa et al. [179] present an EV model that is similar to a battery model. Our model is based on [14] and [179] and considers multiple trips in a day [132]. In addition, we consider hybrid vehicles.

4.2.9 Combined heat and power (CHP) Model

In this subsection, the CHP model is outlined. We explain also considerations and strategies used in the formulation. The CHP model is modeled by

$$\begin{aligned}
y^{\tau}_{CHP} &\geq z^{t}_{CHP} \;\forall\; t \in T, \tau \in \{t, t+1, \ldots, \min\{t + \lceil d^{on}_{CHP}/\Delta t\rceil - 1, |T|\}\} \\
y^{\tau}_{CHP} &\leq 1 - zd^{t}_{CHP} \;\forall\; t \in T, \tau \in \left\{t, t+1, \ldots, \min\left\{t + \left\lceil d^{off}_{CHP}/\Delta t\right\rceil - 1, |T|\right\}\right\} \\
z^{t+1}_{CHP} &\leq 1 - y^{t}_{CHP} \;\forall\; t \in T\backslash\{|T|\} \\
zd^{t+1}_{CHP} &\leq y^{t}_{CHP} \;\forall\; t \in T\backslash\{|T|\} \\
z^{t}_{CHP} &\geq y^{t}_{CHP} - y^{t-1}_{CHP} \;\forall\; t \in T\backslash\{1\} \\
zd^{t}_{CHP} &\geq -y^{t}_{CHP} + y^{t-1}_{CHP} \;\forall\; t \in T\backslash\{1\} \\
1 &\geq zd^{t}_{CHP} + z^{t}_{CHP} \;\forall\; t \in T \\
z^{1}_{CHP} &\geq y^{1}_{CHP} - y^{last_day}_{CHP}
\end{aligned} \tag{4.44}$$

$$\begin{aligned}
y^{1}_{CHP} &= y^{ini}_{CHP} \\
P^{1}_{CHPe} &= P^{ini}_{CHPe}
\end{aligned} \tag{4.45}$$

$$\begin{aligned}
P^{t+1}_{CHPe} &\geq -\max\left\{P^{1,\mu}_{CHP,max}, P^{1,\eta}_{CHP,max}\right\} zd^{t+1}_{CHP} + P^{t}_{CHPe} - 60\Delta t_2 r^{down}_{CHP} w^{t}_{down} \;\forall\; t \in T\backslash\{|T|\} \\
P^{t+1}_{CHPe} &\leq \max\left\{P^{1,\mu}_{CHP,max}, P^{1,\eta}_{CHP,max}\right\} z^{t+1}_{CHP} + P^{t}_{CHPe} + 60\Delta t_2 r^{up}_{CHP} w^{t}_{up} \;\forall\; t \in T\backslash\{|T|\} \\
1 &\geq w^{t}_{up} + z^{t+1}_{CHP} \;\forall\; t \in T\backslash\{|T|\} \\
1 &\geq w^{t}_{down} + zd^{t+1}_{CHP} \;\forall\; t \in T\backslash\{|T|\} \\
w^{t}_{up} &\leq y^{t}_{CHP} \;\forall\; t \in T \\
w^{t}_{down} &\leq y^{t}_{CHP} \;\forall\; t \in T
\end{aligned} \tag{4.46}$$

$$\begin{aligned}
P^{t}_{CHPe} &\geq \max\left\{P^{1,\mu}_{CHP,max}, P^{1,\eta}_{CHP,max}\right\} y^{t}_{CHP} \;\forall\; t \in T \\
P^{t}_{CHPe} &\leq \min\left\{P^{nb^{\mu}_{CHP},\mu}_{CHP,max}, P^{nb^{\eta}_{CHP},\eta}_{CHP,max}\right\} y^{t}_{CHP} \;\forall\; t \in T
\end{aligned} \tag{4.47}$$

$$P^t_{CHPe} + P^t_{CHPt} = P^t_{CHP,fuel}\bar{\eta} \ \forall \ t \in T \tag{4.48}$$
$$P^t_{CHPt} = P^t_{CHPe}\bar{\mu} \ \forall \ t \in T$$

$$C^t_{CHP} \geq P^t_{CHP,fuel} P_{KW} \Delta t_2 \ \forall \ t \in T \tag{4.49}$$

$$\begin{aligned} z^t_{CHP}, zd^t_{CHP} &\in \{0,1\} \ \forall \ t \in T \\ y^t_{CHP} &\in \{0,1\} \ \forall \ t \in T \\ w^t_{up}, w^t_{down} &\leq 1 \ \forall \ t \in T \\ w^t_{up}, w^t_{down} &\geq 0 \ \forall \ t \in T \end{aligned} \tag{4.50}$$

Constraints (4.44) control the on/off status of the CHP. Constraints (4.45) initialize the status variable and the associated electricity production. Constraints (4.46) enforce ramp-up and ramp-down limits. Constraints (4.47) place bounds on the electricity generated by the CHP. Constraints (4.48) relate to the CHP operation. Constraints (4.49) measure the CHP fuel cost. Constraints (4.50) impose the variable domains.

Our model is based on [80] and [81] where efficiency is a function of the electrical power generated. The image of that function has values that are close to each other, so we consider the average efficiency to be a parameter rather than a variable. Variables z^t_{CHP} and zd^t_{CHP} can be relaxed because of Constraints (4.47).

4.2.10 Model for A_{IEUI}: Set of inelastic appliances with uninterruptible operation

The model for inelastic appliances with uninterruptible operation is outlined in this subsection.

With $\Phi_a = |T| - (\lceil D_a/\Delta t_2 \rceil - 1)$, A_{IEUI} is modeled by

$$x^{t+h}_a \geq P^h_a y^t_a \ \forall \ a \in A^t_{IEUI}, \ \forall \ t \in T, \ \forall \ h \in \{0,1,\ldots,\lceil D_a/\Delta t_2 \rceil - 1\} : \ t + h \leq |T| \tag{4.51}$$

$$x^t_a \leq \sum_{i=\max\{1,t-(\lceil D_a/\Delta t_2 \rceil - 1)+1\}}^{t} P^{t-i}_a y^i_a \ \forall \ a \in A^t_{IEUI}, \ \forall \ t \in T \tag{4.52}$$

$$y^t_a = 0 \ \forall \ a \in A^t_{IEUI}, t \in T : t > \Phi_a \tag{4.53}$$

$$\sum_{t=1}^{\Phi_a} y^t_a + \zeta_a = 1 \ \forall \ a \in A^t_{IEUI} \tag{4.54}$$

$$\sum_{tt=1}^{\Phi_a} tty_a^{tt} \geq \sum_{t=1}^{\Phi_b} ty_b^t + \lceil D_b/\Delta t_2 \rceil (1-\zeta_b) - |T| y_{b,a}$$
$$\forall\ a \in A_{IEUI}^t,\ \forall\ b \in A_{IEUI}^t,\ \forall\ k \in A_{IEUI} : a \in A_{IEUI}^{t,k}, b \in A_{IEUI}^{t,k} \quad (4.55)$$

$$\sum_{tt=1}^{\Phi_b} tty_b^{tt} \geq \sum_{t=1}^{\Phi_a} ty_a^t + \lceil D_a/\Delta t_2 \rceil (1-\zeta_a) - |T|(1-y_{b,a})$$
$$\forall\ a \in A_{IEUI}^t,\ \forall\ b \in A_{IEUI}^t,\ \forall\ k \in A_{IEUI} : a \in A_{IEUI}^{t,k}, b \in A_{IEUI}^{t,k} \quad (4.56)$$

$$\begin{aligned} U_a^t &\geq 0\ \forall\ a \in A_{IEUI}^t,\ \forall\ t \in T \\ U_a^t &\geq S_a y_a^t - t y_a^t\ \forall\ a \in A_{IEUI}^t,\ \forall\ t \in T \\ U_a^t &\geq -DS_a y_a^t + t y_a^t\ \forall\ a \in A_{IEUI}^t,\ \forall\ t \in T \end{aligned} \quad (4.57)$$

$$\begin{aligned} \zeta_a &\geq 0\ \forall\ a \in A_{IEUI}^t \\ y_a^t &\in \{0,1\}\ \forall\ a \in A_{IEUI}^t,\ \forall\ t \in T \\ y_{b,a} &\in \{0,1\}\ \forall\ a \in A_{IEUI}^t,\ \forall\ b \in A_{IEUI}^t\ \forall\ k \in A_{IEUI} : a \in A_{IEUI}^{t,k}, b \in A_{IEUI}^{t,k} \end{aligned} \quad (4.58)$$

Constraints (4.51) and (4.52) assign the load profile of task $a \in A_{IEUI}^t$ to time $t \in T$. Constraints (4.53) eliminate solutions where the appliance cannot start its operation. Constraints (4.54) ensure that the task is done at most once, between the beginning of the horizon and the last start time permitting the completion of the task. Constraints (4.55) and (4.56) prevent overlap between tasks for the same appliance. Constraints (4.57) measure the discomfort arising from the deviation from the preferred time. Constraints (4.58) impose the variable domains.

A_{IEUI} is a set of inelastic appliances with uninterruptible operation (see [163]). In practice, the operation of these appliances is represented by a load profile. Load profiles forecast the power variation over a period of time for an appliance, frequently as an average. For example, Tsagarakis et al. [189] use aggregated load profiles, while [149] uses load profiles for specific machines. The former use a time-use survey (TUS) to construct the load profiles. However, the consumption found through TUS diaries can be distinct from the load measurements obtained by submetering [180]. The latter approach uses controlled tests to measure consumption, and the resulting profiles provide a good approximation. UK-DALE [100] is an open-access data-set giving the consumption of domestic appliances in the UK. The data are based on measurements of real electricity consumption.

Our model is task-oriented, an idea from [87] that proposes a model with parameters to

indicate how many times each appliance will be used. In our case, we consider individual load profiles for each use of each appliance. Therefore, our model includes appliances that are used intermittently according to the classification in [163].

4.2.11 Model for A_{phases}: Set of appliances with interruptible phases operation

The model for appliances with interruptible phases operation is outlined in this subsection. With $\mho_a^1 = |T| - \left(\left\lceil \sum_{p=1}^{PH_a} D_{a,p}/\Delta t_2 \right\rceil - 1\right)$, $\mho_a^2 = |T| - (\lceil D_{a,PH_a}/\Delta t_2 \rceil - 1)$, and $\mho_a^3 = (\lceil D_{a,PH_a}/\Delta t_2 \rceil)$, A_{phases} is modeled by

$$x_a^{t+h} \geq P_{a,p}^h y_{a,p}^t \; \forall \; a \in A_{Phases}^t, \; \forall \; t \in T, \; \forall \; p \in \{1, 2, \ldots, PH_a\}, \\ \forall \; h \in \{0, 1, \ldots, \lceil D_{a,p}/\Delta t_2 \rceil - 1\} : \; t + h \leq |T| \quad (4.59)$$

$$x_a^t \leq \sum_{p=1}^{PH_a} \sum_{i=\max\{1, t-(\lceil D_{a,p}/\Delta t_2 \rceil - 1)+1\}}^{t} P_{a,p}^{t-i} y_{a,p}^i \; \forall \; a \in A_{Phases}^t, \; \forall \; t \in T \quad (4.60)$$

$$y_{a,p}^t = 0 \quad \forall \; a \in A_{Phases}^t, \; \forall \; p \in \{1, 2, \ldots, PH_a\}, \; \forall \; t \in T : t > |T| - \left(\left\lceil D_{a,|PH_a|}/\Delta t_2 \right\rceil - 1\right) \quad (4.61)$$

$$\sum_{t=1}^{|T|-(\lceil D_{a,p}/\Delta t_2 \rceil - 1)} y_{a,p}^t + \Psi_{a,p} = 1 \; \forall \; a \in A_{Phases}^t, \; \forall \; p \in \{1, 2, \ldots, PH_a\} \quad (4.62)$$

$$\sum_{tt=t}^{|T|} y_{a,p}^{tt} + \sum_{tt=1}^{t-1+\lceil D_{a,p}/\Delta t_2 \rceil} y_{a,p+1}^{tt} \leq 1 \; \forall \; a \in A_{Phases}^t, \\ \forall \; p \in \{1, 2, \ldots, PH_a - 1\}, \; \forall \; t \in T \; : \; t \; < \; |T| + 1 - \lceil D_{a,p}/\Delta t_2 \rceil \quad (4.63)$$

$$\sum_{tt=1}^{\mho_a^1} tty_{a,1}^{tt} \geq \sum_{t=1}^{\mho_b^2} ty_{b,PH_b}^t + \mho_b^3(1 - \Psi_{b,1}) - |T| y_{b,a}^p \\ \forall \; a \in A_{Phases}^t, \; \forall \; b \in A_{Phases}^t, \; \forall \; k \in A_{Phases} : a \in A_{Phases}^{t,k}, b \in A_{Phases}^{t,k} \quad (4.64)$$

$$\sum_{tt=1}^{\mho_b^1} tty_{b,1}^{tt} \geq \sum_{t=1}^{\mho_a^2} ty_{a,PH_a}^t + \mho_a^3(1 - \Psi_{a,1}) - |T|(1 - y_{b,a}^p) \\ \forall \; a \in A_{Phases}^t, \; \forall \; b \in A_{Phases}^t, \; \forall \; k \in A_{Phases} : a \in A_{Phases}^{t,k}, b \in A_{Phases}^{t,k} \quad (4.65)$$

$$\begin{aligned} U_a^t \geq 0 \ \forall \ a \in A_{Phases}^t, \ \forall \ t \in T \\ U_a^t \geq S_a y_{a,1}^t - t y_{a,1}^t \ \forall \ a \in A_{Phases}^t, \ \forall \ t \in T \\ U_a^t \geq -DS_a y_{a,1}^t + t y_{a,1}^t \ \forall \ a \in A_{Phases}^t, \ \forall \ t \in T \\ U_a^t \geq F_a y_{a,PH_a}^t - t y_{a,PH_a}^t \ \forall \ a \in A_{Phases}^t, \ \forall \ t \in T \\ U_a^t \geq -DF_a y_{a,PH_a}^t + t y_{a,PH_a}^t \ \forall \ a \in A_{Phases}^t, t \in T \end{aligned} \tag{4.66}$$

$$\begin{aligned} \Psi_{a,p} \geq 0 \ \forall \ a \in A_{Phases}^t, \ \forall \ p \in \{1, 2, \ldots, PH_a\} \\ y_{a,p}^t \in \{0,1\} \ \forall \ a \in A_{Phases}^t, \ \forall \ t \in T, \ \forall \ p \in \{1, 2, \ldots, PH_a\} \\ y_{b,a}^p \in \{0,1\} \ \forall \ a \in A_{Phases}^t, \ \forall \ b \in A_{Phases}^t \ \forall \ k \in A_{Phases} : a \in A_{Phases}^{t,k}, b \in A_{Phases}^{t,k} \end{aligned} \tag{4.67}$$

Constraints (4.59) and (4.60) assign the load profile of each phase p of task $a \in A_{phases}^t$ to time $t \in T$. Constraints (4.61) eliminate solutions where the appliance cannot start its operation. Constraints (4.62) ensure that the task is done at most once, between the beginning of the horizon and the last start time permitting the completion of the task. Constraints (4.63), from [38], are precedence constraints between consecutive phases of the same task. Constraints (4.64) and (4.65) prevent overlap between tasks for the same appliance. Constraints (4.66) measure the discomfort arising from the deviation from the preferred time. Constraints (4.67) impose the variable domains.

Each load profile is separated into sequential phases, and the operation can be interrupted between phases. The appliances in A_{phases} include dishwashers [21], washing machines [161], and dryers [149].

4.2.12 Other constraints and objective function

Other constriants as well the objective function that are part of the whole optimization model are outlined in this subsection.

IBR constraints:

$$E_g^{t,i} \leq E_{th}^t \ \forall \ t \in T, \ \forall \ i \in B \tag{4.68}$$

$$\Delta t \sum_{t \in T} E_g^{t,i} \leq E\_bl^i \ \forall \ i \in B \tag{4.69}$$

$$\Delta t E_g^{t,i} \leq E\_bl^i y_g^i \ \forall \ t \in T, \ \forall \ i \in B \tag{4.70}$$

$$\sum_{i \in B} y_g^i \leq 1 \tag{4.71}$$

$$y_g^i \in \{0,1\} \ \forall \ i \in B \tag{4.72}$$

Constraint (4.68) limits the energy that can be bought. Constraints (4.69) to (4.72) are the main IBR constraints: (4.69) ensures that the daily consumption is within the capacity; (4.70) controls the activation of the blocks; (4.71) ensures that at most one block is used; and (4.72) are the binary restrictions.

Flow Conservation:

$$\sum_{a \in A} x_a^t = 10^3 (p_{EVbatt}^{ch,t} + P_{bat}^{ch,t} - P_{bat}^{dch,t} - p_{EVbatt}^{dch,t} - P_{CHPe}^t) + E_{pv}^t - E_v^t + E_{wt}^t + \sum_{i \in B} E_g^{t,i} \; \forall \; t \in T \tag{4.73}$$

The coupling constraints (4.73) ensure energy conservation.

Financial Incentives:

$$C^t = \Delta t \left[\lambda^t \left(\sum_{i \in B} (1 - \varpi^i) E_g^{t,i} \right) - \nu^t E_v^t \right] \forall \; t \in T \tag{4.74}$$

$$E_v^t \leq E_{th}^t \; \forall \; t \in T \tag{4.75}$$

Constraints (4.74) represent the cost at each time t, given by the energy acquisition cost for block i minus the energy sold plus the price of CHP. Constraint (4.75) limits the energy that can be sold. Variable E_v^t represents the case where the customer can inject electricity into the grid. In some markets, the customer receives in exchange an energy credit for future consumption. In this case, we set $E_v^t = 0$, add $E_{av}^{t-1} - E_{av}^t$ in the right hand side of (4.73) and replace Constraint (4.75) by $E_{av}^0 = 0$ to initialize the power credit variable.

Objective function:

$$\min_{\Xi} \; w_c \left(\sum_{t \in T} C^t + C_{ev} + C_{CHP}^t \right) + w_t \sum_{t \in T} \sum_{a \in A} V_a^t + w_u \left(\sum_{a \in A_{phases}^t} \sum_{p=1}^{|PH_a|} \Psi_{a,p} + \sum_{a \in A_{IEUI}^t} \zeta_a + \sum_{t \in T} \sum_{a \in A^t} U_a^t \right) \tag{4.76}$$

We minimize a weighted sum of comfort and cost (4.76), where the cost is given by (4.74) and the EV cost.

4.3 Data and Instances

In this section we discuss our data and how we create the instances.

4.3.1 Locations

Brazil will be one of the largest smart-grid markets by 2023 [65]. The country has a total installed capacity of 161 GW [12], which is expected to grow to 224 GW by 2030 [62, Table 6.26] via initiatives such as the Cities of the Future Project [32]. An analysis of the smart grid stage in Brazil appears in [54]. The climatic data was taken from [9, Chapter 14]. We calculated the temperature based on 5% dry-bulb design conditions. The wind speed data was taken from [111].

4.3.2 Prices

In Brazil, there are two pricing options: the conventional tariff and the white tariff. The conventional tariff is constant, whereas the white tariff is a TOU pricing with a single price for weekends and holidays and three weekday prices:

1. Peak hours: Three consecutive daily hours defined by the distributor.
2. Intermediate peak hours: The hour before and the hour after the peak hours.
3. Nonpeak hours: The remaining hours of the day.

We use the electricity prices published in April 2017 for the white tariff. We summed two tariffs, following [121, p. 57].

The IBR pricing defined by federal law [26] specifies certain discounts:

1. For the portion of consumption below 30 kWh/month, the discount is 65%.
2. For the portion between 31 and 100 kWh/month, the discount is 40%.
3. For the portion between 101 and 220 kWh/month, the discount is 10%.

We divided the monthly limits defined above by 30 days. This makes our model less realistic, but since smart meters track and report energy consumption in minutes, we assume that a pricing scheme over a day will be more important than one for the whole month. The law applies to a subgroup of the population, but we apply it to everyone.

Brazil has a net metering incentive. If the electricity bought from the grid is less than that injected, the customer receives an energy credit for future consumption. In addition, we assume that, as in other markets, Brazil's consumers will in the future have the opportunity to sell electricity, i.e., a *feed-in tariff*. Thus, we consider $\nu^t = \lambda^t/2$ for all $t \in T$.

4.3.3 Capacity

We set the capacity E^t_{th} to 75 kW, which is the residential capacity in Brazil.

4.3.4 PV and Solar Collector

We take the data from data-sheets or use the estimates in [56]. We consider the PVs *Canadian Solar CS5P250M*, *Yingli Solar JS150*, and *Siemens SM110* and the solar collectors *CSi Sodramar*, *TERMOMAX*, *Soletrol*, and *Sunda Seido 10*. The ground reflectance was generated from the uniform distribution U(0.13,3) according to [9, Table 5, Chapter 14].

4.3.5 Wind Turbines

The data comes from the data-sheets for the *Raum Energy 3.5 kW Wind Turbine System* and the *Raum Energy 1.3 kW Wind Turbine System*.

4.3.6 HVAC

For the house, we generated resistance values from a uniform distribution (see [172]), converting the units to (m^2 ^{o}C.h/J). The house height is 3.048 m, with $A_{ceiling} = A_{floor} = 100$ m^2. We set $P_{heating} = P_{cool} = 60\,W/m^2 \times A_{floor}$, an approximate value suggested by some manufacturers. We set A_{ul} between 0.7 and 2.8. We set IDF to 0.031 for cooling and 0.086 for heating. The other parameters are $T^t_f = 23^oC\ \forall\ t \in T$, $H^t_p = 97.57\,W\ \forall\ t \in T$.

4.3.7 Water Heaters and Shower

We use $T^{chu}_f = T^{wh}_f = 50^oC$ (see [118]). We set $P_{wh} \sim U(4000, 5000)\,W$ (see [172]). The heat resistance is given by $U(12, 25)^oFft^2h/Btu$ converted to (m^2 ^{o}C.h/J). We take the WH area and diameter from the data-sheets for Giant-142ETE, Giant-152ETE, Giant-172ETE, Rheem-PROPH50, Rheem-PROPH65, and Rheem-PROPH80. We use the diameter to calculate $(UA)_{wh}$ and V_{tank}. We set $T^{max} = 100^oC$ and $E_{wh} = 1$.

We took the temperature of the water from the street (T^t_{inlet}) from [42, Graphic 4]. We projected the missing intervals so that the last projected value is equal to the first collected value.

For fr^t_{wh} and fr^t_{chu}, we used the data available in [53]. For each client, we aggregate the daily consumption in intervals of Δt. Inter-period consumption is calculated proportionally. P_{chu} is obtained from the data-sheets for Lorenzetti's showers.

4.3.8 Batteries

We used the following values from [217]: $E_{bat} = 24\,\text{kWh}$, $SOC_{min} = 20\%$, $SOC_{max} = 100\%$, $p^{ch}_{max} = 4\,\text{kW}$, $p^{dch}_{max} = 4\,\text{kW}$, $p^{ch}_{min} = 0.3\,\text{kW}$, $p^{dch}_{min} = 0.3\,\text{kW}$, $\eta^{ch} = 0.91$, $\eta^{dch} = 0.91$, $\mu = 1$. According to [30], in a low-storage system the float charge losses represent around 100 W, so $p_{loss} = 0.1\,\text{kW}$.

4.3.9 Fridge

The fridge is described in [25] and [24]. The other parameters are $T^{start}_{freezer} = -13^o\text{C}$, $T^{start}_{refri} = 6^o\text{C}$, $P_{comp} \sim U(150, 170)\,\text{W}$ considering the permanent regime from [41], $T^{freezer}_f = -18^o\text{C}$, and $T^{refri}_f = 2^o\text{C}$.

4.3.10 Electric Vehicles

We used the Nissan Leaf's battery specifications [138]: $EV_{bat} = 24\,\text{kWh}$, $EVSOC_{max} = 90\%$, $EVSOC_{min} = 0\%$ and $EVP^{ch}_{max} = EVP^{dch}_{max} = 3.6\,\text{kW}$. The other parameters are based on the battery parameters: $EVP^{ch}_{min} = EVP^{dch}_{min} = 0.3\,\text{kW}$, $EV\mu = 1$, and $EVp_{loss} = 0.1\,\text{kW}$.

The range of the Leaf model is 160 km and its battery capacity is 24 kWh [179]. We calculated $km^{100} = EV_{bat}/Electricity\ consumption = (24\,kWh)/(150\,Whkm^{-1}) = 160\,\text{km}$, as in [179].

We simulated the battery-charging model for 7 h. At time 0, the SOC was 0. With the specified rate of 3.6 kW/h, the SOC should be 25.2 kWh after 7 h. We therefore defined $\eta^{dch}_{ev} = 24/25.2 \approx 0.95$. Moreover, we set $\eta^{dch}_{ev} = \eta^{ch}_{ev}$.

The number of trips is set to $n_{trip} \sim U(1, 4)$ and t^s_{start} and t^s_{end} are generated randomly. The first trip has a minimum duration of 8 h, the second 4 h, the third 1 h, and the fourth 0.5 h.

The other parameters are $price\_gas = 3\,\$/\text{l}$, $cons\_gas = 10\,\text{km/l}$, $EVSOC\_last\_day = 50\%$, $Km^s_{next} \sim U(0, km^{100})\,km\ \forall\ s \in \{1, ..., n_{trip}\}$, $EVSOC^{end}_{min} \sim U(EVSOC_{ret}, \text{MM})\%$, where MM = maximum value of $EVSOC_{ret}$, and finally, $EVSOC_{ret} \sim U(0, 30)\%$.

4.3.11 CHP

We take the data from [81, Table 4] and the data-sheet for CHP CP5WN-SPB. For that CHP, $rate^{fuel}_{CHP} = \frac{0.72\,gallon/h}{17.8\,kWh} = \frac{3.79\,l/gallon \times 0.72\,gallon/h}{17.8\,KWh} = 0.153\,l/kWh$.

Thus, the values are: $d^{on}_{CHP} = d^{off}_{CHP} = 60\,\text{min}$, $nb^{\mu}_{CHP} = nb^{\eta}_{CHP} = 3$, $r^{down}_{CHP} = r^{up}_{CHP} = 0.05\,\text{kW/min}$, $y^{last\_day}_{CHP} = y^{ini}_{CHP} = 0$, and $P^{ini}_{CHPe} = 0\,\text{kW}$. Fixing μ and $\eta \in \{1, 2, 3\}$ we set $P^{k,\mu}_{CHP,min}$ and $P^{k,\eta}_{CHP,min} \in \{0, 0.2, 0.5\}\,\text{kW}$, $P^{k,\mu}_{CHP,max}$ and $P^{k,\eta}_{CHP,max} \in \{0.2, 0.5, 1\}\,\text{kW}$,

$\eta^k_{CHP,p} \in \{0, 80, 85\}$, and $\mu^k_{CHP,p} \in \{0, 40, 35\}$.

We set the overall efficiency to the average of the efficiencies given by the piecewise linear function, discarding null efficiencies. Thus, $\bar{\eta} = 0.825$ and $\bar{\mu} = 0.375$.

4.3.12 A_{IEUI} and A_{phases}

We use the data from [100]. We start the analysis from the first day that has measured data at midnight. Missing data is assumed to indicate no consumption. We aggregated the power data into 10-min intervals based on the average values. We calculated probabilities for the time and duration of the use of each appliance. Using these probabilities, we chose values for S_a, the preferred starting time, and D_a, the duration of use. We obtain P^h_a from the aggregated power in the interval between t and $t + D_a$. Finally, we set $DS_a = D_a + U(0, 4)$.

For A_{phases}, we performed the steps above for each phase. Dishwashers have three phases: washing, draining, and drying [21]. Washing machines have three phases: water heating, washing, and spinning [161]. Dryers have two phases: with and without heat [149]. In [149], the duration of the dryer's second phase is between 5 and 15 min, so we consider the final 10 min of the load profile to be the second phase.

4.4 Results and Discussion

The scheduling problem is solved in this section, using various models. We selected the references from Table 4.1 with at least seven submodels. For a fair comparison, we replaced the comfort constraints in every model by a fixed start time for the appliances based on load profiles, and fixed bounds for desired temperatures for the thermal appliances. Thus, comfort is equivalent for every model and the objective function considers only the cost. The parameters not previously defined are as follows: $H = 24$, $|T| = 2$, and $w_c = w_u = w_t = 1$. Each instance has the same set of features for each model compared: same parameters for prices, same set of appliances, etc.

4.4.1 Models from Shirazi and Jadid [173]

In this subsection, we compare results using our models and models from [173]. We consider the appliance models in [173, 174] with the following adjustments:

1. We assume that $S^{ESS}_t = S^{ess}_t$.

2. The available data corresponds to time windows and power for the four appliances

in [173, Table 1] and electricity prices in [173, Figure 3]. Since the devices based on load profiles have a fixed usage initialization, we use the data from Section 4.3 instead of that from [173].

3. For the freezer and fridge, the computation of β^{fr}, α^{fr} and γ^{fr} is not specified. We assume that β^{fr} is related to the action of opening and closing the fridge doors, α^{fr} is related to the evaporator temperature, and γ^{fr} is related to the losses.

4. For HVAC, α^{ac} and α^{ht} are undefined. We assume that $EP_t = EP_t^{\Theta} : \Theta \in \{\text{ac, ht}\}$. The parameters β^{ac}, β^{ht}, ρ^{ac}, and ρ^{ht} are computed as in our model, considering infiltration and losses based on the structure of the house.

5. For lighting, there is no constraint that associates illumination level with consumption. Therefore, we do not consider this.

We start our experiments with an "initial" combination composed of A_{IEUI}, fridges, WTs, PVs, IBR constraints, and selling options. We progressively add more appliances. For example, in Table 4.3, Ins. 2 includes the appliances considered in Ins. 1 plus an ESS.

Table 4.3 Costs for model from [173] and our model.

Ins.	Combination	[173] cost ($)	Our cost ($)
1	"initial"	4.02	4.02
2	Ins. 1 + ESS	1.61	1.49
3	Ins. 2 + HVAC	1.93	6.83
4	Ins. 3 + CHP, WH	1.93	6.83
5	Ins. 4 + A_{phases}, Shower	-	9.06
6	Ins. 5 + EV	-	30.03
7	Ins. 4 + Boiler, TSS	1.93	-

In Ins. 1, we assign consumption profiles over the horizon and respect the bounds on the freezer and fridge temperatures. Both models give the same cost.

In Ins. 2, we add a battery, a type of ESS. The efficiencies for the discharging and charging operations are set to 100%. The model of [173] allows the battery to be off during the entire horizon, but with charging and discharging. Their cost is 8% higher than ours. There are two reasons for this. First, our model considers the SOC at the beginning of an interval, whereas [173] considers it at the end. Thus, in the final interval our model records a discharge while the model from [173] does not. Second, we have lower bounds on the charge and discharge variables. If we remove these two differences, we find the same solution.

In Ins. 3, for the model of [173], HVAC adds 32 cents to the bill while our model adds around 440 cents. Like the ESS, the HVAC is off throughout the horizon, but it contributes to the indoor temperature. As we will see in Ins. 9, the main issue in this experiment is the solar gain.

In Ins. 4, both models adjust the use of fridge and batteries, achieving the same cost as in Ins. 3.

In Ins. 5, 6, and 7, we add appliances that are considered either by our model or by [173], obtaining results for just one of the models.

In Ins. 3, the HVAC and the battery cannot emit or absorb energy if they are not turned on. For example, a battery could have the constraint set $AC_b = \{\text{BatPower}_t \leq \text{BatCapacity} \times y_t^{\text{on,off}} \forall\, t \in T\}$, where $y_t^{\text{on,off}}$ is binary, and similar steps give the constraint set AC_h for HVAC. Table 4.4 shows the results when we add the sets AC_b and AC_h.

Table 4.4 Costs for model from [173] and our model, with additional constraints from [173].

Ins.	Combination	[173] cost ($)	Our cost ($)
1	“initial"	4.02	4.02
8	Ins. 1 + ESS, AC_b	2.13	1.49
9	Ins. 8 + HVAC	2.13	6.83
10	Ins. 9 + AC_h	infeasible	6.83
11	Ins. 8 + solar gain	infeasible	6.83
12	Ins. 10 + disjoint set	2.28	6.83
13	Ins. 12 + solar gain	7.34	6.83

For Ins. 8, we note that the model from [173] has a cost around 43% higher than ours. The cost for [173], compared with Ins. 2, is increased because of the battery losses. For Ins. 9, HVAC works without consumption because the activation constraints are not considered. When we add these constraints in Ins. 10, [173] becomes infeasible. Moreover, in Ins. 9, our model consumes energy trying to keep the indoor temperature within the bounds. This does not happen in [173], as shown in Figure 4.5. The model from [173] does not consider solar gain. This has a considerable effect on the indoor temperature [13], so our model consumes more energy and is more expensive.

When we add solar gain in Ins. 11, [173] becomes infeasible. Ins. 12 assumes that the time windows (TWs) for the A/C and heating form a disjoint set. The model from [173] now gives a feasible solution. However, there is still no consideration of solar gain, and finding the optimal disjoint set of TWs is difficult since there are $2^{|T|}$ possible combinations. If we remove the solar gain from the analysis, our model decreases the cost by around 280%. Ins. 13

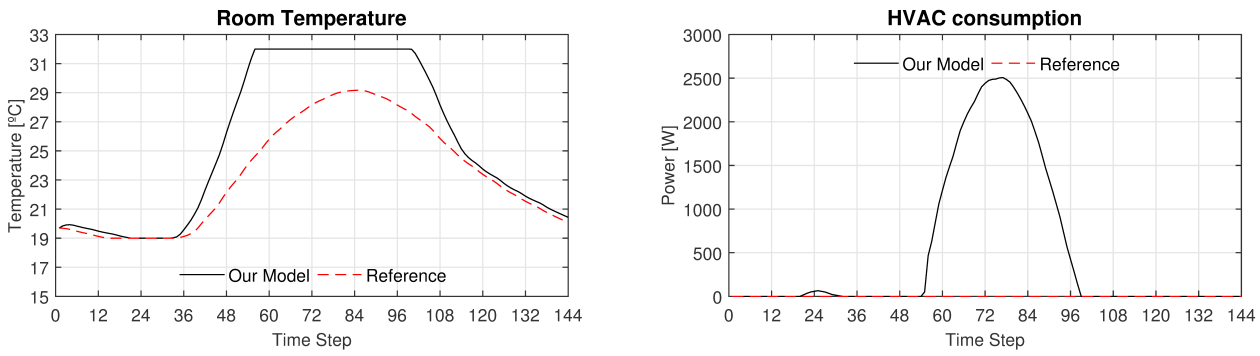

Figure 4.5 Results for temperature of Ins. 9.

adds solar gain to Ins. 12 with only A/C for the disjoint set of TWs for the HVAC to avoid infeasibility. The model from [173] becomes, monetarily, more expensive than ours.

The thermal energy storage model in [173] follows the ESS model, so a similar analysis can be performed. The CHP in [173] comes from [104], and we present this analysis in Section 4.4.3. Although the model from [173] gives a cost that is lower by about R$1715 (544USD), our model is more realistic.

4.4.2 Models from Anvari-Moghaddam et al [13, 14]

In this subsection, we compare results using our models and models from [13,14]. The models from [13,14] consider equivalent batteries, WH, and underfloor HVAC models. Moreover, they have the same energy flow conservation constraints.

We discussed the limitations of the battery models in Section 4.2.6. The WH model from [13, 14] is

$T_{st}(t+1) = T_{st}(t) + \frac{V_D^{th}(t)}{(V_{tot})}(T_{cw} - T_{st}(t)) + \frac{P_{aux}^{th}(t)+P_{CHP}^{th}(t)}{V_{tot}C_w} - \frac{A_{st}}{R_{st}}(T_{st}(t) - T_b(t)) \; \forall \; t \in T\backslash\{|T|\}$, where V_{tot} is the total WH volume; $V_D^{th}(t)$ is the hourly hot water demand at time t; $T_{cw}(t)$, $T_b(t)$, and $T_{st}(t)$ are the entering cold water, environment around the WH, and hot water temperatures at time t, respectively; A_{st} is the surface area of the WH; and R_{st} is the thermal resistance of the WH insulation material. Using our parameter Δt_2, we have:

$T_{st}(t+1) = \frac{V_D^{th}(t)}{(V_{tot})}(T_{cw} - T_{st}(t)) + \Delta t_2 \frac{P_{aux}^{th}(t)+P_{CHP}^{th}(t)}{V_{tot}C_w} - \frac{\Delta t_2}{V_{tot}C_w}\frac{A_{st}}{R_{st}}(T_{st}(t) - T_b(t)) + T_{st}(t) \; \forall \; t \in T\backslash\{|T|\}$. Note that multiplying demand by the time interval results in V_D^{th}. Also, we use an electrical resistance as the auxiliary power while [13, 14] use a boiler fed by gas. Since gas and electricity have different prices, for a fair comparison, we assume that the three WH models ([14], [13], and ours) use electricity as auxiliary power. Note that the three models link the HVAC and CHP systems.

Our HVAC is directly in contact with the air that heats the principal floor, while the HVACs from [13, 14] are on the basement floor. Otherwise, the models are equivalent. For a fair comparison, we assume that all the models have the HVAC on the main floor.

The CHP model in [14] differs from that in [13] by a binary on/off variable and one constraint. We test both versions. The *schedulable tasks and residential load* model has more constraints in [14] than in [13], but as we set the starting time for the appliances based on the load profiles, the models are feasible.

Finally, since [13] considers WTs and PVs, we add these to [14]. The conservation constraints for both come from [13, Equation 37] with $\delta = 1$.

We start our experiments with an "initial" combination composed of the A_{IEUI} and A_{phases} appliances, WTs, PVs, IBR constraints, and selling options. We progressively add more appliances; see Table 4.5.

Table 4.5 Costs for models from [13, 14] and our model.

Ins.	Combination	[14] cost ($)	[13] cost ($)	Our cost ($)
1	"initial"	3.9506	3.9506	3.9506
2	Ins. 1 + ESS	-5.2055	-5.2055	1.3134
3	Ins. 2 + SOC_{min}	1.3102	1.3102	1.3134
4	Ins. 3 + D_A	1.2716	1.2716	2.0013
5	Ins. 1 + HVAC	8.7767	8.7767	8.7767
6	Ins. 3 + HVAC	6.6601	6.6601	6.6629
7	Ins. 6 + D_A	6.5999	6.5999	7.3859
8	Ins. 5 + WH, $\text{CHP}_{\text{ini}}^{\text{off}}$	16.6304	infeasible	9.7961
9	Ins. 5 + WH, $\text{CHP}_{\text{ini}}^{\text{on}}$	infeasible	infeasible	10.5269
10	Ins. 9 + D_A	infeasible	infeasible	-4.4723
11	Ins. 8 + D_A	16.6304	infeasible	-2.4028

In Ins. 1, we assign consumption profiles over the horizon. All the models give the same cost.

In Ins. 2, we add a battery. The efficiencies for the charging and discharging operations are, again, set to 100%. For [13, 14] we do not place an upper bound on the initial SOC. Their SOC starts at the maximal value allowed, which gives a result 296% cheaper than our model.

Suppose SOC_{min} is the bound on the initial SOC. We add SOC_{min} to the models from [13,14] in Ins. 3. Then, their results are 0.24% cheaper than our result because they do not specify a minimal power for the charging and discharging variables. If we also add these constraints, we obtain the same cost as for our model.

In Ins. 4, we change the efficiencies to the values in [14]. D_A refers to the data from [14]. Their

cost is 36.5% lower than our cost. The most important part of this difference is explained by the energy construction in the battery constraints linked with the energy conservation flow in [13, 14] (see Section 4.2.6).

In Ins. 5 and 6, we test HVAC and HVAC with ESS, respectively. The efficiencies in the battery model are 100%. The results are identical for Ins. 5, and they are slightly different for Ins. 6 for the same reason as in Ins. 3. However, for Ins. 7, with D_A, the [13, 14] results are 10.6% cheaper than ours because of the energy creation.

In Ins. 8, we test the CHP with the WH and HVAC. The CHP is off in the first interval, indicated by $\text{CHP}_{\text{ini}}^{\text{off}}$ in Table 4.5. In the [14] results, CHP and the boiler were not used. The only way to increase the water temperature is by increasing the room temperature, but this solution is 69.8% more expensive than our solution. In [13] the ramp-up constraints do not allow the start-up of the CHP. Moreover, the off status is not allowed. Therefore, the [13] model is infeasible.

In Ins. 9, we changed the CHP status at the first interval. It is on with a maximal production of electrical power, indicated by $\text{CHP}_{\text{ini}}^{\text{on}}$ in Table 4.5. Constraint 17 from the [14] model makes the problem infeasible, and the upper bound on P_{CHPt}^{t} in the [13] model makes the problem infeasible.

Ins. 10 and 11 are identical to Ins. 8 and 9, but with D_A. The analysis for Ins. 8 and 9 applies. For Ins. 11, our model sells electricity while the [14] model buys it. Our solution is around 114% (R$19.03) less expensive than the [14] solution. This represents an annual cost of ≈ R$6947 (2205 USD).

4.4.3 Models from Kriett and Salani [104]

In this subsection, we compare results using our models and models from [104]. There are two models from [104] that we did not consider in the analysis: the fridge model (29–31 in [104]) and the HVAC model (32–33 in [104]). These models have a scheduled consumption solution as input. For each interval, the models postpone or advance the time when the appliance will be turned on in that input solution. Thus, [104] assumes that the cooling goods (food), for the fridge, and the living space (air), for the HVAC, have enough thermal inertia to act as a buffer. We do not know how to determine the initial buffers, needed as parameters. We assume we have a scheduled solution for the fridge and a null initial buffer for the cooling goods. We consider only a fridge, and we optimize the electricity cost using the models from [104] and our model. The solution found by [104], shown in Figure 4.6, is not feasible because the temperatures become too high.

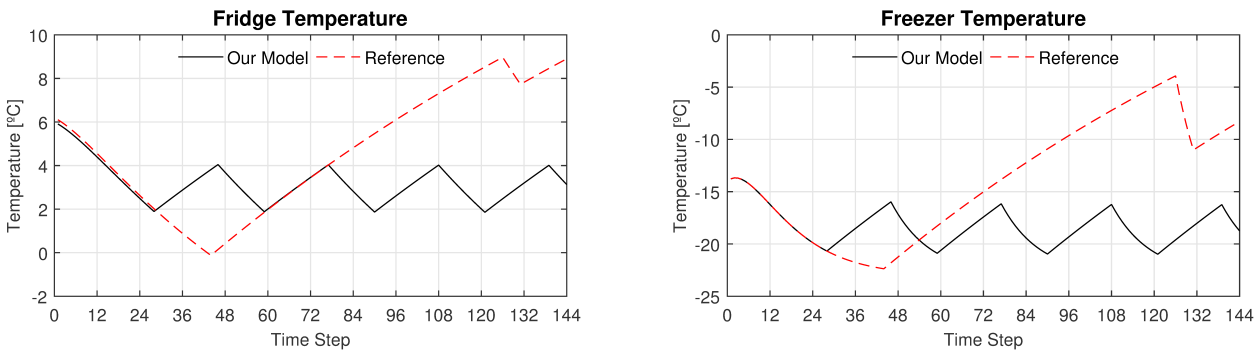

Figure 4.6 Results for temperature of reference fridge model from [104] and our model.

We started our experiments with an "initial" combination composed of the A_{IEUI} and PV appliances, IBR constraints, and selling options. WTs are considered in all the instances except 1, 2, 3, and 6. We progressively add more appliances; see Table 4.6.

In Ins. 1, we assign consumption profiles in the horizon and consider the production from the PV. Both models give the same cost.

In Ins. 2, we add the ESS. In contrast to [173], the ESS model in [104] is designed specifically for a flywheel. The [104] solution continuously charges and discharges simultaneously to maintain feasibility. It is 1.12 times more expensive than our solution.

Given the continuous charging and discharging operation of Ins. 2, in Ins. 3 we assume that the ESS power variables in [104] should be allowed to be zero, allowing the model to either charge or discharge. We change Constraints 10 from [104] to: $y_t p^{ess,r}_{min} \leq p^{ees,r}_t \leq y_t p^{ess,r}_{max} \; \forall \; r \in \{eex, eim\}, t \in T$, where $y_t \in \{0,1\}$ is an on/off variable at time t. This is represented by ESS* in Table 4.6. In [104], the battery does not always charge and discharge at the same time. This explains the cost decrease compared to Ins. 2.

Ins. 4 uses the appliances from Ins. 1 plus CHP. The CHP is off in the first interval. The costs for the two models are almost the same. In our model CHP is used between intervals 99 and 123, and in the [104] model CHP is not used. This will be discussed in our analysis of Ins. 11.

In Ins. 5, we add the production from WT. There is no WT in [104], but it decreased the cost by a factor of 4 compared with the cost for Ins. 1. We therefore considered WT for the next experiments.

In Ins. 6, we add ESS to Ins. 5. The [104] solution continuously charges and discharges at the same time to maintain feasibility: it is 5.6 times more expensive than our solution.

Table 4.6 Costs for model from [104] and our model.

Ins.	Combination	[104] cost ($)	our cost ($)
1	“initial"	12.6557	12.6557
2	Ins. 1 + ESS	11.6846	10.4669
3	Ins. 2 + ESS*	11.6463	10.4669
4	Ins. 1 + CHP	12.6557	12.3806
5	Ins. 1 + WT	3.5393	3.5393
6	Ins. 5 + ESS	4.5219	0.8055
7	Ins. 6 + ESS*	4.5219	0.8055
8	Ins. 6 + EV	infeasible	21.8308
9	Ins. 8 + CHP	infeasible	21.8308
10	Every appliance	infeasible	30.0261
11	Ins. 5 + CHP	3.5393	3.521
12	Ins. 11 + off grid, WS	infeasible	20.7146
13	Ins. 5 + EV	infeasible	23.3725
14	Ins. 5 + EV	infeasible	3.9683
15	Ins. 5 + EV*	11.0408	3.9683
16	Ins. 15 + ESS	10.6995	2.7601
17	Ins. 16 + CHP	10.6995	2.7601

The difference between the [104] solution and our solution is larger in Ins. 6 than in Ins. 2. Moreover, we can compare the cost reduction after the addition of WT, using the results from Ins. 2 and 6. We reduced the cost by a factor of 13 while the [104] model reduced it by 2.6. This is because when there is energy coming from WT, the battery has to be used more to sell energy at high prices. If the battery model has limitations, increased use of the battery will have an impact on the cost. If batteries are not considered, the differences are reduced, as shown by the solutions for Ins. 4 and 11.

We use ESS* for Ins. 7, as in Ins. 3. Compared to Ins. 6, the results do not change because $y_t = 1 \ \forall \ t \in T$. In Ins. 8, 9, and 10, the addition of EVs makes the models from [104] infeasible. We will explain this below.

Ins. 11 has the same appliances as Ins. 5 plus CHP. The CHP is off in the first interval. Our model and the [104] model give similar costs. In our model CHP is used between intervals 113 and 118; in the [104] model it is not used. This is because the ramp-up and ramp-down constraints in [104] do not allow the CHP to change state. This can be problematic when there is more demand or in off-grid systems.

In Ins. 12, we force the use of CHP via an off-grid system. If a surplus of energy occurs, it is lost, i.e., we waste the surplus (WS). Since fuel is more expensive than electricity in our

data, the cost of meeting the demand is higher, and it cannot be met by the [104] model because of the ramp-up and ramp-down constraints.

In Ins. 13, we consider the appliances from Ins. 5 plus EV. The infeasibility in the [104] model is because that model cannot consider the case where the vehicle departs at time k_0, returns at time k_1, and departs again at time k_2 ($k_2 > k_1 > k_0$). This implies noncyclic behavior since there is an odd number of departure-arrival events. The bounds $E_t^{evh,ub}$ and $E_t^{evh,lb}$ in the [104] model cannot handle this case.

In Ins. 14, we change the EV parameters to allow only one departure, where the vehicle is plugged in at interval 7 and the departure is at interval 110. Here, the scenario is appropriate for the [104] model, but there is no zero energy assignment when the EV is traveling because of Constraint 22 from [104]. In Ins. 15, we changed this constraint to: $e_t^{evh} = e_{t-1}^{evh} + (p_t^{evh,eex}\eta^{evh,eex} - \frac{p_t^{evh,eim}}{\eta^{evh,eim}})\Delta t_2 + k_t^{evh}(E_t^{evh,ub} - e_{t-1}^{evh})\ \forall\ t \in T$. This change is indicated by EV* in Table 4.6. It corrects the problem of Ins. 14, but the inequalities 21 from [104] do not allow the power variables to be zero. This increases the cost, and our cost is around 278% cheaper.

Ins. 16 adds ESS to Ins. 15; Ins. 17 adds CHP to Ins. 16. For both models, ESS reduces the final cost, but CHP does not (it is not used). Our cost is 389% (R$7.93) cheaper. This represents an annual cost of $\approx$ R$2894 (918 USD).

4.4.4 Application: Day-to-day scheduling

We now present an application of our model to a house in Belo Horizonte, Brazil, during the summer. We used a computer equipped with an 1.9 Ghz Intel Core i5-4300U CPU. Figures 4.7 and 4.8 show the forecast data, the electricity price, and the behavior of the appliances in the optimal solution.

In the Water Temperature and Water Temperature in Shower plots, a Temp. wish value of zero means that the user does not care about the temperature. The plots show that the temperature needs are almost met. For instance, the water temperature is acceptable for the shower and for general use after step 36. The temperature before step 12 is unacceptable because the WH power and the thermal energy provided by CHP cannot sufficiently increase the initial temperature in the interval before the first and second uses. This is confirmed by the plot *Fraction of time with power on*, which shows that WH is on from the start until near step 12. The CHP operates at a maximal speed until step 12. The air temperature deviates from the target around 12 a.m. because the A/C power is insufficient. Note that in *Fraction of time with power on* the A/C is on whenever the temperature is above the target. The

fridge and freezer quickly adjust their internal temperatures.

Discharge mode is preferred for the batteries when the price is high. The customer does not buy energy between steps 96 and 125 because it is too expensive. Moreover, CHP is preferred around those times. The EV makes its planned trips and is used for storage when electricity is expensive, e.g., in the steps around 100. The appliances with load profiles are used during the permitted time windows.

There are 105,391 constraints and 14,886 variables. Around 30% of the variables are integers. CPLEX solved the problem in 36.64 s.

4.5 Conclusion

The number of smart homes is expanding worldwide. In parallel, research into HEMS is exploring how to use energy in an optimal way. One approach is to use realistic models of smart-home appliances. However, more realistic models are more difficult to solve. This work proposes a HEMS model that achieves a compromise: it is realistic but can be solved in a reasonable time. First, we proposed new fridge, shower, and EV appliance models. Then, we developed a mixed integer linear optimization model that minimizes the cost while maintaining a high level of user comfort. To illustrate the effectiveness of our model, we used real data and demonstrated that the inclusion of more details and constraints impacts the user cost. For the instances considered, our model gave results that are between 8% and 389% cheaper than those from comparable models, over a horizon of 24 hours, which corresponds to annual savings ranging from 544USD to 2205USD.

Acknowledgments

This work is supported by a full scholarship from CNPq-Brazil.

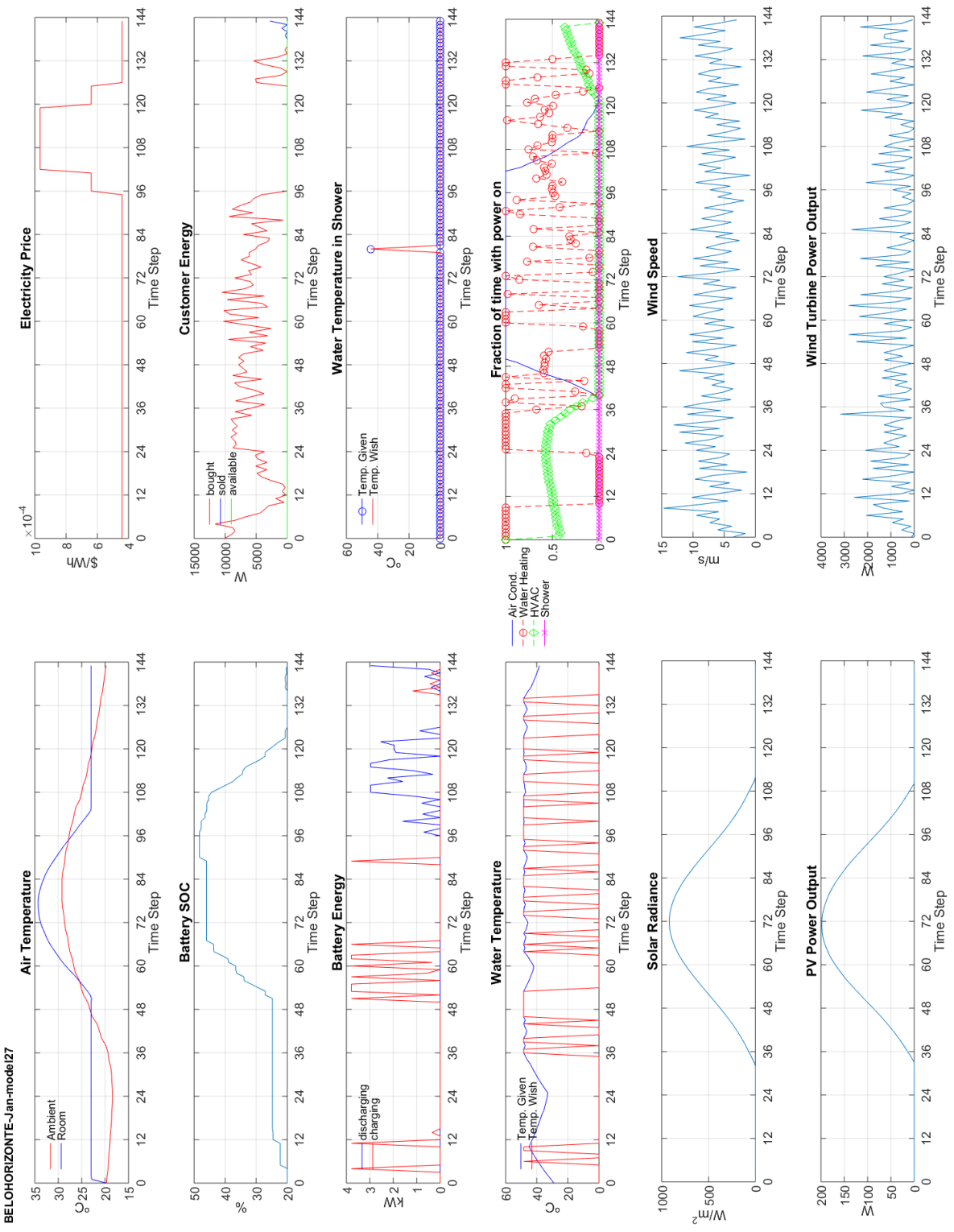

Figure 4.7 Results for Belo Horizonte in January.

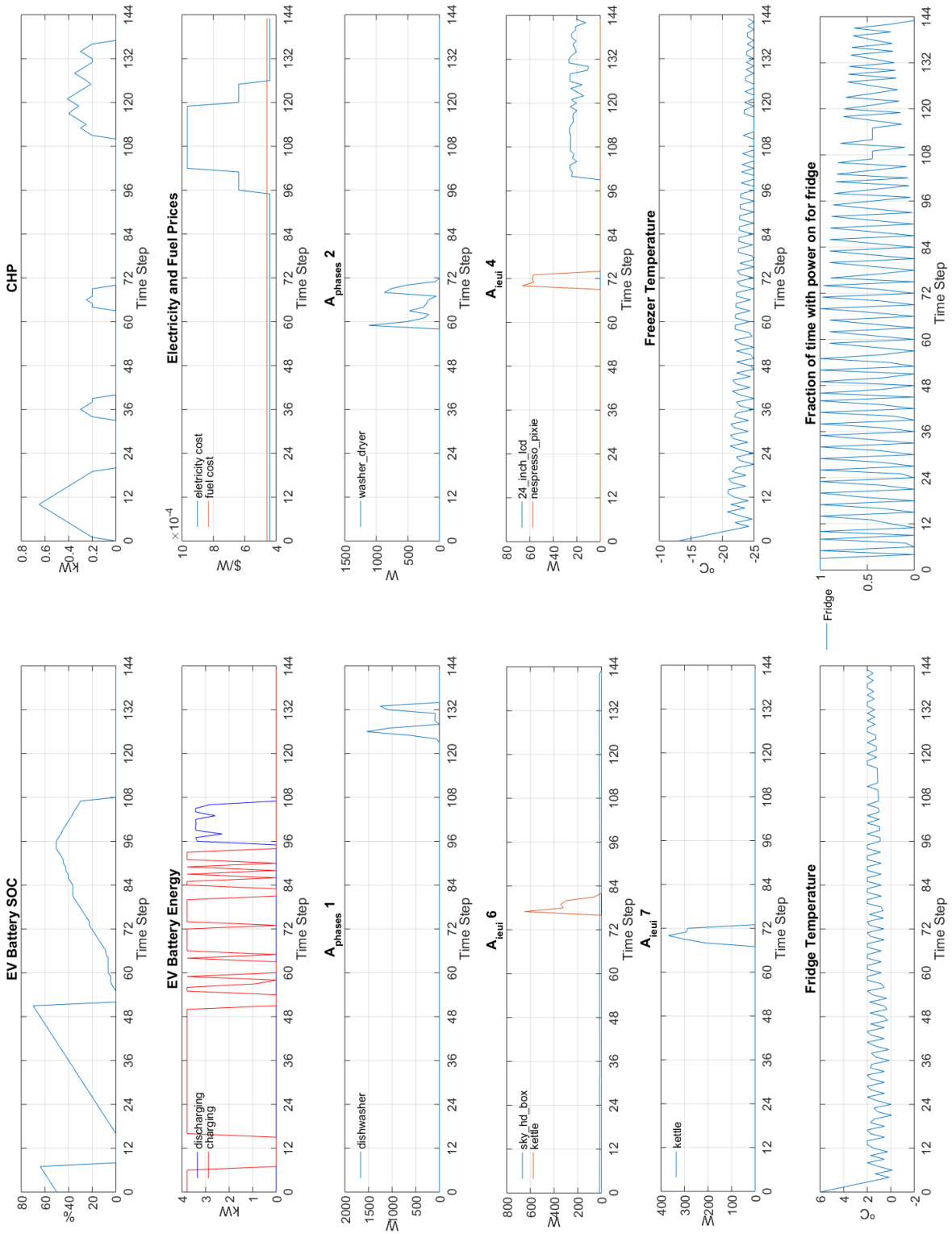

Figure 4.8 Results for Belo Horizonte in January.

Nomenclature Sets

A - Set of electric appliances.
$A_{IEUI} \subseteq A$ - Set of appliances with uninterruptible operation.
A^t_{IEUI} - Set of tasks from appliances $\in A_{IEUI}$.
$A^{t,a}_{IEUI} \subseteq A^t_{IEUI}$ - Set of tasks from A^t_{IEUI} of the same appliance $a \in A_{IEUI}$.
$A_{Phases} \subseteq A$ - Set of appliances with interruptible phases.
A^t_{Phases} - Set of tasks from appliances $a \in A_{Phases}$.
$A^{t,a}_{Phases} \subseteq A^t_{Phases}$ - Set of tasks from A^t_{Phases} of the same appliance $a \in A_{Phases}$.
$A^t \in \{A^t_{Phases} \cup A^t_{IEUI}\}$ - Set of appliance tasks.
B - Set of blocks in IBR.
D_{air} - Set of durations for hot or cold air needs.
D_{chu} - Set of durations for shower needs.
D_{wh} - Set of durations for hot water needs.
T - Set of time sub-intervals for scheduling horizon.
Ξ - Set of all variables.

Nomenclature Constants

Timing
H - Number of hours in scheduling horizon (hours).
$\Delta t_2 = H/|T|$ - Duration of each time sub-interval (hours).
$\Delta t = 60\Delta t_2$ - Duration of each time slot (minutes).
Let t be an index to represent a sub-interval of time. If we divide a horizon of $H = 24$ hours into two sub-intervals, then $\Delta t = 12$, $|T| = 2$, $t \in T = \{1, 2\}$, where $t = 1$ represents the time from 00:00h to 11:59h and $t = 2$ represents the remaining time.

Policy
E_bl^i - Energy consumption limit of block $i \in B$ (Wh).
E^t_{th} - Grid power capacity at sub-interval $t \in T$ (W).
ϖ^i - Discount to stay in block $i \in B$ (%).
λ^t - Energy consumption price at $t \in T$ (\$/Wh).
ν^t - Energy selling price at $t \in T$ (\$/Wh).

Weights
w_c - Weight factor for cost (1/\$).
w_t - Weight factor for temperature discomfort ($1/^o$C).
w_u - Weight factor for starting time discomfort (1/h).

PV
E^t_{pv} - Power from photovoltaic panels at $t \in T$ (W).

WT
E^t_{wt} - Power from wind turbines at $t \in T$ (W).

HVAC

A_{body} - Person's body area inside home (m^2).
$A_{ceiling}$ - Area of ceiling (m^2).
A_{wall} - Area of wall (m^2).
A_{window} - Area of window (m^2).
C_{air} - Heat capacity (J/kg^{o}C).
H^t_{sun} - Solar radiation heat power at sub-interval t (W/m^2).
n_{ac} - Number of air changes (1/h).
$P^t_{activity}$ - Human activity metabolic rates at $t \in T$ (W/m^2).
P_{cool} - Rated power for air-conditioner (W).
$P_{heating}$ - Rated power for heater (W).
$R_{ceiling}$ - Heat resistance of ceiling (m^2 ^{o}C.h/J).
R_{wall} - Heat resistance of wall (m^2 ^{o}C.h/J).
R_{window} - Heat resistance of window (m^2 ^{o}C.h/J).
$SHGC$ - Solar Heat Gain Coefficient average.
T^t_f - Desired inside air temperature at $t \in T$ (^{o}C).
T^t_o - Ambient temperature at sub-interval $t \in T$ (^{o}C).
V_{house} - Volume of house (m^3).
ρ_{air} - Air density (kg/m^3).

Water Heater

$C_p = 4190 J/kg^oC$ (Thermal capacity).
E_{wh} - Binary constant, set to 1 if WH present.
fr^t_{wh} - Hot water flow rate for WH at $t \in T$ (l/m).
P_{wh} - Rated power for WH (W).
T^{wh}_f - Preferred temperature for hot water (^{o}C).
T^t_{in} - Water temperature from solar collector at $t \in T$ (^{o}C).
T^{max} - Maximal temperature for water (^{o}C).
$(UA)_{wh}$ - Loss coefficient area product for WH ($W/^oC$).
V_{tank} - Volume of water heater (WH) (dcm^3).

Shower

$C_e = 4190 J/kg^oC$ (Water specific heat).
fr^t_{chu} - Hot water flow rate for shower at $t \in T$ (l/min).
P_{chu} - Rated power for shower resistance (W).
T^{chu}_f - Preferred water temperature for shower (^{o}C).
T^t_{inlet} - Street water temperature at $t \in T$ (^{o}C).

Fridge

P_{comp} - Rated power for fridge's compressor (W).
$T^{start}_{freezer}$ - Initial freezer temperature (^{o}C).
T^{start}_{refri} - Initial fridge temperature (^{o}C).
$T^{freezer}_f$ - Desired freezer temperature (^{o}C).
T^{refri}_f - Desired fridge temperature (^{o}C).

Battery

E_{bat} - Battery capacity (kWh).
P^{ch}_{max} - Maximum charging power for battery (kW).
P^{ch}_{min} - Minimum charging power for battery (kW).
P^{dch}_{max} - Maximum discharging power for battery (kW).
P^{dch}_{min} - Minimum discharging power for battery (kW).
p_{loss} - Power float loss of battery (kW).
SOC_{max} - Maximum battery SOC without float loss (%).
SOC_{min} - Minimum battery SOC (%).
η^{ch} - Charging efficiency of inverter battery.
η^{dch} - Discharging efficiency of inverter battery.
μ - Charging/discharging efficiency of batter.

Load Profiles

D_a - Duration of task $a \in A^t_{IEUI}$ (h).
$D_{a,p}$ - Duration of phase p of task $a \in A^t_{Phases}$ (h).
DF_a - Latest finishing time for task $a \in A^t$ (h).
DS_a - Latest starting time for task $a \in A^t$ (h).
F_a - Preferred finishing time for task $a \in A^t$ (h).
P^h_a - Fixed power of task $a \in A^t_{IEUI}$ at interval h of load profile (W).
$P^h_{a,p}$ - Fixed power for phase p of task $a \in A^t_{Phases}$ at interval h of load profile (W).
PH_a - Number of phases of task $a \in A^t_{Phases}$.
S_a - Preferred starting time for task $a \in A^t$ (h).

Eletric Vehicle

$cons\_gas$ - Distance covered with one liter of fuel (km/l).
EV_{bat} - EV battery capacity (kWh).
EVP^{ch}_{max} - Maximum charging power of EV battery (kW).
EVP^{ch}_{min} - Minimum charging power of EV battery (kW).
EVP^{dch}_{max} - Maximum discharging power of EV battery (kW).
EVP^{dch}_{min} - Minimum discharging power of EV battery (kW).
EVp_{loss} - Power float loss of EV battery (kW).
$EVSOC\_last\_day$ - EV battery SOC at $t = 0$ (%).
$EVSOC_{max}$ - Maximum EV battery SOC (%).
$EVSOC_{min}$ - Minimum EV battery SOC (%).
$EVSOC^{end}_{min}$ - Minimal SOC when EV departs (%).
$EVSOC_{ret}$ - Forecast SOC when EV arrives (%).
$EV\eta^{ch}$ - Charging efficiency of inverter EV battery.
$EV\eta^{dch}$ - Discharging efficiency of inverter EV battery.
$EV\mu$ - Charging/discharging efficiency of EV battery.
km^{100} - Car autonomy with SOC at 100% (km).
Km^s_{next} - Distance forecast for next trip s (km).
n_{trip} - Number of complete trips in day.
$P_{gas} = \frac{price\_gas}{consu\_gas}$ - Fuel price per km traveled ($/km).
$price\_gas$ - Fuel price per liter ($/l)
t^s_{end} - Step time at which EV departs for trip s; it leaves at beginning of period.
t^s_{start} - Step time at which EV returns for trip s; it arrives at end of period.

CHP

d^{off}_{CHP} - CHP minimal time off once turned off (min).
d^{on}_{CHP} - CHP minimal time on once turned on (min).
nb^{η}_{CHP} - Number of pieces in overall piecewise efficiency function.
nb^{μ}_{CHP} - Number of pieces in piecewise efficiency function for electrical generation.
P^{ini}_{CHPe} - Initial value for variable P_{CHPe} (kW).
$P_{KW} = rate^{fuel}_{CHP} \times price\_gas$ - CHP price per kW ($/kWh).
$P^{k,\eta}_{CHP,max} \; \forall \; k = \{1..nb^{\eta}_{CHP}\}$ - Maximal power at breakpoint k in overall CHP piecewise efficiency function (kW).
$P^{k,\eta}_{CHP,min} \; \forall \; k = \{1..nb^{\eta}_{CHP}\}$ - Minimal power at breakpoint k in overall CHP piecewise efficiency function (kW).
$P^{k,\mu}_{CHP,max} \; \forall \; k = \{1..nb^{\mu}_{CHP}\}$ - Maximal power at breakpoint k in CHP piecewise efficiency function for electrical generation (kW).
$P^{k,\mu}_{CHP,min} \; \forall \; k = \{1..nb^{\mu}_{CHP}\}$ - Minimal power at breakpoint k in CHP piecewise efficiency function for electrical generation (kW).
$price^{on}_{CHP}$ - CHP start-up cost ($).
$rate^{fuel}_{CHP}$ - Fuel price per kWh for CHP (l/kWh).
r^{down}_{CHP} - Maximum ramp down for CHP (kW/min).
r^{up}_{CHP} - Maximum ramp up for CHP (kW/min).
y^{ini}_{CHP} - Initial value for variable y_{CHP}.
$y^{last\_day}_{CHP}$ - Binary, set to 1 if CHP is on at $t = 0$.
$\bar{\eta}$ - Overall efficiency average.
$\eta^{k}_{CHP,p} \; \forall \; k = \{1..nb^{\eta}_{CHP}\}$ - Image at breakpoint k in overall CHP piecewise efficiency function (%).
$\bar{\mu}$ - Electrical generation efficiency average.
$\mu^{k}_{CHP,p} \; \forall \; k = \{1..nb^{\mu}_{CHP}\}$ - Image at breakpoint k in CHP piecewise efficiency function for electrical generation (%).

Nomenclature Variables

Discomfort

U^{t}_{a} - Time discomfort due to deviation from target for appliance a at $t \in T$ (h).
V^{t}_{a} - Temperature discomfort due to deviation from target temperature of appliance a at $t \in T$ (^{o}C).
ζ_a - Discomfort for not doing task $a \in A^{t}_{IEUI}$ (h).
$\Psi_{a,p}$ - Discomfort for not doing phase p of task $a \in A^{t}_{Phases}$ (h).

HVAC

T^{t}_{room} - Room temperature at sub-interval $t \in T$ (^{o}C).
y^{t}_{air} - On/off binary for air-conditioner operation at $t \in T$.
y^{t}_{HVAC} - On/off binary for heating operation at $t \in T$.
z^{t}_{air} - Fraction of Δ_t in $t \in T$ during which air-conditioner is on.
z^{t}_{HVAC} - Fraction of Δ_t in $t \in T$ during which heating is on.

WH

$T^{t}_{out,wh}$ - Water heater output temperature at $t \in T$ (^{o}C).
y^{t}_{wh} - On/off binary for water heater operation at $t \in T$.

Shower

$T^t_{chu\_hand}$ - Shower water temperature manually adjusted at sub-interval t (^{o}C).
$T^t_{out,chu}$ - Shower output water temperature at $t \in T$ (^{o}C).
$y^t_{chu,hot}$ - On/off binary for shower operation at $t \in T$.

Battery

$P^{ch,t}_{bat}$ - Charging power of battery (kW).
$P^{dch,t}_{bat}$ - Discharging power of battery (kW).
SOC^t - Battery's state of charge at sub-interval t (%).
$y^{ch,t}_{bat}$ - On/off binary for battery charging at $t \in T$.
$y^{dch,t}_{bat}$ - On/off binary for battery discharging at $t \in T$.
y^t_{float} - Binary to activate battery float losses at $t \in T$.

Fridge

$T^t_{freezer}$ - Freezer temperature at sub-interval t (^{o}C).
T^t_{refri} - Fridge temperature at sub-interval t (^{o}C).
y^t_{comp} - On/off binary for fridge's compressor at $t \in T$.

Eletric Vehicle

C_{ev} - Fuel cost used in electric vehicle (EV) ($).
C^s_{ev} - Cost related to fuel used in trip s ($).
$EVSOC^t$ - EV battery's state of charge at $t \in T$ (%).
Km^s_{fuel} - Number of km for trip s using fuel (km).
$P^{ch,t}_{EVbat}$ - Charging power of EV battery (kW).
$P^{dch,t}_{EVbat}$ - Discharging power of EV battery (kW).
$y^{ch,t}_{EVbat}$ - On/off binary for EV battery charging at $t \in T$.
$y^{dch,t}_{EVbat}$ - On/off binary for EV battery discharging at $t \in T$.
$y^t_{EVfloat}$ - Binary to start EV battery float losses at $t \in T$.

CHP

C^t_{CHP} - CHP cost operation at sub-interval $t \in T$ ($).
P^t_{CHPe} - CHP electrical power output at $t \in T$ (KW).
$P^t_{CHP,fuel}$ - CHP power input from fuel at $t \in T$ (KW).
P^t_{CHPt} - CHP thermal power output at $t \in T$ (KW).
w^t_{down} - Fraction of Δ_t in $t \in T$ in which CHP ramps down.
w^t_{up} - Fraction of Δ_t in $t \in T$ in which CHP ramps up.
y^t_{CHP} - On/off binary for CHP operation at $t \in T$.
z^t_{CHP} - Binary to determine if CHP is turned on at $t \in T$.
zd^t_{CHP} - Binary to determine if CHP is turned off at $t \in T$.

A^t_{IEUI}

y^t_a - Binary that indicates whether or not operation of task $a \in A^t_{IEUI}$ starts at sub-interval t.
$y_{a,b}$ - Binary that indicates if task $a \in A^t_{IEUI}$ has to be done after task $b \in A^t_{IEUI}$ is finished.

A^t_{Phases}

$y^t_{a,p}$ - Binary that indicates if phase p of task $a \in A^t_{Phases}$ starts at sub-interval t.
$y^p_{a,b}$ - Binary that indicates if task $a \in A^t_{Phases}$ has to be done after task $b \in A^t_{Phases}$ is finished.

Other

C^t - Monetary cost at $t \in T$ ($).
E^t_{av} - Fixed power credit available at $t \in T$ (W).
E^t_g - Fixed power taken from grid at $t \in T$ (W).
$E^{t,i}_g$ - Fixed power taken from grid at $t \in T$ for block $i \in B$ (W).
E^t_v - Fixed power injected into grid at $t \in T$ (W).
x^t_a - Fixed power consumption of appliance a at $t \in T$(W).
y^i_g - Binary to determine whether or not block $i \in B$ is selected.

ADDITIONAL COMMENTS ON CHAPTER 4

The first comment is related to the relevance of local renewable generation to smart homes. The usage of renewable generation is not mandatory in a smart home. However, considering the COP21 (2015 Paris), in which participants agreed that greenhouse gas (GHG) emissions will be reduced as much as possible, governments want to decrease GHG emissions. Photovoltaic panels (PV) is one possibility for that reduction [140]. This work considers that the installation of a PV system is expected to save money from a householder perspective, otherwise the householder will not make an investment in that system. The best way to use the electricity generated by a PV could be determined by the optimization of the home energy usage, which brings us to the concept of smart home.

A second comment considers the need of extra constraints for HVAC models to avoid short operation cycles. If a thermal appliance $a \in A$ has operational constraints that impose the on state during a certain amount of time once it is turned on, such constraint must be added in the appliance model of $a \in A$. It is also important to avoid overcharge operation. This work considers the possibility in which an appliance should work, for instance, for 9 minutes instead of 10 minutes (the full interval). Impose the appliance to work for a full interval can force the appliance to operate in overcharge mode.

A third comment is about how to obtain data for the power coefficient of wind turbines. For C_{p2}, as in [195], this thesis uses a constant that represents a maximum value for the power coefficient, which is given in data sheets.

Another comment is related to the orientation and the structure of windows considered in the home. This work considers the same windows structure since it did not study the effect of different materials or layers for windows in the optimal solution. Following [172], the windows are turned to the south.

To improve the consistency of units for WH, the data for the validation example of the WH model is given also in the metric system as follows: $T^1_{out,wh} = 25^oC$, $x^t_{wh} = 5\,\text{kW}\ \forall\ t \in T$, the surface area of the WH equals $0.46\,\text{m}^2$, $(\text{UA})_{wh} = 22.01\ W/^oC$, $T^t_{in} = 40^oC\ \forall\ t \in T$, $v_{tank} = 303$ dcm^3, $fr^t_{wh} = \ddot{f}\ \forall\ t \in T$ (litter/min) and $\ddot{f} \in \{0, 3.79, 18.92, 37.85\}$.

Another comment is related to the value used for T^{max}. For security reasons, T^{max} must be around 60^oC: 100^oC is too high. However, by penalizing discomfort level function in the objective and setting $T^{max} > 60$ allows the model to decide the best temperature at each time step without any impact in the user comfort: see figure below.

Although not explicitly indicated in Chapter 4, this thesis considers a plug-in hybrid electric

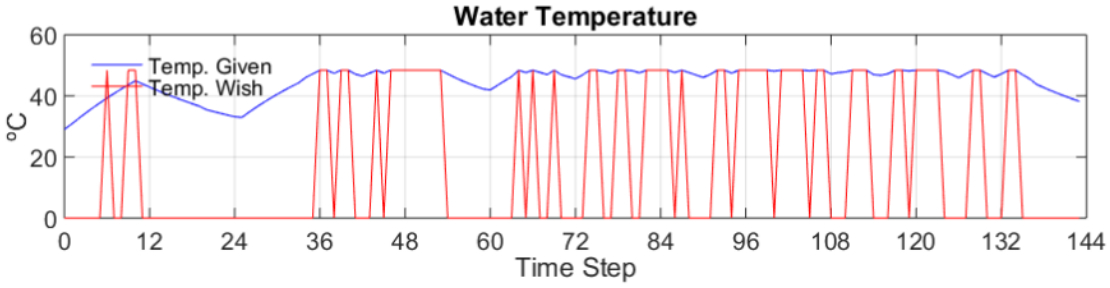

vehicle. Hence, electricity and fuel are considered for EV.

An important comment is related to the annual cost of ≈ R$6947 (2205 USD), at the end of Section 4.4.2. For Instance 11 in Table 4.5, the cost of the proposed model is R$19.03 cheaper that the one resulting of models from [13, 14]. Considering one year, an approximation for the annual extra cost is R$19.03 × 365 = R$6947 (2205USD). That amount of money should be planned following to results of models from [13, 14], but not the in model proposed in this thesis. Hence, the user can plan the 2205USD for other needs using the model presented in this thesis, which corroborates the need of a representative model for smart home scheduling, one of the motivations for this thesis.

Another important aspect is that the data needed as input for the models is largely difficult to obtain. However, in the reality, if a householder desires to set up a smart home, there is already sensors for residences to measure external air and water temperature, wind speed, solar radiation, load consumption by appliance, which were the most difficult data to obtain for a specific user.

Finally, the last comment is related to the choice of Perez's model for PV. The Perez model is considered [56] as the most accurate model to simulate the solar radiation available at the surfaces of the panels and collectors in the minute time scale.

CHAPTER 5 ARTICLE 2: A GENERAL FRAMEWORK FOR CUSTOMIZED TRANSITION TO SMART HOMES

Authors: Michael David de Souza Dutra, Miguel F. Anjos and Sébastien Le Digabel.
International Journal of Energy Research, 2019.[1]

Abstract: Smart homes have the potential to achieve efficient energy consumption: households can profit from appropriately scheduled consumption. By 2020, 35% of all households in North America and 20% in Europe are expected to become smart homes. Developing a smart home requires considerable investment, and the householders expect a positive return. In this context, this work addresses the following question: what and/or when equipment should be bought for a specific site to gain a positive return on the investment? This work proposes a framework to guide the smart-home transition considering customized electricity usage. The framework is based on linear models and gives a payback analysis of each combination of equipment acquisition for a specific user. The results quantify the dependence of the payback on the site and the application.

Keywords: Smart Home, Energy Management System, Payback, Return on Investment.

5.1 Introduction

With the growth of smart grids worldwide [59, 65] and the increased use of demand-response pricing mechanisms in the residential sector, the number of smart homes is expected to increase significantly. Governments support this trend for two reasons. First, distributed generation by smart homes allows investment in the grid infrastructure to be postponed. Second, the environmental impact is reduced if local renewable generation is used. Smart home owners may be interested in making a profit (or at least reducing their electricity bill) or maintaining a certain level of comfort via the scheduling of appliances [47].

Householders need to know, at least, the simple payback period of the investment in smart-home transition. A possibility for the investment is the acquisition of smart-home components (SHCs), which is defined to be the appliances, machines, and technologies available for smart homes, such as photovoltaic panels (PVs), wind turbines (WTs), combined heating and power (CHP), energy storage systems (ESSs), water heaters (WHs), electric vehicles (EVs), heating,

[1] Available in [46]

ventilation, and air-conditioning (HVAC), and solar collectors (SCs). As mentioned in [7], *"... the consideration of either net present values or discounted payback periods are the most useful approaches as these consider the future value of money"*. This work uses the simple payback period instead of net present values (NPV) or discounted payback periods (DPP), since there is no accurate data available for maintenance costs of all specific SHCs considered in this paper. However, if those data are given, the last step of the framework has the flexibility to incorporate NPV and DPP. Moreover, throughout this work, the term "payback" designates simple payback.

The main contributions are that this work creates a general framework that gives a payback analysis of each SHC combination for a specific user, and it investigates whether there is a synergistic effect in the payback and the return on investment.

The remainder of this paper is organized as follows. Section 5.2 presents related work, and Section 5.3 presents the proposed framework. Section 5.4 discusses the mathematical model, which is based on [47], and gives computational results. Section 5.5 provides concluding remarks.

5.2 Related Work

To the best of our knowledge, a general framework that provides a payback analysis of each possible SHC acquisition combination for a specific user is not yet available.

Xu et al. [203] propose a scheduling model that finds the best combination and the optimal capacities of batteries, water tanks, and ice/heat storage units under time-of-use electricity prices. They consider PV, SC, WH, CHP, and HVAC as well as these storage devices. Their mixed-integer linear program (MILP) minimizes the total cost of electricity, natural gas, and the investment cost of the storage devices. For each of the three cities considered, the authors compare a solution from a deterministic scenario with solutions that consider the solar radiation and demand profiles to be uncertain. Their tree method considers the expected cost in all scenarios jointly. The costs are minimized and projected over a one-year horizon. The results show that thermal storage units and water tanks are profitable, but batteries have short lifetimes and high investment costs.

Van der Stelt et al. [192] present a techno-economic analysis of household batteries and community energy storage, i.e., an ESS shared by several houses, for residential prosumers with smart appliances. Using real demand and PV generation data from 39 households in the Netherlands, the authors calculate the levelized costs of energy and the payback period for the ESS systems. Shiftable appliances are also considered. They formulate an MILP that

minimizes the cost of energy acquisition from the grid. They assume that the user can inject electricity into the grid but without remuneration. The horizon is one year. They find that the savings are too small to recover the investment costs within the lifetime of the systems: the payback ranges from 26 to 43 years.

Akinyele & Rayudu [6] present a comprehensive review of energy storage technologies with their technological development status and capital costs. They show a high cost (500–2500 $/kWh) for lithium-ion batteries.

Monyei et al. [129] propose a biased load manager home energy management system for low-cost residential buildings using the Matlab simulation environment. A case study in Naira (Nigeria) shows that the payback is between 8.4 and 25 years.

Barbieri et al. [19] study the profitability of μ-CHP systems for residential buildings. They show that the Stirling engine has the best performance, with payback of 7 and 14 years if prices are respectively 3000 and 6000 €/kW. They build a simulation model in Excel in which there is a scheduling optimization problem for a μ-CHP component that is solved by a genetic algorithm.

Asaee et al. [16] investigate, in a Canadian context, the energy system, greenhouse gas (GHG) emissions, and economic performance of a co-generation system based on an internal combustion engine (ICE). The analysis is based on the whole building through simulation with the ESP-r software. As the capital cost estimation was not available, the measure used was the tolerable capital cost. The results showed that the ICE is cost-effective.

Barbieri et al. [20] conclude, in 2012 for the UK, that the absence of subsidies and, in particular, a reduction in taxes on natural gas did not make certain μ-CHP technologies attractive. Later, Conroy et al. [40] studied a Stirling engine in the UK, comparing the economic performance and the GHG of the μ-CHP against a condensing gas boiler. They found that the payback is 13.8 years higher than that for the boiler. Their study was based on field trial data for June 2004 to July 2005.

In the UK context, Merkel et al. [122] propose a scheduling MILP to minimize the total annual cost. While the μ-CHP is more detailed, the thermal storage is represented by a temporal balancing equation and the boiler has power-limit constraints. They use three weeks per season with a scaling factor to represent a year. They find that the payback for a system with boilers and μ-CHP is not economical in three of the five buildings. For the other two buildings, the paybacks are 18.6 and 19.2 years. With thermal storage and μ-CHP, the system is profitable for all five buildings, with a payback between 13.1 and 17.3 years.

Six et al. [177] study market opportunities for μ-CHP in Flanders using simulation with

TRNSYS. The results show that the payback is greater than the life-span of the project.

Dufo-López et al. [57] present an hourly management method for energy generated in grid-connected wind farms using battery storage (wind–battery systems) and hydrogen (wind–hydrogen system); these are analyzed technically and economically. They calculate the investment cost and discounted present values for large systems (2.5 MW for WT and 2 MWh for batteries). They perform a simulation over one year with the GRHYSO software to represent the system life-span of 20 years. They find that when the electricity selling price is higher than the market average, a system composed of batteries and WTs is more cost-effective than wind-only systems.

Akter et al. [7] present an Australian case: they propose a framework that assesses a battery system with PVs. The results show that the payback and net present value (NPV) of this system are worse than those for systems with PVs only. PVs are found to be profitable in on-grid systems but unprofitable in off-grid systems because of the waste of energy, after a threshold of installed capacity. The authors consider different tariffs and reductions in CO_2 emissions, using simulation to explore the scenarios for a project with a life-span of 25 years.

Cherrington et al. [37] perform a financial analysis of two installations in Cornwall (UK) to determine the impact of different feed-in tariffs (FITs) in a PV system with a capacity around 2 kW. The capital cost is £11000. Given annual inflation of 8%, a grid injection limit from PV generation of 50%, an annual efficiency loss, and an annual reduction in the total installation cost, the authors find paybacks in the range of 9–12 years and net profit in the range of £14400–32543. However, a similar study [148] that considers a PV of 3 kW with the same capital cost and annual inflation of 6% shows that PV without FIT is not profitable in 17 of 20 British cities. With FIT and a grid injection limit from PV generation of 50%, in all 20 cities the PV capital cost is decreased by £1000–7000. The authors perform a simulation using the PVSyst software in which the PV generation profiles are estimated by the average of twelve PV hourly outputs.

Aagreh et al. [1] present a feasibility analysis for a small hotel of combinations of PV, WT, an off-grid system with a battery, and an on-grid system. They perform a simulation with the HOMER software for a 25-year horizon. In the on-grid case, when the price for selling electricity back to the grid is null, the payback for the PV system exceeds the life-span. When the selling price is half of the market price, PVs become profitable for small capacities. WT systems without batteries and PVs are profitable (see Tables 2 and 3 of [1]) for the cases considered. The paybacks for system with batteries are not given.

Mamouri & Bénard [94] present an evaluation of solar water heaters in 26 dispersed locations in Michigan for an average life-span of 20 years. They use the System Advisor Model

simulation software and find a payback between 8.1 and 9.3 years.

Xie et al. [202] study a detailed house design using the SketchUp modeling software. They analyze the payback for PVs, SC, a hybrid of PV and thermal panels (PVT), heat pumps, phase-changing materials, and μ-CHP systems. The results show paybacks of at least 6.5, 13, and 11 years for WH, μ-CHP, and PVs/PVT, respectively.

To the best of our knowledge, there are no studies of EV payback in the context of smart homes. However, a comprehensive ownership cost model to calculate the costs of purchase and use has been developed [8].

The literature has focused on payback for isolated or specific sets of SHC. The results suggest that each system will have its own payback. However, current research does not explore SHC acquisition for a specific user. As mentioned in [6], the benchmarking costs of ESS depend on the application and the site. This work assumes that every system depends on the application. The goal is a tool to assist householders in their decisions about the transition to a smart home. This work is related to [203] and [192] since this work too uses optimization methods.

5.3 Framework

The proposed framework is illustrated in Figure 5.1: the ellipses represent optimization problems and the rectangles represent results.

Let SHC^{-} be the set of SHC that are not already available at the house. The goal is to calculate the payback and the return on investment of every combination in SHC^{-}. The first step is to determine the compromise between cost and comfort level. These are conflicting objectives, and there are multiple Pareto-optimal solutions. Hence, multi-objective optimization (MOO) [48] can be applied to obtain an approximate Pareto front (APF) of this trade-off.

A detailed model has been presented [47] to find an optimal trade-off between cost and comfort by minimizing a weighted sum of the two objectives. This work adapts it to the APF approach. The model schedules the energy consumption for one day in T time intervals with a fixed length. The appliances are grouped as follows:

- A: Set of electrical appliances;
- $A_I \subseteq A$: Set of appliances with uninterruptible operation;
- A_I^*: Set of tasks for appliances in A_I.
- $A_P \subseteq A$: Set of appliances with interruptible phases;

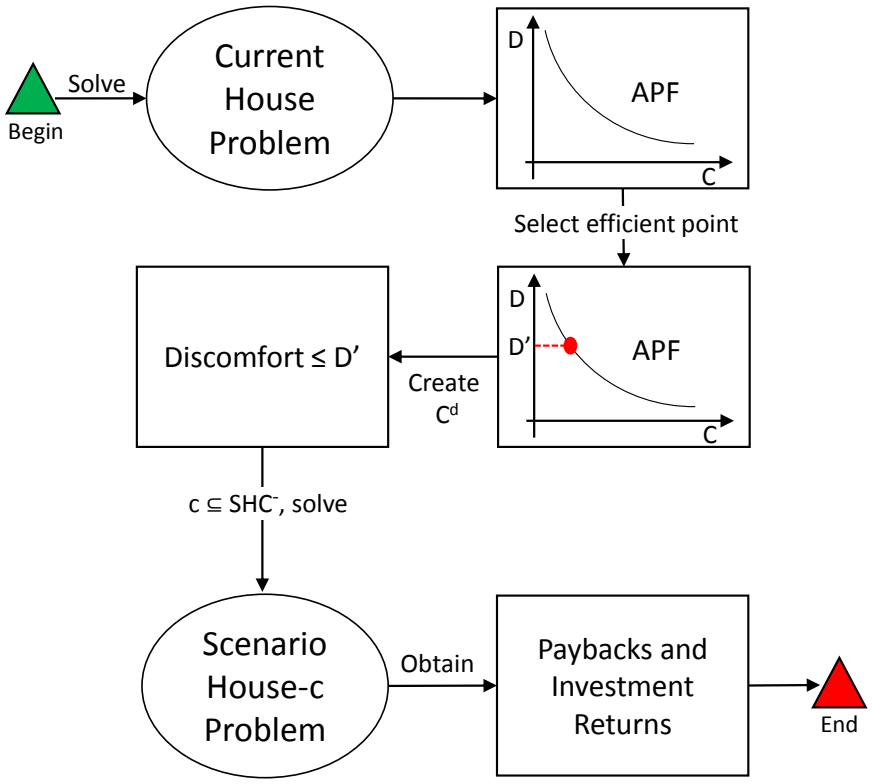

Figure 5.1 Proposed framework.

- A_P^*: Set of tasks for appliances in A_P;
- $A^* = \{A_P^* \cup A_I^*\}$: Set of tasks for appliances in A.

Let $\mathcal{X}$ be the space of all variables and $\boldsymbol{\Xi} \in \mathcal{X}$ a solution. The full set of constraints in $\mathcal{X}$ is available in [47], which are omitted here. The functions f_c, f_t, f_u, and f_d represent, respectively, the total cost, the thermal discomfort, the usage-time discomfort, and the total discomfort:

- $f_c(\boldsymbol{\Xi}) = \sum_{t \in T} \left(C_b^t - C_s^t + C_{CHP}^t \right) + C_{ev},$
- $f_t(\boldsymbol{\Xi}) = \sum_{t \in T} \sum_{a \in A} V_a^t,$
- $f_u(\boldsymbol{\Xi}) = r_1 \left[\sum_{k \in A_p^*} \sum_{p=1}^{P_k} \Psi_{k,p} + \sum_{k \in A_I^*} \zeta_k \right] + r_2 \sum_{t \in T} \sum_{k \in A^*} U_k^t$

where variables: C_b^t [$] and C_s^t [$] represent the cost at $t \in T$ of buying and selling energy, respectively, C_{CHP}^t [$] is the combined heating power (CHP) operation cost at $t \in T$, C_{ev} [$]

is the fuel cost for a hybrid vehicle, V_a^t [^{o}C] is the discomfort related to the deviation from the target temperature of appliance a at $t \in T$, U_k^t [hour] is the discomfort related to the deviation from the target time for task k at $t \in T$, ζ_k [hour] is the discomfort related to the omission of task $k \in A_I^*$ and $\Psi_{k,p}$ [hour] is the discomfort related to the omission of phase p of task $k \in A_P^*$. For parameters, let define P_k as the number of phases of task $k \in A_P^*$, $r_1 \in \mathcal{R}$ as the discomfort factor per task not performed and $r_2 \in \mathcal{R}$ as the discomfort factor per usage-time deviation.

Let define the "Current House Problem" to be

$$\min_{\Xi} \left[f_c(\Xi), f_d(\Xi) = \alpha_t f_t(\Xi) + \alpha_u f_u(\Xi) \right] \tag{5.1}$$

$$\Xi \in \mathcal{X}^{\mathcal{BASE}} \tag{5.2}$$

where α_t [discomfort/^{o}C] and α_u [discomfort/hour] are discomfort factors. $\mathcal{X}^{\mathcal{BASE}}$ represents the same space of $\mathcal{X}$, but every variable of an appliance $a \in SHC^-$ is set to zero in $\mathcal{X}^{\mathcal{BASE}}$. The first step uses the above model to compute an APF, which is shown in the first rectangle in Figure 5.1. The next step is to select an efficient point on the APF. Suppose the decision-maker has selected a point with discomfort level D': see the red point in the second rectangle in Figure 5.1. Then, D' is used in the constraint $C^d : f_d(\Xi) \leq D'$. This is represented by the third rectangle.

For each subset $c \subseteq SHC^-$, the framework solves the optimization problem SHP^c with the constraint C^d and the constraint(s) for the components in c. The flow conservation constraint is modified to consider the components from the current house in addition to the components of c. Suppose $SHC^- = \{$PV,WH,EV$\}$ and $c = \{$EV,WH$\}$. Then SHP^c is

$$\min_{\Xi} \quad f_c(\Xi) \tag{5.3}$$

$$\text{s.t.} \quad f_d(\Xi) \leq D' \tag{5.4}$$

$$\Xi \in \mathcal{X}^{\mathcal{EV}} \tag{5.5}$$

$$\Xi \in \mathcal{X}^{\mathcal{WH}} \tag{5.6}$$

$$\Xi \in \mathcal{X}^{\mathcal{BASE}} \tag{5.7}$$

Objective function (5.3) is the same as (5.1). Constraint (5.4) ensures a maximum discomfort level D'. In Constraints (5.5) and (5.6), $\mathcal{X}^{\mathcal{EV}}$ and $\mathcal{X}^{\mathcal{WH}}$ means a set of feasible points for EV and WH constraints, respectively. Constraints (5.5) and (5.6) control the operation of the EV and WH, respectively. Finally, (5.7) are the constraints from (5.2) with the flow conservation constraint adjusted to consider the EV and WH.

The payback is computed in the last framework step, which is represented by the last rectangle in Figure 5.1. Let D^p be the project duration, Pay^B the payback period, s^{slp} the savings over the life-span, T^I the total investment, and I^R the return on investment. The payback is calculated [7] as $Pay^B = D^p T^I / s^{slp}$ and $I^R = s^{slp} - T^I$. If Pay^B is greater than the life-span then the project is not cost-effective.

5.4 Results and Discussion

In this section, the framework is applied to three case studies. This work considers an horizon of 25 years, and the exchange rates used are 1 USD = 0.71 GBP, 1 USD = 1.27 CAD, and 1 USD = 3.3 BRL. The houses have appliances with distinct daily tasks A^t, a fridge, a shower, and an HVAC system. The houses considered are located in Belo Horizonte (BH), Brazil; London, U.K.; and Montreal, Canada.

For BH and London, this work does not consider inflation; it assumes that the customer wishes to acquire a system now. A total of 1024 systems are evaluated based on an annual savings approach: 365 days are optimized and the sum of the daily savings gives the annual savings. The total saving for a specific project is the product of the annual saving and the duration.

For Montreal, this work considers inflation: the cost of the SHCs and electricity prices change over time. A total of 64 systems are evaluated. The optimization is applied daily from 2019 to 2080, covering projects starting between 2019 and 2055, since each has a duration of 25 years. If a project starts in January 2020, sum the savings of the next 365×25 days is done to obtain the total savings . At the end, the output is: what and when the SHCs for a specific user in Montreal should be acquired such that it will be profitable.

For the appliances $a \in A_{IEUI} \cup A_{Phases}$, a dataset with real daily load profiles is available [100]. A set of load profiles is created for each day of the week. In the optimization, for each day of the week, a load profile is randomly selected from the corresponding set. Thermal mass of building, solar radiation, wind speed, etc., are considered in constraints proposed in [47], which are also used in this work. For more details, hypotheses and justifications for all decisions related to the SHC models and pricing policies are defined in [47]. In addition, $\alpha_u = \alpha_t = 1$.

5.4.1 BH Case

The BH house does not have PV, Battery, WT, SC, WH, EV, or μ-CHP. Let use $SHC^- = \{$PV 3.5 kW, PV 6.5 kW, Battery 26 kWh, Battery 13 kWh, WT 3 kW, WT 7 kW, SC, WH,

EV, μ-CHP}. When similar components are in the same subset $c \subseteq SHC^{-}$, they are replaced by a new component with a capacity equal to the sum of the capacities of these components. The house does not have the infrastructurefor natural gas, so the ICE is set to μ-CHP. Table 5.1 summarizes the set SHC^{-}. The first column lists the element and the second column gives its brand and model. In the second column, some SHCs have the number of units that must be acquired to achieve the desired capacity, for instance, the PV 3.5kW need 14 units of CS CS5P-250M to achieve a capacity of 3.5kW. The third column gives the warranty, which is considered to be the life-span, and the fourth and fifth columns give the prices, in USD and BRL respectively. The sixth column gives the total price including installation cost and additional materials/equipment. Unless otherwise stated, no maintenance costs is considered: when the warranty ends, the SHC is replaced. Warranty is used for life-span only to show an example for framework usage. In reality, the life-span is an input set by the user. The total daily distance (in km) for EVs is drawn from the uniform distribution U[0,70]. The PV simulation model considers many parameters such as sun position, PV orientation, ground reflectance, latitude, longitude and solar radiation. For the solar radiation, the percentage of clouds are used for each month from [200], which is shown in Figure 5.2. This avoids overestimating the solar radiation by assuming clear skies. The other parameters are set as in [47].

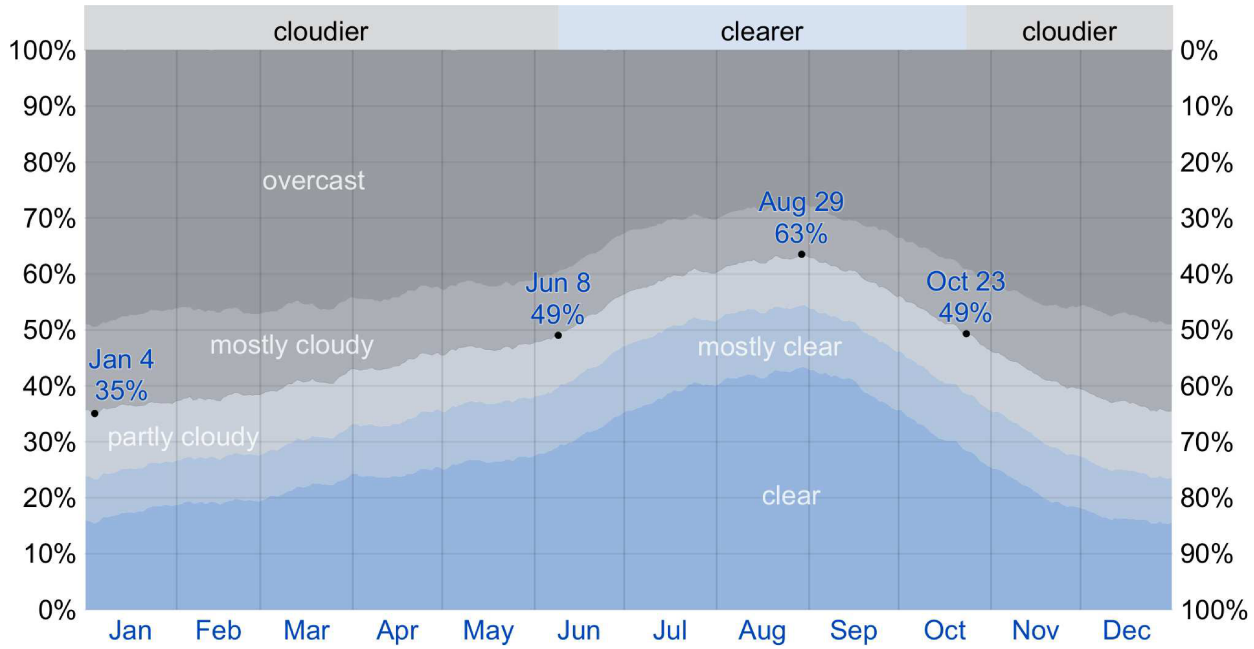

Figure 5.2 Percentage of time spent in each cloud cover band at BH, categorized by the percentage of the sky covered by clouds: clear $< 20\%$; mostly clear $< 40\%$; partly cloudy $< 60\%$; mostly cloudy $< 80\%$; overcast $> 80\%$. Source: [200].

Table 5.1 SHC summary for BH case

SHC	Brand and Model	Life-span (years)	Price (USD)	Price (R$)	Total Cost (R$)
PV 3.5 kW	14 × CS CS5P-250M	25[a]	14 × 225 [75]	11781[b]	17671.50
Battery 26 kWh	2 × Tesla Powerwall	10 [185]	12500 [185]	41250[b]	61875
WT 3 kW	3 × Bergey Excel 1 kW	5[a]	3 × 4995[c]	49450.5[b]	74175.75
SC	Coupled Tempersol [184]	5[a]		1400 [184]	2100
WH	Rheem 80G	10 [160]	1899 [160]	6266.7[b]	9400.05
EV	2018 Nissan Leaf	5[a]	30000 [137]	120000 [191]	43500
μ-CHP	Yanmar CP5WN-SNB	2[a]		3950 [83]	5925
PV 6.5 kW	26 × CS CS5P-250M	25 [a]	26 × 225 [75]	21879[b]	32818.5
Battery 13 kWh	1 Tesla Powerwall	10 [185]	6600 [185]	21780[b]	32670
WT 7 kW	Bergey Excel 1 kW + Bergey Excel 6 kW	5[a]	10000[c]	330000[b]	49500
WT 10 kW	Bergey Excel 10 kW	10 [23]	31770[c]	104841[b]	104841

a: According to the manufacturers's datasheet
b: Value converted from USD to BRL
c: Given by the manufacturer
CS: Canadian Solar

APF Results

The ϵ-constraint algorithm [107, Algorithm 1] is used to obtain an APF, which is shown in Figure 5.3. The efficient solutions found in Figure 5.3 could be presented to the DM, but to aid the selection process MDIPNW [39] was used to select an efficient point with coordinate (C',D'). With this coordinate, the framework creates a constraint C^d to control the maximum level of discomfort.

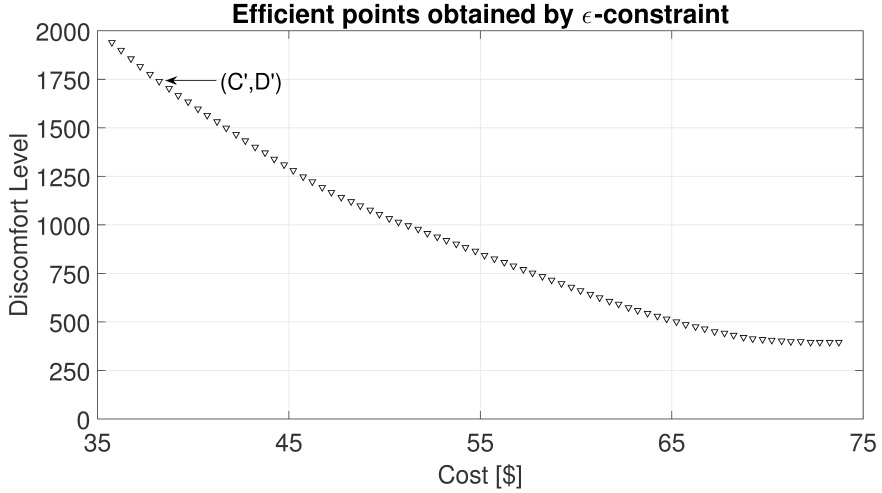

Figure 5.3 APF and point selected to construct C^d.

Solving SHP^c

For each subset $c \subseteq SHC^-$ defined in Section 5.4.1, the problem SHP^c is solved. The number of sets is $2^n - 1$ because $c = \varnothing$ represents the existing scenario, which was handled in the

first step of the framework.

Payback and Investment Return

Since some SHCs have life-spans below 25 years, the total cost was increased in proportion. For instance, the 3 kW WT has a life-span of five years, so there is a need of five units to cover 25 years.

For each SHP^c, the total investment is found by summing the total cost of each component of c, as well as the payback and the return on investment: see formulas given in Section 5.3.

BH Results

Table 5.2 BH results

Component	Payback (years)	Return on investment (thousand R$)
PVs, 3.5 kW	7.57	40.632
PVs, 6.5 kW	8.59	62.656
PVs, 10 kW	9.13	87.784
WTs, 7 kW	19.58	68.489
WTs, 10 kW	22.60	41.809
SC	11.41	12.513

Table 5.2 summarizes the cost-effective combinations. An interesting finding is the relationship between the renewable generators. The expected synergy does not occur: the sum of their separate investment returns (IRs) is greater than the combined IR.

In this case, batteries are too expensive. Every set c with a battery has an IR lower than that without a battery; sometimes the former value is negative. The price of a Tesla battery pack must decrease to 223.5 USD to pay for itself without renewable generation. Systems composed of a battery and renewable generation have a negative IR. In these systems, the price of a 26 kWh battery must be 1650 USD to match the IR of a 3.5 kW PV system; 100 USD to match that of an SC system; and 1500 USD to match that of a 7 kW WT system.

The price of an EV must be at most 58073 R$ to be cost-effective. If the DM is going to buy a car costing x R$, the price of an EV must be at most $x + 58073$ R$. If one considers a life-span of 10 years for EVs, the price must be at most 116140 R$.

SC is a better option for water heating because a) WH systems, or b) WH and SC systems, or c) μ-CHP, WH, and SC systems are not cost-effective. μ-CHP is not cost-effective even if its price is halved because of its short life-span; it starts to be profitable if its life-span increases to 13 years. However, the payback could be interesting if a μ-CHP powered by

natural gas were available. In an industrial context, [105] showed a discounted payback in less than five years for a μ-CHP powered by natural gas in a city near BH.

For this customer, the set $\{10\,\text{kW PV}, \text{SC}, 7\,\text{kW WT}\}$ gives the best IR (141.282 thousand R$) with a payback in 17.14 years. The set $\{3.5\,\text{kW PV}\}$ has the smallest positive payback.

5.4.2 London Case

Table 5.3 SHC summary for London case

SHC	Brand and Model	Life-span (years)	Price (USD)	Price (£)	Total Cost (£)
PV 3.5 kW	CS CS5P-250M	25[a]		5906.25 [158]	5906.25
Battery 26 kWh	2 × Tesla Powerwall	10 [185]	12500 [185]	8875[b*]	13312.50
WT 3 kW	3 × Bergey Excel 1 kW	5[a]		15000 [157]	15000.00
SC	Pure Energy 16	15[a]		4500 [156]	4500.00
WH	Megaflo Eco Unvented Indirect 300L	2[a]		1319.5* [58]	1979.25
EV	2018 Nissan Leaf	5[a]		21990 [139]	21990.00
μ-CHP	BlueGen	10[a]		15500* [155]	23250.00
PV 6.5 kW	CS CS5P-250M	25[a]		10968.75 [158]	10968.75
Battery 13 kWh	1 Tesla Powerwall	10 [185]	6600 [185]	4686[b*]	7029.00
WT 7 kW	Bergey Excel 1 kW + Bergey Excel 6 kW	5[a]		36000[d]	36000.00
WT 10 kW	Bergey Excel 10 kW	10 [23]	31770[c]	22556.7[b*]	33835.05

a: According to the manufacturers's datasheet
b: Value converted from USD to GBP
c: Given by the manufacturer
CS: Canadian Solar
d: Sum of 1 WT 1 kW and 1 WT 6 kW from [157]
*: Does not include installation cost

The same SHC^{-} as for BH is considered. The acquisition price per kWh is that for the tariff *HomeEnergy Fix Mar 2019*, from British Gas. The time of use has two stages: £0.175 from 7:00 a.m. to 10:59 p.m. and £0.0912 otherwise [27, 190]. The selling price per kWh is set to £0.0524 following the FIT export tariff in [141]. The price of natural gas is £0.0361/kWh from the tariff *Safeguard PAYG* [27]. The fuel price is set to the average diesel price in April 2018 [147]: £1.25/L. The ground temperature was obtained from [199], and the house's heat resistance is based on [197, Table 2]. The Weibull parameter for wind speed is taken from [82, Table 8.5 - London Array I]. The nominal power of 5 kW for HVAC is considered to be at least 50% of the measuring heating capacity from [79]. The total daily distance (in km) for EVs is drawn from the uniform distribution U[0,70]. The parameters for the economic analysis are given in Table 5.3. It is similar to Table 5.1, but some elements in the column "Price (£)" include the total cost of equipment and installation. Other costs are added in the column "Total Cost (£)." Unless otherwise stated, no maintenance costs is considered: when the warranty ends, the SHC is replaced. For the solar radiation, the percentage of clouds is used for each month from [200], which is shown in Figure 5.4. The other parameters are set as in [47].

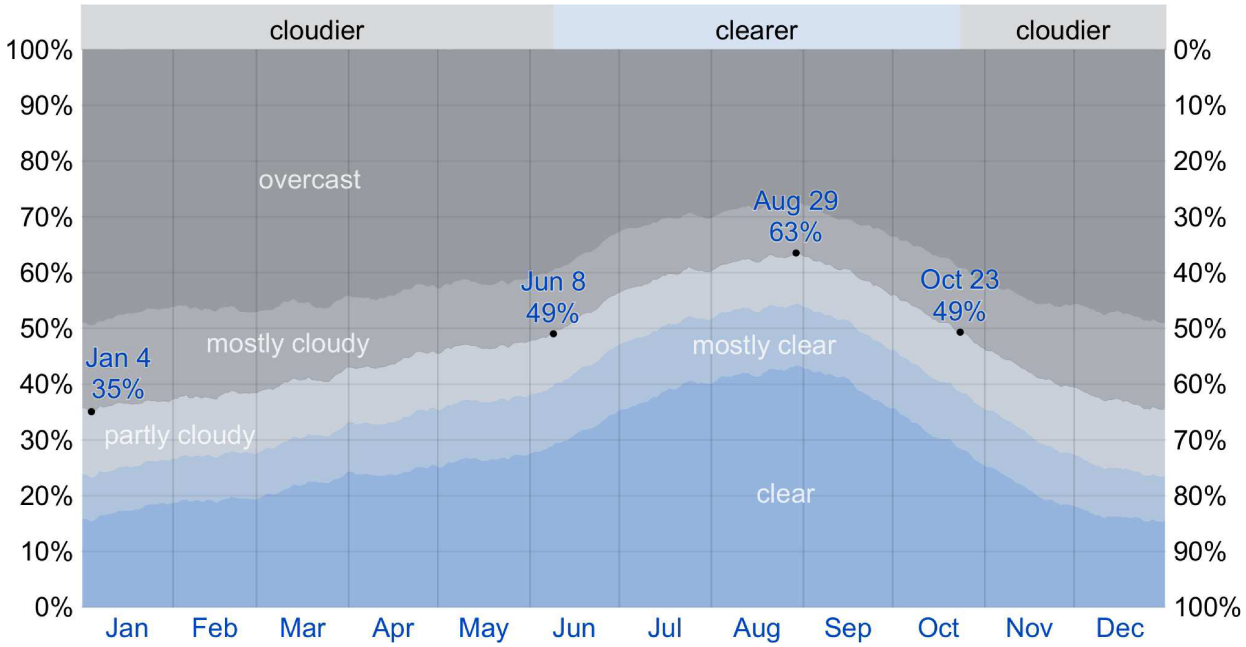

Figure 5.4 Percentage of time spent in each cloud cover band at London. Source: [200].

London Results

Table 5.4 London results

Component	Payback (years)	Return on investment (thousand R$)
PVs, 3.5 kW	17.30	2.789
PVs, 6.5 kW	18.72	3.619
PVs, 10 kW	22.01	2.241
WTs, 10 kW	9.09	98.676

Table 5.4 summarizes the cost-effective combinations. PVs have a payback inversely proportional to the nominal power, and the best IR is for the medium size. The estimates found by the proposed framework are worse than [37] and better than [148]. Compared with [37], the payback found by the proposed framework is larger by 5–7 years, and the IR is lower by £12–30 k for the 3.5 kW PV. An important difference between this study and [37] is that this work does not consider annual inflation of 8%. For a payback of 12 years in this study, the total savings over 25 years increase to £1500, which happens if electricity increases by 8% annually. For [148], in London, a 3 kW PV system with FIT has to cost at most £5 k to be self-sustaining. If the 3.5 kW PV costs £8.6 k, the framework's results will still have a positive IR. A difference between this work and that in [148] is that this work uses a detailed optimization method over a whole year. Thus, the PV energy will be used in an optimal way,

which can reduce the payback.

The framework can also be used to determine the best sizing for some SHCs. From Table 5.2, the best capacity size for PV is between 3.5kW and 10kW based on the economic measures. The framework could be executed again replacing the PV 3.5kW and PV 10kW by PV 5kW and PV 8.5kW, respectively, so that find a better approximation for the best size of the PV.

SC would not be cost-effective even if its life-span were 25 years. If its price drops to £2065, it starts to be profitable. A two-year life-span for WH makes it a costly option. It must increase its life-span to 14 years or decrease its price to £192 to become cost-effective.

Only the 10 kW WT has a positive IR. For an annual mean wind speed above 7 m/s, since the 10 kW WT has a cost of £5640/kW, this result is in line with [182, Table 13] that specifies a viable initial cost below £7548/kW for the generation capacity.

As for BH, batteries are too expensive. Lower battery capacities have lower losses. For the system with a 10 kW WT and a 13 kWh battery, the battery cost must decrease to 1000 USD to match the IR of the corresponding system without a battery. With the exception of systems with a 10 kW WT, every system composed of ESS and PVs or ESS and SC has a negative IR.

Although batteries are not profitable, EV is cost-effective if the life-span is 10 years: the payback is 23.81 years with an IR of £2.731 k. Taking into account the UK plug-in grant [78] of £4500, the payback drops to 18.94 years with an IR of £13.981 k.

BlueGen is unprofitable: the payback is 83 years. It remains unprofitable if the life-span of this μ-CHP increases to 25 years. However, with a life-span of 25 years and the same costs as in [122], the payback is 17.52 years, which is in line with the results of [122]. Given the FIT tariff of £0.1454 in June 2018 for CHP [141], BlueGen is profitable (17.91 years and £22.84 k). If an ICE were used, such as the one in Table 5.1, the μ-CHP would never be profitable.

The best payback is for {10 kW WT}. With the plug-in grant and an EV lifespan of 10 years, the best set becomes {10 kW WT, EV} (11.34 years and £120.558 k).

5.4.3 Montreal Case

In Montreal, it is generally believed that PV is not profitable because of the low price of electricity. The appliances that are not currently available are PV, EV, battery, and SC. Thus, the set SHC^{-} is composed of PV 3.5 kW, Battery 26 kWh, SC, EV, PV 6.5 kW, and Battery 13 kWh. Although Montreal is cold for almost half of the year, SC is used [188]. CHP is discouraged by governmental programs for GHG reductions; even natural gas is considered undesirable [150].

The acquisition price per kWh is given in [89]. Beyond a fixed price for electricity availability, the tariff can be seen as an inclining block rate (IBR) with two blocks: \$0.0591/kWh if the consumption is below 36 kWh per day and \$0.0912/kWh otherwise. To represent this, one can consider a block with a capacity of 36 kWh and a discount of 35% that can be completely used. Note that the utility does not pay for electricity injected into the grid but gives the customer a credit in kWh that is valid for two years. It is considered to be equivalent to the utility buying electricity at the selling price, but this work assumes that the compensation can be applied after two years.

The fuel prices are set to the average diesel price in April 2018 [28]: 1.40 CAD. The nominal power for HVAC is set to 5 kW. The ground temperature is assumed to be between 5^oC and 10^oC, following [167, Figure 12]. The house's heat resistance is taken from sections 34 and 37 of *Quebec's Regulation Respecting Energy Conservation in New Buildings*. The total daily distance (in km) for EVs is drawn from the uniform distribution U[0,70]. The other parameters are set as in [47].

According to Hydro-Quebec [90], electricity prices follow the consumer price index (CPI), which varies between 0.5% and 3% annually for 1997 to 2017 [92]. Ran et al. [71, page 23] show that from 2010 to 2017 there was a 61% reduction in the residential PV system cost benchmark and from 2016 to 2017 there was a 6% reduction. This work assumes that PV prices fall by 6% per year, but, to take into account the effect of learning curves [146], the percentage is multiplied by 0.98 at the beginning of each year to give a more conservative decrease. Following [93, page 12], this thesis considered a decreasing cost of 10.3% per year for batteries; this is multiplied by 0.9 each year to give a more conservative decrease. The same value is used for the decreasing cost of EVs, since batteries are considered a key component in terms of overall cost and performance [60]. SC technologies are already well developed and can be bought at low prices [153], so an annually decreasing cost is not applied. The parameters for the economic analysis are given in Table 5.5. The installation costs, a component of the *Total Cost*, were provided by local suppliers.

Table 5.5 SHC summary for Montreal case

SHC	Brand and Model	Life-span (years)	Price (USD)	Price (CAD)	Total Cost (CAD)
PV 3.5 kW	14 × CS CS5P-250M	25[a]	14 × 225 [75]	4533.9[b]	10881.3
Battery 26 kWh	2 × Tesla Powerwall	10 [185]	12500 [185]	15875[b]	23812.50
SC	Heliodyne GOBI 408-001	10[a]	1070.99 [159]	1360.16[b]	2040.24
EV	2018 Nissan Leaf	5[a]	30000 [137]	38100[b]	38100
PV 6.5 kW	26 × CS CS5P-250M	25[a]	26 × 225 [75]	8420.1[b]	20208.24
Battery 13 kWh	1 Tesla Powerwall	10 [185]	6600 [185]	8382[b]	12573

a: According to the manufacturers's datasheet
b: Value converted from USD to CAD
CS: Canadian Solar

Montreal Results

For the solar radiation, this work considered the percentage of clouds for each month [200], which is shown in Figure 5.5.

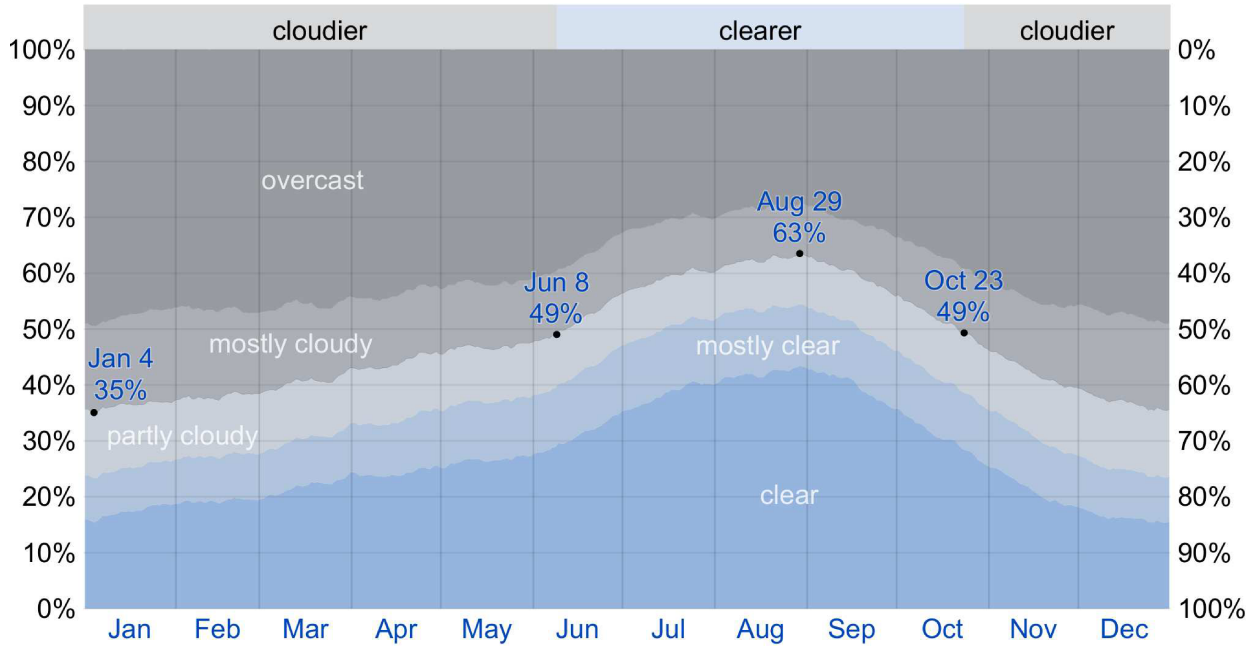

Figure 5.5 Percentage of time spent in each cloud cover band at Montreal. Source: [200].

The annual savings for some subsets $c \subseteq SHC^{-}$ are shown in Figure 5.6. The total savings, for the duration of the project, are given in Figure 5.7. For example, in Figure 5.6, each year from 2019 to 2079 has an annual saving for each component. For instance, the 3.5 kW PV has an annual saving of $297 in 2019, increasing to $381 in 2079. There is no significant difference between 13 kW and 26 kW batteries: In Figures 5.6 and 5.7 they overlap one to another.

Figure 5.8 shows the payback for the 3.5 kW PV. In Figures 5.8 to 5.12 the x axis gives the start year for the project and the y axis gives the payback in years. The dashed red line indicates the life-span of 25 years. Three possible scenarios for inflation is considered. If it is 3% for 25 years after the installation year (2019), the expected payback is around 24 years. If it is 0.5% for 25 years after 2024, the payback is 25 years. If it is between 0.5% and 3%, the 3.5 kW PV will have a payback below its life-span between 2019 and 2024. An upper bound (UB) on the start of the project is 2024, since the system starts to be cost-effective for the most conservative value of inflation. A lower bound (LB) is 2019 since the system is cost-effective for 3% inflation.

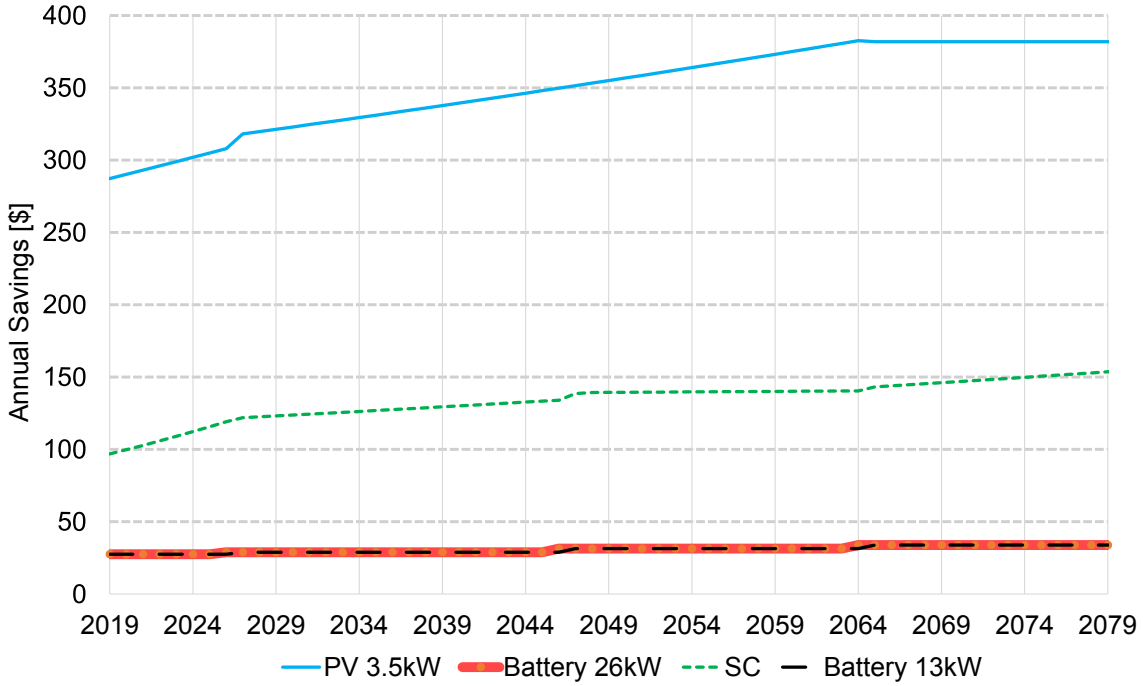

Figure 5.6 Annual saving ($) for some $c \subseteq SHC^{-}$.

For a 6.5 kW PV system, the LB is 2019 and the UB is 2025. For a PV 10 kW PV, the LB is 2020 and the UB is 2025.

The SC system will not be profitable until 2028, as shown in Figure 5.9. With 1.75% inflation, the payback is 38 years if the project starts in 2019. A similar system had a payback above 75 years [88]. In this work, the heat-transfer fluid is a closed loop of water with self-draining. In [88], it is a glycol-based coolant with a circulation pump. The system considered in this work is around three times less expensive than the glycol-based one, which explains the difference in the payback results.

Batteries are not used since there is a flat tariff so they are not cost-effective. EV is cost-effective after 2037: see Figure 5.10. The EV payback increases with the price of electricity. This is because the main source of savings is the replacement of fuel by electricity.

If the EV life-span is 10 years, the payback is positive after 2021; see Figure 5.11. If one includes the purchase rebate of $8000 from the Drive Electric program of the Quebec government [187], the EV payback occurs between 2028 and 2031.

To summarize, in a scenario with higher inflation, the best option is to install a PV system in 2019–2020 and to use an EV after 2028 if the life-span is 5 years. Under conservative inflation, the best option is to install a PV system in 2024–2025 and to use an EV after 2031

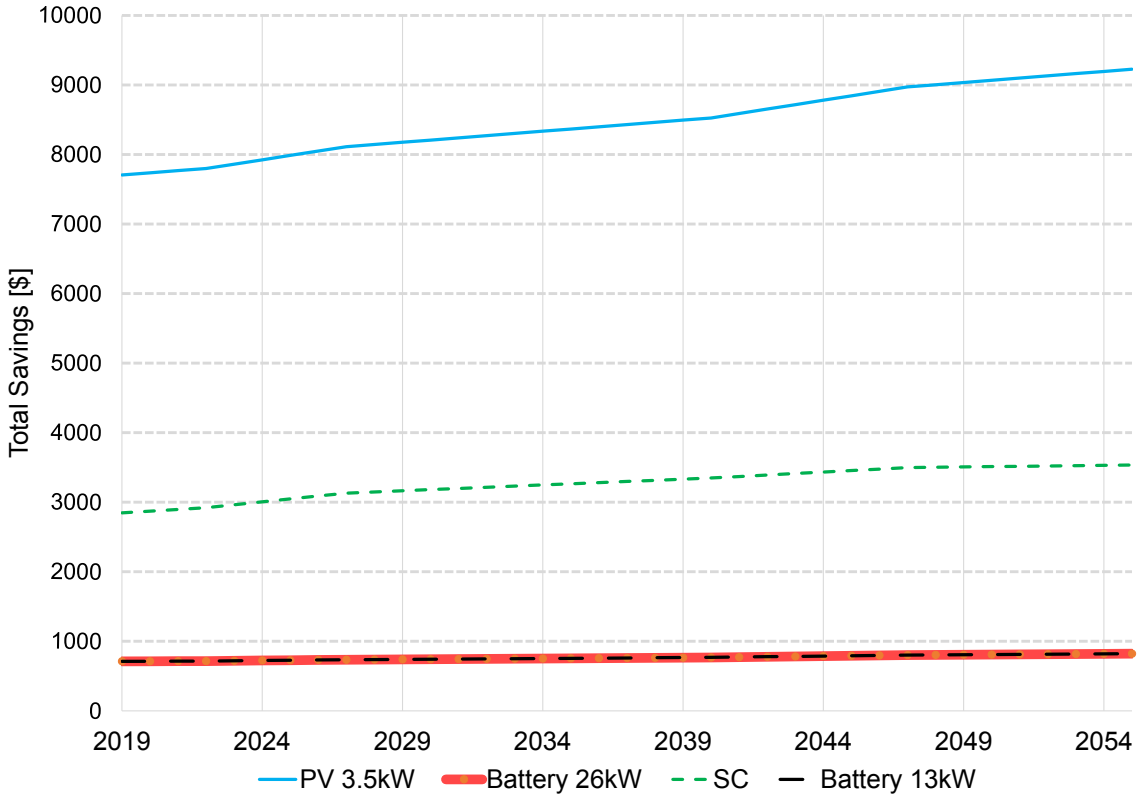

Figure 5.7 Total savings ($) from the year that project starts for some $c \subseteq SHC^{-}$.

if the life-span is 5 years. Batteries and SC should not be used.

5.5 Conclusions

Transforming a house into a smart home requires considerable investment. This work has proposed a framework to guide the transition to smart homes given customized electricity usage. The framework gives a payback analysis of each SHC acquisition combination for a specific user. The framework was tested on examples in Belo Horizonte, London, and Montreal. For BH and London, this work considered 1024 systems based on 8760 optimized hours (1 year). For Montreal, this work considered 64 systems based on 534360 optimized hours (60 years). The results quantify the dependence of the payback on the site and application, e.g., EV is attractive in London but not BH. The examples illustrate the versatility of the proposed framework. In future work, users model proposed in this work could be used in the context of coordination of multiple smart homes by demand response.

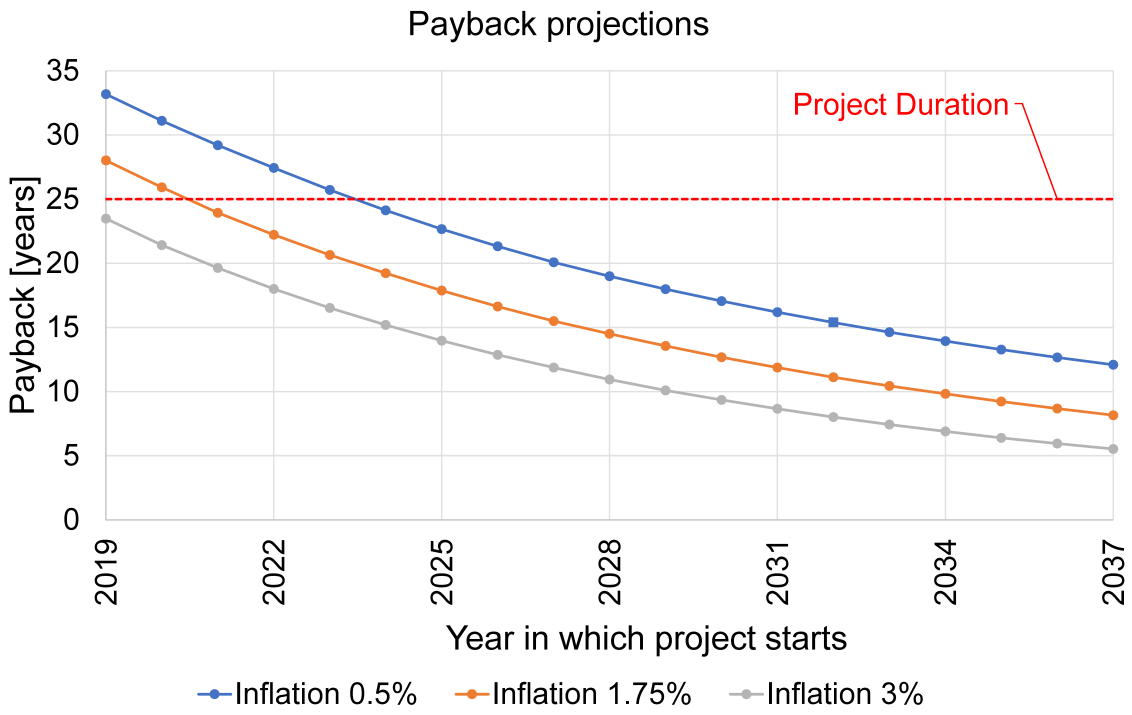

Figure 5.8 Payback for 3.5 kW PV in Montreal.

Acknowledgments

This work is supported by a full scholarship from CNPq-Brazil.

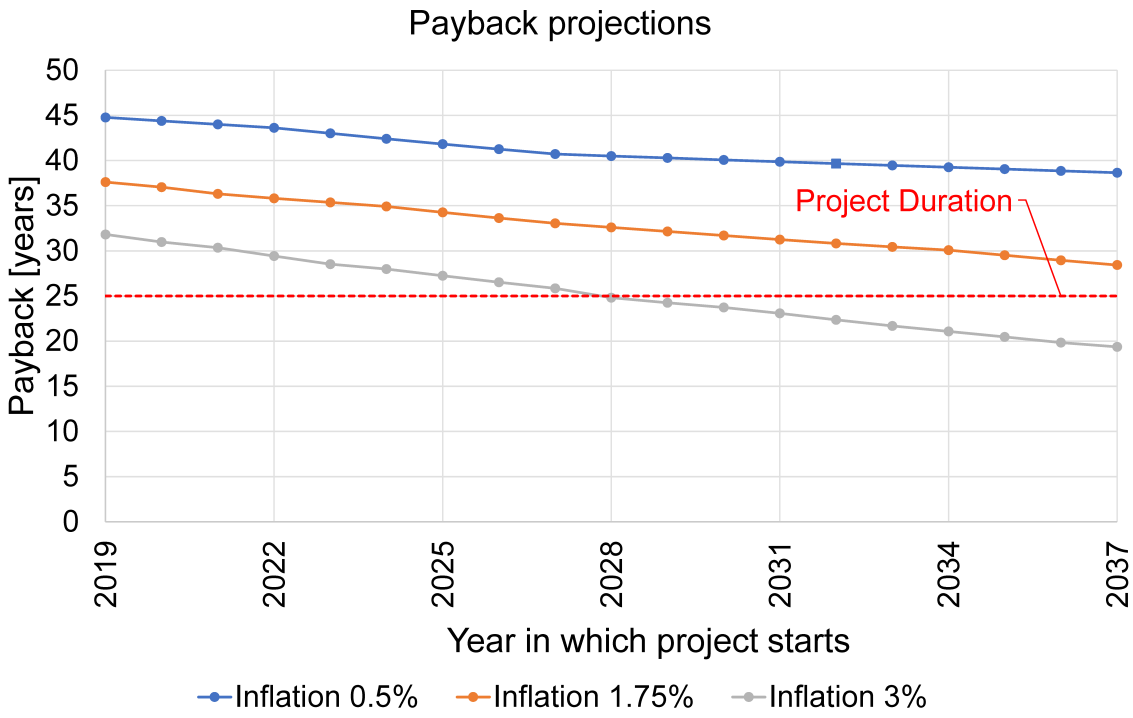

Figure 5.9 Payback for SC in Montreal.

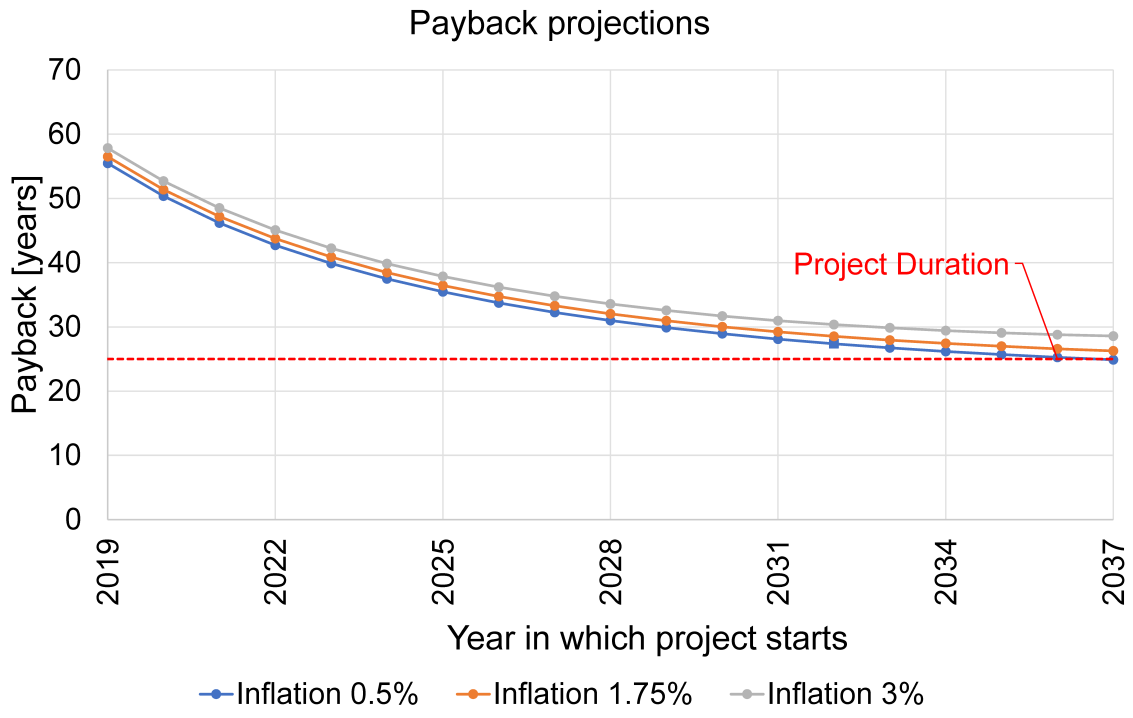

Figure 5.10 Payback for EV in Montreal.

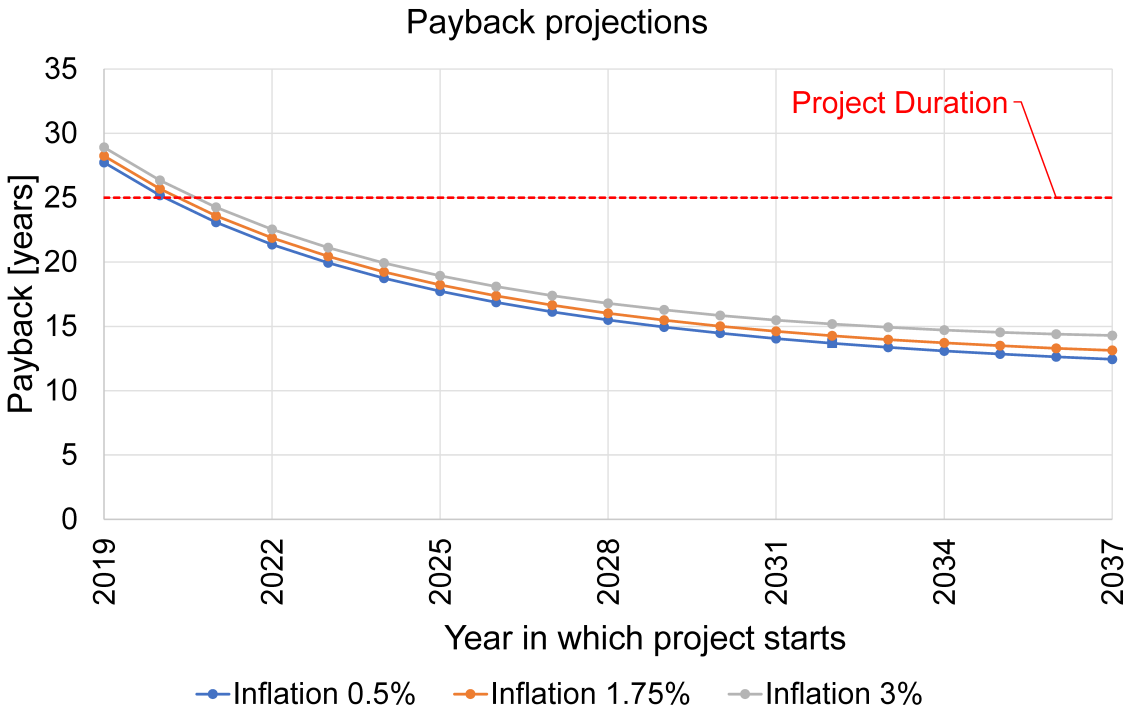

Figure 5.11 Payback for EV with life-span of 10 years in Montreal.

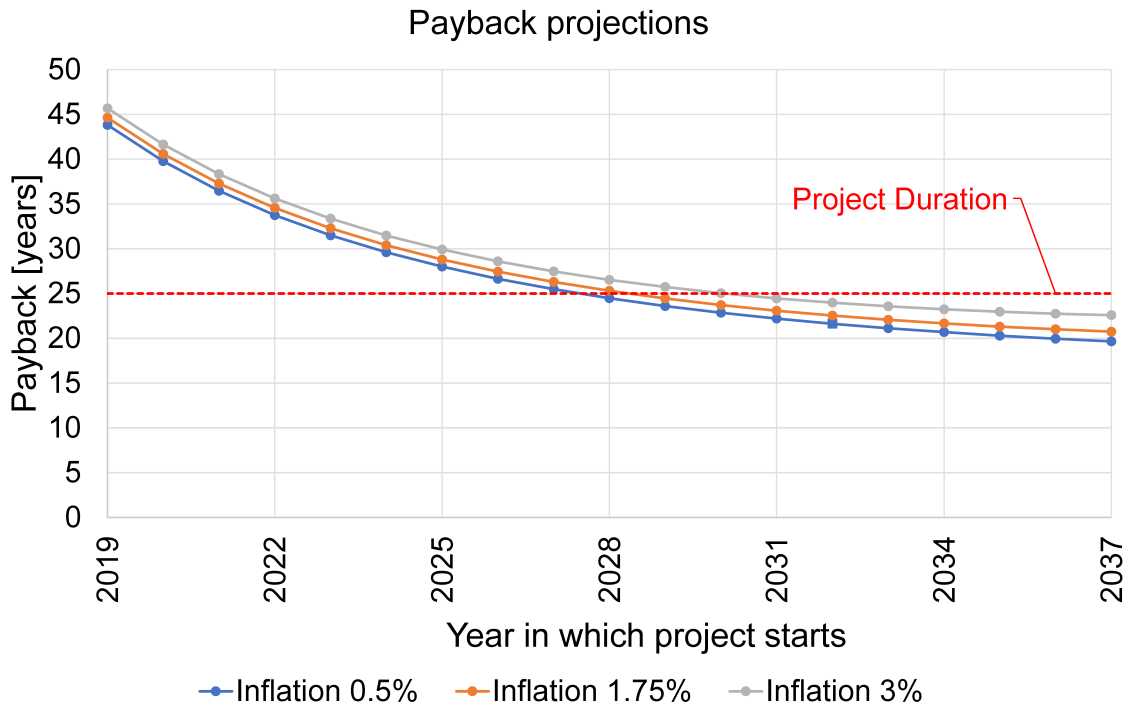

Figure 5.12 Payback for EV with purchase rebate in Montreal.

CHAPTER 6 A FRAMEWORK FOR PEAK SHAVING THROUGH THE COORDINATION OF SMART HOMES[1]

Abstract: In demand–response programs, aggregators balance the needs of generation companies and end-users. This work proposes a two-phase framework that shaves the aggregated peak loads while maintaining the desired comfort level for users. In the first phase, users determine their planned consumption. For the second phase, this work presents a bilevel model with mixed-integer variables and reformulate it as a single-level model. This work proposes an exact centralized algorithm and a decentralized heuristic. Computational results show that the heuristic gives small optimality gaps and is much faster than the centralized approach.

6.1 Introduction

One of the challenges for an electricity generation company (GENCO) is the variability in the demand. It may try to influence customers to change their consumption to fit a desired load shape via, for example, demand–response (DR) programs. Such programs generally offer incentives for consumption adjustment. Reviews of DR are available in [31, 52, 108, 175, 193], and [142] reports its recent applications worldwide in the residential sector.

Individual residences make only a small contribution to the overall DR strategy. An aggregator acts as an intermediary between a group of users and a GENCO [74], and a GENCO may itself act as an aggregator [142].

High peak demand periods have a negative impact on the reliability and stability of the power grid, so the GENCO desires a consumption curve that is as flat as possible [108, 151]. When a price-based DR is used, consumers respond to price signals by moving their demand to a cheaper period, which creates new rebound peaks [113]. Moreover, for domestic electric water heaters, price-based DR alone is not enough to change the user behavior to favor the GENCO [109].

Incentive-based DR programs avoid new peaks and increase user participation. They pay customers to shift and/or reduce their consumption for a given time period. Direct load control (DLC) is common in the residential sector, and curtailable load (CL), defined as a DR program that gives monetary incentives to users so that it adopts a specific load consumption, is more appropriate for larger consumers [142]. However, consumers have reported that the

[1] Available in [45]

incentives were insufficient and their comfort levels were impacted [86]. Moreover, DLC incurs a computational burden and leads to privacy issues [67].

This work considers the following question: *what incentive should be paid to maximize the social welfare while maintaining an acceptable level of comfort?*

The organization of this work is as follows. Section 6.2 presents a literature review and outlines the contributions of this work. Section 6.3 introduces the mathematical models and two algorithms designed to answer the question. Section 6.4 discusses the computational results, and Section 6.5 provides concluding remarks.

6.2 Related Works

In this section, a literature review related to coordination and aggregation of multiples homes is made. According to [123], the existing literature on distributed methods for DR can be classified into two categories. The first consists of simplified models with continuous variables [18,67,73,183]. The second category consists of more realistic mixed-integer models that consider inter-temporal device couplings. A similar classification is possible for models: more detailed models increase the user's profit while maintaining the desired comfort level. This work uses the appliance models from [47], so it belongs in the second category, in contrast to studies that consider simplified models or do not use specific appliance models (e.g., [67, 95, 151, 209, 210]).

There are at least two strategies for decreasing peak load while satisfying consumers. The first is to treat the DR problem as a single-level social welfare maximization problem (SWMP) by finding a trade-off between cost and/or a utility discomfort function for the consumers and a utility function for the GENCO (income, community's comfort, etc.). Lu *et al.* [117] classify SWMP methods into three types:

1. Single-objective optimization [96]: it considers either the users goal or the GENCO goal but not both;
2. Weighted sum multiobjective optimization [33, 50, 67, 85, 86, 99, 101, 112, 119, 123, 130, 136, 152, 171, 198, 204]: its limitation is the need to choose weights;
3. Pareto-front multiobjective optimization [70,116,166,214]: it may have lower scalability because of the time to construct an approximation to the Pareto front or use simplified models to reduce the CPU time.

The second strategy, which this work uses, is a bilevel formulation with the upper level

representing the GENCO (the leader) and N lower levels representing N electricity consumers (the followers). Linear bilevel problems are $\mathcal{NP}$-hard [49].

A linear bilevel problem can be reformulated as a single-level mixed-integer linear program (MILP) [17, 133, 201, 213, 219] using the Karush–Kuhn–Tucker (KKT) conditions [49]. However, this is not possible if a lower-level problem has discrete variables, as in this work. It is also possible to use a Stackelberg game model in which the upper and lower levels are solved iteratively until equilibrium is reached. This approach is used by [66, 67, 106, 208, 209], and [115], but they do not consider CL or specific appliance models for users. In addition, some of these studies use the weighted-sum approach [67, 209].

This work is related to [165], which proposes a bilevel optimization problem to coordinate DR for a set of users. The service provider announces the load profiles to the householders. Each user then returns adjustments to its profile. This process is repeated until no further improvements are made. The objective function at the upper level minimizes the standard deviation between a current load and a target load, while the lower-level objective functions minimize the user costs. The optimization problem is solved in two steps. In the first step, the energy expenses of the individual customers are minimized. Then, for each user, a constraint that limits the user cost is added to the upper-level problem. The connection between this work and this framework is the use of the same constraint to reformulate the bilevel problem as a single-level one. However, this work differs in that it determines a personalized monetary incentive for each customer, uses specific models for home appliances, has cost minimization as the objective function for the GENCO, and executes each phase only once.

6.2.1 Contribution

This work proposes a scalable framework involving mixed-integer variables for the coordination of user consumption. It minimizes the user costs while maintaining their comfort and also minimizes the GENCO costs. Detailed appliance models are used. The framework is divided into two phases. The first phase minimizes the energy expenses of individual customers. In the second phase, the framework assumes that the users participate in a DR program and will accept requests that do not impact their cost or comfort. Thus, this work proposes a bilevel problem in which the upper level represents the GENCO and each lower-level problem is assigned to a customer. This is reformulated into a single-level problem as in [165]. Two algorithms are developed: an exact centralized approach and a decentralized heuristic. The solution encourages the users, via monetary incentives (CL), to adopt a new consumption that minimizes the peak loads and the costs for the GENCO. No existing study has all of these features.The proposed framework can also be used for regulation review, for instance

in Brazil, where the current DR program is not economically attractive for consumers [194].

6.2.2 Limitation

The present work does not consider personalized user tariffs for two reasons. First, current rules (e.g., in Brazil and Quebec) do not allow different tariffs for different customers in the same neighborhood. Second, such tariffs increase the complexity of the optimization model. If the tariff is a variable, then the model becomes nonlinear since the costs are products of the tariffs and the energy consumption, which is also a variable. This work considers fixed tariffs and linear models.

6.3 Framework

This section presents the two-phase framework. In the first phase, each user finds its best consumption schedule and sends that information to the aggregator. In the second phase, the aggregator finds a solution that better coordinates the customers from the GENCO perspective.

6.3.1 Model for users

The set $\mathcal{N}$ represents the users. Their appliances and features [47, Table 1] are represented by the models from [47]. Each model schedules the energy consumption for one day in T time intervals indexed with t, with length Δ_t, and the appliances are grouped as follows:

- A: Set of electrical appliances;
- $A_I \subseteq A$: Set of appliances with uninterruptible operation;
- A_I^*: Set of tasks for appliances in A_I.
- $A_P \subseteq A$: Set of appliances with interruptible phases;
- A_P^*: Set of tasks for appliances in A_P;
- $A^* = \{A_P^* \cup A_I^*\}$: Set of tasks for appliances in A.

Let $\mathcal{X}$ be the space of all variables and $\boldsymbol{\Xi} \in \mathcal{X}$ a solution. The functions f_c, f_t, f_u, and f_d represent, respectively, the total cost, the thermal discomfort, the usage-time discomfort, and the total discomfort:

- $f_u(\boldsymbol{\Xi}) = r_1 \left[\sum_{k \in A_p^*} \sum_{p=1}^{P_k} \Psi_{k,p} + \sum_{k \in A_I^*} \zeta_k \right] + r_2 \sum_{t \in T} \sum_{k \in A^*} U_k^t,$
- $f_t(\boldsymbol{\Xi}) = \sum_{t \in T} \sum_{a \in A} V_a^t,$
- $f_c(\boldsymbol{\Xi}) = \sum_{t \in T} \left(C_b^t - C_s^t + C_{CHP}^t \right) + C_{ev},$
- $f_d(\boldsymbol{\Xi}) = \alpha_t f_t(\boldsymbol{\Xi}) + \alpha_u f_u(\boldsymbol{\Xi})$

where variables: C_b^t [$] and C_s^t [$] represent the cost at $t \in T$ of buying and selling energy, respectively, C_{CHP}^t [$] is the combined heating power (CHP) operation cost at $t \in T$, C_{ev} [$] is the fuel cost for a hybrid vehicle, V_a^t [^{o}C] is the discomfort related to the deviation from the target temperature of appliance a at $t \in T$, U_k^t [hour] is the discomfort related to the deviation from the target time for task k at $t \in T$, ζ_k [hour] is the discomfort related to the omission of task $k \in A_I^*$ and $\Psi_{k,p}$ [hour] is the discomfort related to the omission of phase p of task $k \in A_P^*$. For parameters, let define P_k as the number of phases of task $k \in A_P^*$, $r_1 \in \mathcal{R}$ as the discomfort factor per task not performed and $r_2 \in \mathcal{R}$ as the discomfort factor per usage-time deviation.

Let Θ_n be the set of appliances, machines and smart home components [46] not available for the user $n \in \mathcal{N}$, and $\boldsymbol{\Xi}_n \in \mathcal{X}$ be the vector of variables for the user $n \in \mathcal{N}$, which contains real and binary variables. The vector $\boldsymbol{\Xi}_n$ can be used as an input for the functions defined above considering that every variable related to the appliance $a \in \Theta_n$ is set to zero. Each user also imposes its own constraints, which specify the feasible region $\mathcal{F}_n \subseteq \mathcal{X}$. Thus, each user $n \in \mathcal{N}$ have the following MILP:

$$\min_{\boldsymbol{\Xi}_n} \quad f_c(\boldsymbol{\Xi}_n) \tag{6.1}$$

$$\text{s.t.} \quad f_d(\boldsymbol{\Xi}_n) \leq D_n \tag{6.2}$$

$$\boldsymbol{\Xi}_n \in \mathcal{F}_n. \tag{6.3}$$

The objective function (6.1) is the cost of user $n \in \mathcal{N}$. Constraint (6.2) limits the maximum discomfort D_n; this parameter can be set using multi-criteria decision analysis and multiobjective optimization (see [46]). Finally, (6.3) are the constraints that represent the flow conservation, the operation of the appliances, the pricing policies, and the energy limits. See [47] for details.

6.3.2 Framework: first phase

Overbars ($\overline{x}$) are used to indicate quantities calculated in the first phase. In this phase, there is no coordination of the users or the DR, and the tariffs are known one day ahead. Each user $n \in \mathcal{N}$ solves Model (6.1)–(6.3) to find a scheduling plan with optimal cost $\overline{C_n}$. That cost and the desired load are returned to the aggregator.

6.3.3 Framework: second phase

Let define parameters: π, ν, and λ as respectively the production cost per Wh, the buying cost per Wh, and the selling price per Wh from the GENCO perspective, β [$] the cost for the hydro-power unit start-up and ω [W] a factor to convert β/ω into ramp-up/down cost per watt. Let define variables: E_n^t [Wh] be the energy obtained from the grid at $t \in T$ by user $n \in \mathcal{N}$, $C_p^t \geq 0$ [$] the energy production cost at $t \in T$ ($C_p^t = \pi\Delta_t \sum_{n\in\mathcal{N}} E_n^t$) and $\kappa_n \geq 0$ [$] the incentive paid to client n to change its consumption. E_n^t is a element of $\boldsymbol{\Xi}_n$.

The GENCO goal is to maximize its profit. The revenue is considered to be the total amount of bills paid by customers, expressed as $\sum_{n\in\mathcal{N}} \overline{C_n}$. The cost has four components. The first is the cost incurred by the variability of the total energy produced for a given horizon, which may be related to the ramp-up and ramp-down costs. The second is that of the energy production. The third is the CL incentive given to customers. The fourth is related to clients' injection of energy into the grid; this is included in the revenue.

The following of this section presents, progressively, the steps to obtain the entire optimization model. First the focus is the objective function only, then constraints, and finally the entire optimization model. The total energy variance for the whole horizon is as follows:

$$\min_{E_n^t} \ \frac{1}{(|T|-1)} \sum_{t\in T} \left(\sum_{n\in\mathcal{N}} E_n^t - \frac{\sum_{t_2\in T}\sum_{n\in\mathcal{N}} E_n^{t_2}}{|T|} \right)^2 \tag{6.4}$$

The objective function (6.4) and Constraints (6.2)–(6.3) form a mixed-integer nonlinear problem, and even small instances are hard to solve. Since E_n^t is one element of $\boldsymbol{\Xi}_n$, a trivial solution is not possible. This work instead uses β/ω as an approximation for the ramp-up/down cost, use e_1^t and e_2^t as gap and surplus variables, and remove the constant (|T|-1) since it does not change the optimal solution. This allows us to reformulate (6.4) as a cost minimization of the total energy variance generated, which is locally an approximation of (6.4):

$$\min_{E_n^t, e_1^t, e_2^t} \ \frac{\beta}{\omega}\left(\sum_{t\in T}\frac{e_1^t+e_2^t}{\Delta_t}\right) \tag{6.5}$$

$$s.t. \left(\sum_{n\in\mathcal{N}} E_n^t - \frac{\sum_{t_2\in T}\sum_{n\in\mathcal{N}} E_n^{t_2}}{|T|}\right) + e_1^t - e_2^t = 0 \ \ \forall\ t\in T \tag{6.6}$$

$$e_1^t, e_2^t \geq 0 \ \ \forall\ t\in T \tag{6.7}$$

If one aggregates the other costs, the GENCO objective function becomes:

$$\min_{\substack{E_n^t, e_1^t, e_2^t,\\ C_p^t, \kappa_n}} \ \frac{\beta}{\omega}\left(\sum_{t\in T}\frac{e_1^t+e_2^t}{\Delta_t}\right) + \sum_{t\in T} C_p^t + \sum_{n\in\mathcal{N}}\kappa_n \tag{6.8}$$

In the first phase, the aggregator can estimate the GENCO energy production cost as $\overline{C_p} = \overline{\sum_{t\in T} C_p^t}$ and the cost of variability as $\overline{R_c} = \overline{\beta/\omega \sum_{t=1}^{|T|}[(e_1^t+e_2^t)/\Delta_t]}$ if there is no DR.

The aggregator cannot increase the incentives. Let the "saved costs" be the amount that the GENCO saves using DR, which must be lower than the incentives spent. This can be modeled as follows:

$$\overline{R_c} - \frac{\beta}{\omega}\sum_{t=1}^{T}\left(\frac{e_1^t+e_2^t}{\Delta_t}\right) + \overline{C_p} - \sum_{t\in T} C_p^t \geq \sum_{n\in\mathcal{N}}\kappa_n \tag{6.9}$$

The aggregator goal is represented by the following optimistic bilevel problem with an upper level representing the GENCO and $|\mathcal{N}|$ lower levels representing the consumers:

$$\min_{\substack{E_n^t, e_1^t, e_2^t,\\ C_p^t, \kappa_n}} \ \frac{\beta}{\Delta_t\omega}\left(\sum_{t\in T}\frac{e_1^t+e_2^t}{\Delta_t}\right) + \sum_{t\in T} C_p^t + \sum_{n\in\mathcal{N}}\kappa_n \tag{6.10}$$

s.t. (6.6), (6.7), (6.9)

$$C_p^t = \pi\Delta_t \sum_{n\in\mathcal{N}} E_n^t \ \forall\ t\in T \tag{6.11}$$

$$\forall\ n\in\mathcal{N} \qquad \min_{\boldsymbol{\Xi}_n} f_c(\boldsymbol{\Xi}_n) \tag{6.12}$$

$$\text{s.t. } (6.2), (6.3)$$

It is worth to mention that the link between the objectives functions (6.10) and (6.12) is

made through variable E_n^t, since it is an element of $\boldsymbol{\Xi}_n$. In a bilevel optimization problem, the leader sets incentives/prices according to its goal, and the consumers respond based on their targets. The term "optimistic" means that if the lower-level problem has multiple optimal solutions, the solution chosen is the one most favorable to the upper-level problem. If the aggregator guarantees a discount or no cost increase, the customers can change their consumption to favor the GENCO. Thus, if the cost with DR for client $n \in \mathcal{N}$ is above $\overline{C_n}$, the GENCO must pay the extra cost with incentives. Therefore, constraints are added to protect users against cost increases:

$$\kappa_n \geq \sum_{t \in T} \left(C_b^t - C_s^t + C_{CHP}^t \right) + C_{ev} - \overline{C_n} \ \forall \ n \in \mathcal{N}. \tag{6.13}$$

The GENCO revenue is fixed in phase one. Thus, additional user costs are in fact costs for the GENCO, and C_b^t is replaced by C_p^t in (6.13). Moreover, this work assumes that the GENCO is not interested in paying for energy injected into the grid since $\pi < \nu < \lambda$. Hence, $C_s^t = 0$ for all $t \in T$ and the objective functions (6.12) are replaced by Constraints (6.14):

$$\kappa_n \geq \sum_{t \in T} \left(C_p^t + C_{CHP}^t \right) + C_{ev} - \overline{C_n} \ \forall \ n \in \mathcal{N}. \tag{6.14}$$

The final aggregator problem is then represented by the following single-level model:

$$\text{(P)} \quad \min_{\substack{E_n^t, e_1^t, e_2^t, \\ C_p^t, \kappa_n, \boldsymbol{\Xi}_n}} \ \frac{\beta}{\omega} \left(\sum_{t \in T} \frac{e_1^t + e_2^t}{\Delta_t} \right) + \sum_{t \in T} C_p^t + \sum_{n \in \mathcal{N}} \kappa_n \tag{6.15}$$

$$\text{s.t.} \quad (6.6), (6.7), (6.9), (6.11), (6.14), (6.2), (6.3).$$

6.3.4 Algorithms

Problem (P) could be solved using commercial solvers, but a centralized approach has little scalability and privacy issues due to the need of data from every consumer [193]. A decentralized approach improves scalability but not necessarily privacy since the model may be solved in a single machine. Ideally, (P) should be solved in a distributed way, with each user solving the problems associated with its consumption in its own home management system. This mitigates privacy concerns and improves scalability.

Let K (a divisor of $|\mathcal{N}|$) be the cluster size, S the heuristic solution, and UB an upper bound for the optimal value of (P). This work proposes a decentralized heuristic (DH): see Algorithm 1. If $K = 1$, DH can be used in a distributed mode.

Algorithm 1 Heuristic DH

Input: $|\mathcal{N}|, K$

Output: UB, S

1: $UB \leftarrow 0$
2: Partition the users into $|\mathcal{N}|/K$ clusters
3: For each cluster c, create an instance I^c of (P)
4: Solve each I^c to optimality, obtaining the solution $\boldsymbol{x}^c$
5: Concatenate $\boldsymbol{x}^c$ for every cluster c into the vector S
6: Calculate UB using S in objective function (6.15)

6.4 Results and Discussion

This section presents the results for the centralized approach (CA) and DH. Data are considered from Belo Horizonte, Brazil. Let set $\beta = \$140.50$ based on the average cost for a hydro-power unit start-up [91, Example 1], $\omega = 50\,\text{MW}$, and $\pi = 0.01\,\$/\text{KWh}$. The other parameters are set as in [47]. The solver is Cplex 12.8.

Table 6.1 summarizes the results and reports CPU times for both CA and DH. The first column gives the number of users. The "gap" columns give the difference between the solution found and the optimal solution: gap $= (UB - Z^*)/UB$, where UB is the value found by DH and Z^* is the optimal value found by CA. If no time is given, CA could not solve the instance within 24 hours.

CA can solve only small instances, which confirms the scalability issues. For $50 \leq |\mathcal{N}| \leq 500$, DH is faster than CA: the speed-up factors are between 2.87 and 14.74 for $K = 1$ and between 1.40 and 6.6 for $K = 10$. In terms of deviation from the optimal value, for $|\mathcal{N}| = 500$ the UB-LB is \$10. If a distributed approach is employed, i.e., $K = 1$, the CPU time improves since it is divided, approximately, by $|\mathcal{N}|$: see Table 6.2. Moreover, DH gives small optimality gaps.

The proposed approach efficiently flattens the load profile: see Figures 6.1 and 6.2. Without coordination, near time 96, there is a large peak due to highest tariff between time step 112 and 125 in the current time-of-use program. Hence, from the users' perspective, it is cheaper to use batteries and thermal storage. This behavior is undesirable from the GENCO perspective.

The peak-to-average ratio (PAR), which is given by

$$\text{PAR} = |T| \left(\max_t \left\{ \sum_{n \in \mathcal{N}} E_n^t \right\} \right) \left(\sum_{t \in T} \sum_{n \in \mathcal{N}} E_n^t \right)^{-1},$$

decreased from 2.06 without coordination to 1.17 in the DH solution for $|\mathcal{N}| = 10^4$ (an

Table 6.1 Results

$\|\mathcal{N}\|$	CPU Time [s]			Gap [%]	
	CA	DH (K=1)	DH (K=10)	DH (K=1)	DH (K=10)
10	10.18	10.08	12.5	0.037	0
50	238.7	83	170.1	0.039	0.003
100	1000	146	410	0.042	0.005
300	8244	559	1245	0.046	0.006
500	12522	940	2084	0.045	0.006
1000	-	1882	4217	-	-
5000	-	24880	22696	-	-
8000	-	40221	39952	-	-
10000	-	50329	43966	-	-

Table 6.2 Estimated CPU time per user for $K = 1$ in a distributed implementation

$\|\mathcal{N}\|$	10	50	100	300	500
Time [s]	1.008	1.66	1.46	1.86	1.88
$\|\mathcal{N}\|$	1000	5000	8000	10000	
Time [s]	1.88	4.98	5.03	5.03	

improvement of 43.2%).

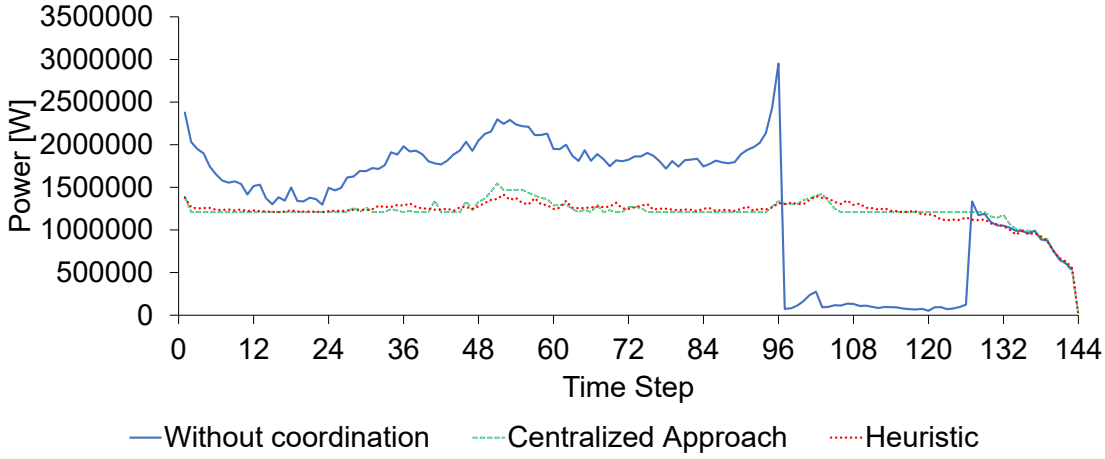

Figure 6.1 System load profile for $|\mathcal{N}| = 500$.

The power in Figures 6.1 and 6.2 is zero at time step $t = 144$. This behavior is explained since there is no consumption after $t = 144$. A constraint could be used to set the energy required at $t = 144$ to be same as the electricity required at $t = 0$, which could even improve the results, but that constraint does not exist in the reality in some cases. A second possibility is to consider the *"steady state of the process"*, but not the *"transient state"*, which in the

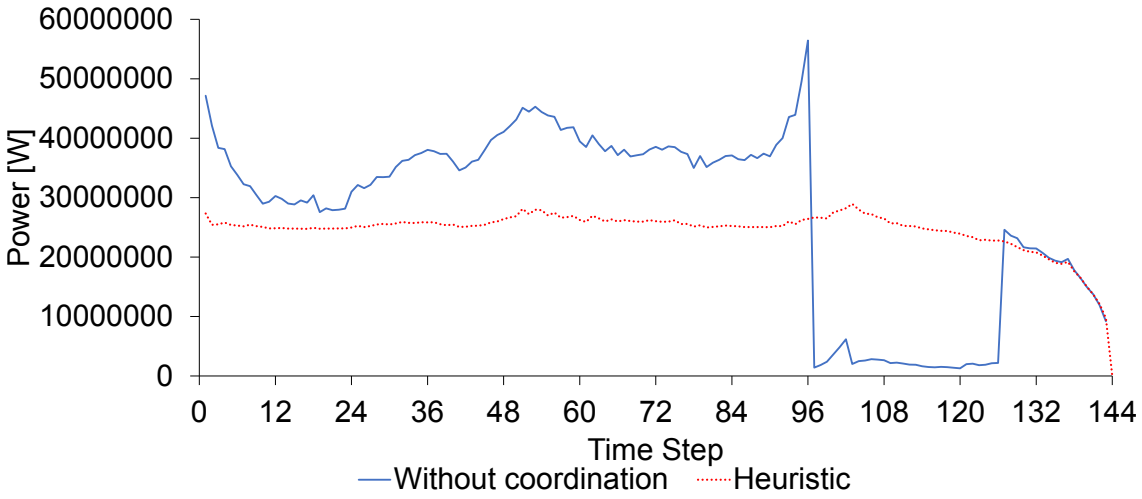

Figure 6.2 System load profile for $|\mathcal{N}| = 10^4$.

case of Figures 6.1 and 6.2 means to analyze the results considering only the range of time steps between, for instance, 24 and 120.

6.5 Conclusions

Price-incentive DR programs can create new rebound peaks. This increases demand variability and is undesirable from the GENCO perspective. This works has proposed a framework that minimizes costs for both users and the GENCO, by shaving aggregated peak loads and maintaining the desired comfort level. The framework results in a formulation that can be solved in a centralized or decentralized way. Centralized methods have scalability issues, so a heuristic was presented with a small optimality gap; it decreases the CPU time by a factor of up to 6.6 compared to the centralized approach. In addition, the DH can be used in a distributed mode if privacy is required.

Acknowledgments

This work is supported by a full scholarship from CNPq-Brazil.

CHAPTER 7 GENERAL DISCUSSION

The general objective of this thesis is to provide modeling and optimization tools for energy management in smart homes. The subject being treated is part of the current effort of smart grids researches. In particular, the thesis focused on the use of energy by two entities of different scales: a single user (home), and an aggregator, which is an entity that aggregates several users (several homes).

Considering a single householder, it is clear that there are several works that have modeled and optimized the equipment used in homes, and for each SHC, several authors presented models of equipment with different degrees of complexity. In this context, this thesis has two contributions.

The first one is given by joining several devices at the same time in the home energy management system scheduling model and including more details and realistic constraints that impact the optimization user cost. Moreover, this work focuses on the development of a mathematical model for smart home components that are representative. The ultimate goal of this thesis is trade-off the complexity and realism of SHCs models so that it could fit the home energy management system in the smart home, from a practical perspective.

he results point that it is relevant to consider how a realistic modeling of the devices will affect the optimized cost and that it is quite important to consider and maintain a desired level of comfort for users, which is assured by the model proposed through utility functions for discomfort level.

In practical terms, the output of the first contribution is an optimization model (M) for an individual customer. The model M integrates reliable appliances models from different domains of the literature while maintaining a resolution complexity small enough such that the model can be solved in a personal computer in a feasible time for practical purposes.

The second contribution related to a single householder has focused on a decision support system tool to support the end user in the process of transition towards a smart home. The question related to the return on investment by the acquisition of smart home components is discussed. The primary objective is to determine which combinations of SHC to consider and when to buy them. Such models, can significantly help users to make a gradual transition to a smart home.

Using model M as a base, in practical terms, the output of the second contribution is a framework (F), customizable for each client, for an investment analysis. Each householder

can use the framework to help in its decision-making process regarding the transition or not to a smart home concept. If yes, F offers an approximation of when and through which technologies the investments of users will be profitable.

Considering multiple householders, this thesis makes use of the aggregator concept to reduce peak load and achieve load leveling. That approach is very interesting for the supplier provider and the user. Customers who opt for smart homes are strong candidates for demand response programs. Using M and parts of F as the basis for a multi-user approach, the third contribution of this research is the development of a method for coordinating the electricity consumption of a community of users together with a generator company for social welfare maximization.

CHAPTER 8 CONCLUSION AND RECOMMENDATIONS

8.1 Concluding remarks

This thesis proposes a mixed integer linear optimization model that minimizes the cost while maintaining a high level of user comfort in the scheduling of smart appliance usage in smart homes. We achieve a compromise: the model is realistic, but can be solved in reasonable time. For the instances considered, the solution found by the model proposed in this thesis saves from 544USD to 2205USD more than other models proposed in the literature.

The aforementioned model was used in the construction of a framework to guide the transition to smart homes given customized electricity usage from an economic perspective. The framework is able to propose the set of appliances, machines and other technologies that have the best return on investment for a given householder.

Using strategies from that framework for individual smart homes, another framework was developed to be used in the context of price-incentive demand response programs. It can avoid new rebound peaks when users minimize their costs, which increases demand variability in a way that is considered to be a concern from the generator company perspective. The framework coordinates multiple houses by shaving aggregated peak loads and keeping the desired comfort level for users, beyond of minimizing cost for users and for the generator company.

8.2 Limitations

In general terms, there are some important limitations throughout this thesis.

The first limitation of this thesis is that it was not tested in real homes. Testing the developed methods in real homes is necessary to validate research from a practical perspective.

The second limitation is the consideration of deterministic data rather than a uncertain data. This means that the behavior of the user, the weather, appliance efficiencies, etc. are treated as certain, which is an assumption that will not happen in reality.

For the individual scheduler model presented in Chapter 4 and used in Chapter 5, a limitation is the lack of an automatic tool to collect data for the user. For instance, a user may not properly understand how to measure the home insulation or the home solar gain, which can impose extra costs by an extern service. In addition, if a modification to the home structure is made such as a new window, the measure process must be repeated. How to construct an

energy model for the home, without human intervention is out of the scope of this research.

The model of wind turbines, HVACs and WHs used are among the easiest models that calculates the power needed, the temperature of the room, and the output water temperature, respectively. The impact of outside temperature on EV was not considered. Thus, more realistic models are required.

Another limitation throughout this thesis is the usage of day-ahead pricing policies (a deterministic data). Consequently, the methods cannot be used in areas that has real time pricing policies. For real time prices, a rolling horizon approach using model predictive control could be used. However, this requires that the user model to be solved is 2 or 3 seconds. So, a decrease in complexity is needed to increase the user model performance. In addition, the formulation proposed for multiple users in Chapter 6 assumes real application of a coordinated planning for several users without considering the possibility of accepting a demand response request one day ahead by the user that is not carried out by him the following day.

Although a representative model is conceived for users, in Chapter 6 only hydro-power units with simple representation is considered. This simplify the entire optimization problem, but improves scalability.

Beyond these limitations, there are also challenges that can hinder the advancement of demand response programs. Various barriers to the development of DR were recently identified and classified by [142]. First, regulatory factors are one type of barrier. For instance, some regions does not have legislation to allow the full potential of DR, such as in Brazil, while in other regions, there are organizations that impose rules that limit it such as the Western Electricity Coordinating Council in the U.S. Second, in some places the market entrance criteria should also be reviewed to increase the participation rate of stakeholders. Third, different entities could use DR for their own benefit, then managing the interactions among these entities, i.e, coordinating their conflicting interests for DR is a challenge. Fourth, important amount of investment is needed for the infrastructures. Finally, the acceptance of end-users is also uncertain.

8.3 Future Work

The thesis was conceived using a deterministic case. However, the majority of real problems have uncertain data. Due to the natural dynamism of reality, sources of uncertainty such as a variation in solar production due to a cloud that passes over the panels must be considered. This can change the solution found in a deterministic context. So, a solution whose disturbance does not produce a sudden change in the objective function performance is desired.

Given these uncertainties, a future work is dedicated to develop a stochastic approach for the methods developed in this thesis.

The thesis used representative models users, but it was not given the same importance for the GENCO model in the bilevel formulation. More realistic models can be used for GENCO in a future work.

Another direction for future work could be to verify if the individual kWcap for appliances is better than the framework proposed in Chapter 5 to determine the best combination of appliances from an economic perspective.

Users could not follow the solution obtained by the GENCO from a bilevel optimization problem. Machine Learning could be used to interact with the lower level optimization problem bringing into the formulation some information about the user acceptance “levels”.

BIBLIOGRAPHY

[1] Aagreh, Y., and Al-Ghzawi, A. Feasibility of utilizing renewable energy systems for a small hotel in Ajloun city, Jordan. Applied Energy 103 (2013), 25–31.

[2] Abdelhamid, M., Pilla, S., Singh, R., Haque, I., and Filipi, Z. A comprehensive optimized model for on-board solar photovoltaic system for plug-in electric vehicles: energy and economic impacts. International Journal of Energy Research 40, 11 (2016), 1489–1508.

[3] Adika, C. O., and Wang, L. Autonomous appliance scheduling for household energy management. IEEE Transactions on Smart Grid 5, 2 (2014), 673–682.

[4] Adika, C. O., and Wang, L. Smart charging and appliance scheduling approaches to demand side management. International Journal of Electrical Power & Energy Systems 57 (2014), 232–240.

[5] Agnetis, A., de Pascale, G., Detti, P., and Vicino, A. Load scheduling for household energy consumption optimization. IEEE Transactions on Smart Grid 4, 4 (2013), 2364–2373.

[6] Akinyele, D. O., and Rayudu, R. K. Review of energy storage technologies for sustainable power networks. Sustainable Energy Technologies and Assessments 8 (2014), 74–91.

[7] Akter, M. N., Mahmud, M. A., and Oo, A. M. T. Comprehensive economic evaluations of a residential building with solar photovoltaic and battery energy storage systems: An australian case study. Energy and Buildings 138 (2017), 332–346.

[8] Al-Alawi, B. M., and Bradley, T. H. Total cost of ownership, payback, and consumer preference modeling of plug-in hybrid electric vehicles. Applied Energy 103 (2013), 488–506.

[9] American Society of Heating, R., and Air-Conditioning Engineers, I. 2013 ASHRAE Handbook - Fundamentals (SI Edition). ASHRAE, 2013.

[10] American Society of Heating, R., and Air-Conditioning Engineers, I. 2015 ASHRAE HANDBOOK Heating, Ventilating, and Air-Conditioning APPLICATIONS (SI Edition). ASHRAE, 2015.

[11] Ancillotti, E., Bruno, R., and Conti, M. The role of communication systems in smart grids: Architectures, technical solutions and research challenges. Computer Communications 36, 17-18 (2013), 1665–1697.

[12] ANEEL. Matriz de energia elétrica. accessed Dec. 2017.

[13] Anvari-Moghaddam, A., Monsef, H., and Rahimi-Kian, A. Cost-effective and comfort-aware residential energy management under different pricing schemes and weather conditions. Energy and Buildings 86 (2015), 782–793.

[14] Anvari-Moghaddam, A., Monsef, H., and Rahimi-Kian, A. Optimal smart home energy management considering energy saving and a comfortable lifestyle. IEEE Transactions on Smart Grid 6, 1 (2015), 324–332.

[15] Arabali, A., Ghofrani, M., Etezadi-Amoli, M., Fadali, M. S., and Baghzouz, Y. Genetic-algorithm-based optimization approach for energy management. IEEE Transactions on Power Delivery 28, 1 (2013), 162–170.

[16] Asaee, S. R., Ugursal, V. I., and Beausoleil-Morrison, I. Techno-economic evaluation of internal combustion engine based cogeneration system retrofits in Canadian houses – a preliminary study. Applied Energy 140 (2015), 171–183.

[17] Audet, C., Hansen, P., Jaumard, B., and Savard, G. Links between linear bilevel and mixed 0–1 programming problems. Journal of Optimization Theory and Applications 93, 2 (1997), 273–300.

[18] Baharlouei, Z., and Hashemi, M. Efficiency-fairness trade-off in privacy-preserving autonomous demand side management. IEEE Transactions on Smart Grid 5, 2 (2014), 799–808.

[19] Barbieri, E. S., Melino, F., and Morini, M. Influence of the thermal energy storage on the profitability of micro-CHP systems for residential building applications. Applied Energy 97 (2012), 714–722.

[20] Barbieri, E. S., Spina, P. R., and Venturini, M. Analysis of innovative micro-CHP systems to meet household energy demands. Applied Energy 97 (2012), 723–733.

[21] Barker, S., Kalra, S., Irwin, D., and Shenoy, P. Empirical characterization and modeling of electrical loads in smart homes. 2013 International Green Computing Conference (IGCC) (2013), 1–10.

[22] Beaudin, M., and Zareipour, H. Home energy management systems: A review of modelling and complexity. Renewable and Sustainable Energy Reviews 45 (2015), 318–335.

[23] Bergey. Bergey Excel 10kW. accessed Apr. 2018.

[24] Borges, B. N. Modelagem semi-empírica de um refrigerador frost-free sujeito a abertura de portas. 2013. Thesis, Universidade Federal de Santa Catarina, Florianópolis, 2013.

[25] Borges, B. N., Hermes, C. J. L., Gonçalves, J. M., and Melo, C. Transient simulation of household refrigerators: A semi-empirical quasi-steady approach. Applied Energy 88, 3 (2011), 748–754.

[26] Brazil. Lei nº 12.212, de 20 de janeiro de 2010, 2010. accessed Dec. 2017.

[27] British Gas. British Gas. accessed Apr. 2018.

[28] Buddy, G. Montréal Fuel Prices. accessed Apr. 2018.

[29] Camarinha-Matos, L. M. Collaborative smart grids – A survey on trends. Renewable and Sustainable Energy Reviews 65 (2016), 283–294.

[30] Castillo-Cagigal, M., Caamaño-Martín, E., Matallanas, E., Masa-Bote, D., Gutiérrez, A., Monasterio-Huelin, F., and Jiménez-Leube, J. PV self-consumption optimization with storage and active DSM for the residential sector. Solar Energy 85, 9 (2011), 2338–2348.

[31] Celik, B., Roche, R., Suryanarayanan, S., Bouquain, D., and Miraoui, A. Electric energy management in residential areas through coordination of multiple smart homes. Renewable and Sustainable Energy Reviews 80 (2017), 260–275.

[32] Cemig. Cities of the future project. accessed Dec. 2017.

[33] Chavali, P., Yang, P., and Nehorai, A. A distributed algorithm of appliance scheduling for home energy management system. IEEE Transactions on Smart Grid 5, 1 (2014), 282–290.

[34] Chen, C., Wang, J., Heo, Y., and Kishore, S. MPC-based appliance scheduling for residential building energy management controller. IEEE Transactions on Smart Grid 4, 3 (2013), 1401–1410.

[35] Chen, X., Wei, T., and Hu, S. Uncertainty-aware household appliance scheduling considering dynamic electricity pricing in smart home. IEEE Transactions on Smart Grid 4, 2 (2013), 932–941.

[36] Chen, Z., Wu, L., and Fu, Y. Real-time price-based demand response management for residential appliances via stochastic optimization and robust optimization. IEEE Transactions on Smart Grid 3, 4 (2012), 1822–1831.

[37] Cherrington, R., Goodship, V., Longfield, A., and Kirwan, K. The feed-in tariff in the UK: A case study focus on domestic photovoltaic systems. Renewable Energy 50 (2013), 421–426.

[38] Christofides, N., Alvarez-Valdes, R., and Tamarit, J. M. Project scheduling with resource constraints: A branch and bound approach. European Journal of Operational Research 29, 3 (1987), 262–273.

[39] Clemente-Císcar, M., San Matías, S., and Giner-Bosch, V. A methodology based on profitability criteria for defining the partial defection of customers in non-contractual settings. European Journal of Operational Research 239, 1 (2014), 276–285.

[40] Conroy, G., Duffy, A., and Ayompe, L. M. Economic, energy and GHG emissions performance evaluation of a Whispergen Mk IV Stirling engine μ-CHP unit in a domestic dwelling. Energy Conversion and Management 81 (2014), 465–474.

[41] da Costa Gomes, G. C. Avaliação do comportamento de refrigeradores domésticos frente a defeitos provocados e emulados. Thesis, Universidade Federal de Santa Catarina, 2015.

[42] da Silva, A. J., Nascimento, C. R. C., da Silva, L. F., and Lucas, T. d. P. B. Análise topoclimática em unidade de conservação urbana a partir da temperatura e umidade relativa do ar. e-Scientia 4, 1 (2011), 21–30.

[43] De Lara, M., Carpentier, P., Chancelier, J.-P., and Leclere, V. Optimization methods for the smart grid. Report commissioned by the Conseil Français de l'Energie, Ecole des Ponts ParisTech (2014).

[44] De Soto, W., Klein, S. A., and Beckman, W. A. Improvement and validation of a model for photovoltaic array performance. Solar Energy 80, 1 (2006), 78–88.

[45] de Souza Dutra, M., Anjos, M., and Le Digabel, S. A Framework for Peak Shaving Through the Coordination of Smart Homes. Tech. Rep. G-2019-16

http://www.optimization-online.org/DB_HTML/2019/02/7090.html, Les cahiers du GERAD, 2019.

[46] De Souza Dutra, M. D., Anjos, M. F., and Le Digabel, S. A general framework for customized transition to smart homes. Tech. Rep. G-2019-09 http://www.optimization-online.org/DB_HTML/2019/01/7049.html, Les cahiers du GERAD, 2019.

[47] de Souza Dutra, M. D., Anjos, M. F., and Le Digabel, S. A realistic energy optimization model for smart-home appliances. International Journal of Energy Research (2019), 1–26.

[48] Deb, K., Pratap, A., Agarwal, S., and Meyarivan, T. A fast and elitist multiobjective genetic algorithm: NSGA-II. IEEE Transactions on Evolutionary Computation 6, 2 (2002), 182–197.

[49] Dempe, S. Foundations of Bilevel Programming. Nonconvex Optimization and Its Applications. Springer US, 2002.

[50] Deng, R., Yang, Z., Chen, J., Asr, N. R., and Chow, M.-Y. Residential energy consumption scheduling: A coupled-constraint game approach. IEEE Transactions on Smart Grid 5, 3 (2014), 1340–1350.

[51] Deng, R., Yang, Z., Chen, J., and Chow, M.-Y. Load scheduling with price uncertainty and temporally-coupled constraints in smart grids. IEEE Transactions on Power Systems 29, 6 (2014), 2823–2834.

[52] Deng, R., Yang, Z., Chow, M.-Y., and Chen, J. A survey on demand response in smart grids: Mathematical models and approaches. IEEE Transactions on Industrial Informatics 11, 3 (2015), 570–582.

[53] DeOreo, W. B., Mayer, P. W., Dziegielewski, B., and Kiefer, J. Residential end uses of water, version 2. Water Research Foundation, 2016.

[54] Di Santo, K. G., Kanashiro, E., Di Santo, S. G., and Saidel, M. A. A review on smart grids and experiences in brazil. Renewable and Sustainable Energy Reviews 52 (2015), 1072–1082.

[55] Du, P., and Lu, N. Appliance commitment for household load scheduling. IEEE Transactions on Smart Grid 2, 2 (2011), 411–419.

[56] Duffie, J. A., and Beckman, W. A. Solar Engineering of Thermal Processes, vol. 4. Wiley New York, 2013.

[57] Dufo-López, R., Bernal-Agustín, J. L., and Domínguez-Navarro, J. A. Generation management using batteries in wind farms: Economical and technical analysis for Spain. Energy Policy 37, 1 (2009), 126–139.

[58] e-tradecounter. Megaflo Eco Unvented Hot Water Cylinders. accessed Apr. 2018.

[59] El-hawary, M. E. The smart grid—state-of-the-art and future trends. Electric Power Components and Systems 42, 3–4 (2014), 239–250.

[60] Element Energy Limited. Cost and performance of EV batteries: Final report for The Committee on Climate Change. Report, Element Energy Limited, 2012.

[61] Energia, Ministério de Minas e. Relatório Smart Grid. Techical report, Ministério de Minas e Energia, 2010.

[62] Energética, Empresa de Pesquisa. Plano Nacional de Energia 2030. EPE, Rio de Janeiro, 2007.

[63] Erdinc, O., Paterakis, N. G., Mendes, T. D. P., Bakirtzis, A. G., and P. S. Catalao, J. Smart household operation considering bi-directional EV and ESS utilization by real-time pricing-based DR. IEEE Transactions on Smart Grid 6, 3 (2015), 1281–1291.

[64] Erol-Kantarci, M., and Mouftah, H. T. Wireless sensor networks for cost-efficient residential energy management in the smart grid. IEEE Transactions on Smart Grid 2, 2 (2011), 314–325.

[65] Fadaeenejad, M., Saberian, A. M., Fadaee, M., Radzi, M. A. M., Hizam, H., and AbKadir, M. Z. A. The present and future of smart power grid in developing countries. Renewable and Sustainable Energy Reviews 29 (2014), 828–834.

[66] Fadlullah, Z. M., Duong Minh, Q., Kato, N., and Stojmenovic, I. GTES: An optimized game-theoretic demand-side management scheme for smart grid. IEEE Systems Journal 8, 2 (2014), 588–597.

[67] Fan, S., Ai, Q., and Piao, L. Bargaining-based cooperative energy trading for distribution company and demand response. Applied Energy 226 (2018), 469–482.

[68] Fazelpour, F., Vafaeipour, M., Rahbari, O., and Rosen, M. A. Intelligent optimization to integrate a plug-in hybrid electric vehicle smart parking lot with renewable energy resources and enhance grid characteristics. Energy Conversion and Management 77 (2014), 250–261.

[69] Fotouhi Ghazvini, M. A., Soares, J., Abrishambaf, O., Castro, R., and Vale, Z. Demand response implementation in smart households. Energy and Buildings 143 (2017), 129–148.

[70] Fotouhi Ghazvini, M. A., Soares, J., Horta, N., Neves, R., Castro, R., and Vale, Z. A multi-objective model for scheduling of short-term incentive-based demand response programs offered by electricity retailers. Applied Energy 151 (2015), 102–118.

[71] Fu, R., Feldman, D., Margolis, R., Woodhouse, M., and Ardani, K. U.S. Solar Photovoltaic System Cost Benchmark: Q1 2017. Tech. rep., National Renewable Energy Laboratory, 2018.

[72] Gao, J., Xiao, Y., Liu, J., Liang, W., and Chen, C. L. P. A survey of communication/networking in smart grids. Future Generation Computer Systems 28, 2 (2012), 391–404.

[73] Gatsis, N., and Giannakis, G. B. Decomposition algorithms for market clearing with large-scale demand response. IEEE Transactions on Smart Grid 4, 4 (2013), 1976–1987.

[74] Gkatzikis, L., Koutsopoulos, I., and Salonidis, T. The role of aggregators in smart grid demand response markets. IEEE Journal on Selected Areas in Communications 31, 7 (2013), 1247–1257.

[75] GoGreenSolar. Water heating cost. accessed Apr. 2018.

[76] Golshannavaz, S. Cooperation of electric vehicle and energy storage in reactive power compensation: An optimal home energy management system considering PV presence. Sustainable Cities and Society 39 (2018), 317–325.

[77] Gottwalt, S., Ketter, W., Block, C., Collins, J., and Weinhardt, C. Demand side management—A simulation of household behavior under variable prices. Energy Policy 39, 12 (2011), 8163–8174.

[78] Gov.UK. plug-in-car-van-grants. accessed May 2018.

[79] GreenMatch. Central Heating Capacity UK. accessed Apr. 2018.

[80] Hawkes, A. D., Brett, D. J. L., and Brandon, N. P. Fuel cell micro-CHP techno-economics: Part 1 – Model concept and formulation. International Journal of Hydrogen Energy 34, 23 (2009), 9545–9557.

[81] Hawkes, A. D., Brett, D. J. L., and Brandon, N. P. Fuel cell micro-CHP techno-economics: Part 2 – Model application to consider the economic and environmental impact of stack degradation. International Journal of Hydrogen Energy 34, 23 (2009), 9558–9569.

[82] Hawkins, S. L. High resolution reanalysis of wind speeds over the British Isles for wind energy integration. PHD thesis, The University of Edinburgh, 2012.

[83] Hikari. Gerador Diesel 6kW. accessed Apr. 2018.

[84] Hong, Y.-Y., Lin, J.-K., Wu, C.-P., and Chuang, C.-C. Multi-objective air-conditioning control considering fuzzy parameters using immune clonal selection programming. IEEE Transactions on Smart Grid 3, 4 (2012), 1603–1610.

[85] Hu, M., Xiao, J.-W., Cui, S.-C., and Wang, Y.-W. Distributed real-time demand response for energy management scheduling in smart grid. International Journal of Electrical Power & Energy Systems 99 (2018), 233–245.

[86] Hu, Q., Li, F., Fang, X., and Bai, L. A framework of residential demand aggregation with financial incentives. IEEE Transactions on Smart Grid 9, 1 (2018), 497–505.

[87] Hubert, T., and Grijalva, S. Modeling for residential electricity optimization in dynamic pricing environments. IEEE Transactions on Smart Grid 3, 4 (2012), 2224–2231.

[88] Hydro-Québec. Performance des chauffe-eau solaires installés au Québec - Rapport final. Report, Laboratoire des technologies de l'énergie d'Hydro-Québec, 2012. Projet pilote sur les chauffe-eau solaires domestiques du Bureau de l'efficacité et de l'innovation énergétiques.

[89] Hydro-Québec. Hydro-Québec's electricity rates for its electricity distribution activities effective April 1,2018, 2018.

[90] Hydro-Quebec. Residential electricity rate increases for the past 25 years. accessed Apr. 2018.

[91] IEEE, Ed. Hydropower unit start-up costs (Chicago, 2002), IEEE Power Engineering Society Summer Meeting.

[92] Institut de l'statistique du Québec. L'inflation. accessed Apr. 2018.

[93] International Energy Agency. Global EV Outlook 2016: Beyond one million electric cars. Report, International Energy Agency, 2016.

[94] J. Mamouri, S., and Bénard, A. New design approach and implementation of solar water heaters: A case study in Michigan. Solar Energy 162 (2018), 165–177.

[95] Javaid, N., Naseem, M., Rasheed, M. B., Mahmood, D., Khan, S. A., Alrajeh, N., and Iqbal, Z. A new heuristically optimized home energy management controller for smart grid. Sustainable Cities and Society 34 (2017), 211–227.

[96] Javaid, N., Ullah, I., Akbar, M., Iqbal, Z., Khan, F. A., Alrajeh, N., and Alabed, M. S. An intelligent load management system with renewable energy integration for smart homes. IEEE Access 5 (2017), 13587–13600.

[97] Javorski Eckert, J., Corrêa de Alkmin e Silva, L., Mazzariol Santiciolli, F., dos Santos Costa, E., Corrêa, F. C., and Giuseppe Dedini, F. Energy storage and control optimization for an electric vehicle. International Journal of Energy Research 42, 11 (2018), 3506–3523.

[98] Johan Fagerberg, A. F. Smart homes and home automation. Tech. rep., Berg Insight, 2015.

[99] Joo, I.-Y., and Choi, D.-H. Distributed optimization framework for energy management of multiple smart homes with distributed energy resources. IEEE Access 5 (2017), 15551–15560.

[100] Kelly, J., and Knottenbelt, W. The UK-DALE dataset, domestic appliance-level electricity demand and whole-house demand from five UK homes. Scientific Data 2 (2015), 150007.

[101] Khalid, A., Javaid, N., Guizani, M., Alhussein, M., Aurangzeb, K., and Ilahi, M. Towards dynamic coordination among home appliances using multi-objective energy optimization for demand side management in smart buildings. IEEE Access 5 (2018), 19509–19529.

[102] Khan, M. A., Javaid, N., Mahmood, A., Khan, Z. A., and Alrajeh, N. A generic demand-side management model for smart grid. International Journal of Energy Research 39, 7 (2015), 954–964.

[103] Kim, T. T., and Poor, H. V. Scheduling power consumption with price uncertainty. IEEE Transactions on Smart Grid 2, 3 (2011), 519–527.

[104] Kriett, P. O., and Salani, M. Optimal control of a residential microgrid. Energy 42, 1 (2012), 321–330.

[105] Landini, C. L., and de Mello Sant'Ana, P. H. Technical, economic, and regulatory analysis of the implementation of micro-cogeneration technology in the Brazilian manufacturing sector. Energy Efficiency 10, 4 (2016), 957–971.

[106] Latifi, M., Khalili, A., Rastegarnia, A., and Sanei, S. Fully distributed demand response using the adaptive diffusion–Stackelberg algorithm. IEEE Transactions on Industrial Informatics 13, 5 (2017), 2291–2301.

[107] Laumanns, M., Thiele, L., and Zitzler, E. An efficient, adaptive parameter variation scheme for metaheuristics based on the epsilon-constraint method. European Journal of Operational Research 169, 3 (2006), 932–942.

[108] Law, Y. W., Alpcan, T., Lee, V. C. S., Lo, A., Marusic, S., and Palaniswami, M. Demand response architectures and load management algorithms for energy-efficient power grids: A survey. 2012 Seventh International Conference on Knowledge, Information and Creativity Support Systems (2012), 134–141.

[109] Lübkert, T., Venzke, M., Vo, N.-V., and Turau, V. Understanding price functions to control domestic electric water heaters for demand response. Computer Science - Research and Development 33, 1–2 (2017), 81–92.

[110] Lee, J.-W., and Lee, D.-H. Residential electricity load scheduling for multi-class appliances with time-of-use pricing. IEEE International Workshop on Smart Grid Communications and Networks (2011), 1194–1198.

[111] Leite, A. P., Falcão, D. M., and Borges, C. L. Modelagem de usinas eólicas para estudos de confiabilidade. Sba: Controle & Automação Sociedade Brasileira de Automatica 17 (2006), 177–188.

[112] Li, N., Chen, L. J., and Low, S. H. Optimal demand response based on utility maximization in power networks. 2011 IEEE Power and Energy Society General Meeting (2011), 1–8.

[113] Li, Y., Ng, B. L., Trayer, M., and Liu, L. Automated residential demand response: Algorithmic implications of pricing models. IEEE Transactions on Smart Grid 3, 4 (2012), 1712–1721.

[114] Liu, R.-S., and Hsu, Y.-F. A scalable and robust approach to demand side management for smart grids with uncertain renewable power generation and bi-directional energy trading. International Journal of Electrical Power & Energy Systems 97 (2018), 396–407.

[115] Liu, Y., Hu, S., Huang, H., Ranjan, R., Zomaya, A. Y., and Wang, L. Game-theoretic market-driven smart home scheduling considering energy balancing. IEEE Systems Journal 11, 2 (2017), 910–921.

[116] Liu, Y., Yuen, C., Huang, S., Ul Hassan, N., Wang, X., and Xie, S. Peak-to-average ratio constrained demand-side management with consumer's preference in residential smart grid. IEEE Journal of Selected Topics in Signal Processing 8, 6 (2014), 1084–1097.

[117] Lu, H., Zhang, M., Fei, Z., and Mao, K. Multi-Objective Energy Consumption Scheduling in Smart Grid Based on Tchebycheff Decomposition. IEEE Transactions on Smart Grid 6, 6 (2015), 2869–2883.

[118] Lévesque, B., Lavoie, M., and Joly, J. Residential water heater temperature: 49 or 60 degrees celsius? The Canadian Journal of Infectious Diseases 15, 1 (2004), 11–12.

[119] McNamara, P., and McLoone, S. Hierarchical Demand Response for Peak Minimization Using Dantzig-Wolfe Decomposition. IEEE Transactions on Smart Grid 6, 6 (2015), 2807–2815.

[120] Melhem, F. Y., Grunder, O., Hammoudan, Z., and Moubayed, N. Optimization and energy management in smart home considering photovoltaic, wind, and battery storage system with integration of electric vehicles. Canadian Journal of Electrical and Computer Engineering-Revue Canadienne De Genie Electrique Et Informatique 40, 2 (2017), 128–138.

[121] Menezes, H. L. d. S. Avaliação da aplicação da modalidade tarifária horária branca: Estudo de caso para consumidores residenciais. Report, Universidade de Brasília, 2015.

[122] Merkel, E., McKenna, R., and Fichtner, W. Optimisation of the capacity and the dispatch of decentralised micro-CHP systems: A case study for the UK. Applied Energy 140 (2015), 120–134.

[123] Mhanna, S., Chapman, A. C., and Verbic, G. A fast distributed algorithm for large-scale demand response aggregation. IEEE Transactions on Smart Grid 7, 4 (2016), 2094–2107.

[124] Ministério da Fazenda. Tesouro Nacional. accessed May 2018.

[125] Ministério da Ciência, Tecnologia e Inovação. Redes Elétricas Inteligentes - Diálogo Setorial Brasil-União Europeia. Techical report, MCTI, 2014.

[126] Ministério de Minas e Energia. Projeção da demanda de energia elétrica para os próximos 5 anos (2016-2020), vol. NOTA TÉCNICA DEA 19/15. EPE, 2015.

[127] Mohseni, A., Mortazavi, S. S., Ghasemi, A., Nahavandi, A., and Talaei abdi, M. The application of household appliances' flexibility by set of sequential uninterruptible energy phases model in the day-ahead planning of a residential microgrid. Energy 139 (2017), 315–328.

[128] Mohsenian-Rad, A.-H., and Leon-Garcia, A. Optimal residential load control with price prediction in real-time electricity pricing environments. IEEE Transactions on Smart Grid 1, 2 (2010), 120–133.

[129] Monyei, C. G., Adewumi, A. O., Akinyele, D., Babatunde, O. M., Obolo, M. O., and Onunwor, J. C. A biased load manager home energy management system for low-cost residential building low-income occupants. Energy 150 (2018), 822–838.

[130] Moon, S., and Lee, J.-W. Multi-residential demand response scheduling with multi-class appliances in smart grid. IEEE Transactions on Smart Grid 9 (2018), 2518–2528.

[131] Najafi-Ghalelou, A., Nojavan, S., and Zare, K. Heating and power hub models for robust performance of smart building using information gap decision theory. International Journal of Electrical Power & Energy Systems 98 (2018), 23–35.

[132] Nguyen, D. T., and Le, L. B. Joint optimization of electric vehicle and home energy scheduling considering user comfort preference. IEEE Transactions on Smart Grid 5, 1 (2014), 188–199.

[133] Nguyen, D. T., Nguyen, H. T., and Le, L. B. Dynamic pricing design for demand response integration in power distribution networks. IEEE Transactions on Power Systems 31, 5 (2016), 3457–3472.

[134] Nguyen, H. T., Nguyen, D. T., and Le, L. B. Energy management for households with solar assisted thermal load considering renewable energy and price uncertainty. IEEE Transactions on Smart Grid 6, 1 (2015), 301–314.

[135] Nguyen, X. H., and Nguyen, M. P. Mathematical modeling of photovoltaic cell/module/arrays with tags in Matlab/Simulink. Environmental Systems Research 4, 1 (2015).

[136] Ni, Z., and Das, A. A new incentive-based optimization scheme for residential community with financial trade-offs. IEEE Access 6 (2018), 57802–57813.

[137] Nissan. Nissan Leaf 2018. accessed Apr. 2018.

[138] NISSAN. Nissan Leaf presentation. accessed Dec. 2017.

[139] Nissan. Nissan Leaf Visia. accessed Apr. 2018.

[140] nrcan.ca. Solar photovoltaic energy, Apr. 2019. accessed May 2019 - https://www.nrcan.gc.ca/energy/renewables/solar-photovoltaic/7303.

[141] Ofgem. Feed-In Tariff (FIT) rates. accessed Apr. 2018.

[142] Paterakis, N. G., Erdinç, O., and Catalão, J. P. S. An overview of demand response: Key-elements and international experience. Renewable and Sustainable Energy Reviews 69 (2017), 871–891.

[143] Paterakis, N. G., Erdinc, O., Bakirtzis, A. G., and Catalao, J. P. S. Optimal household appliances scheduling under day-ahead pricing and load-shaping demand response strategies. IEEE Transactions on Industrial Informatics 11, 6 (2015), 1509–1519.

[144] Pedrasa, M. A. A., Spooner, T. D., and MacGill, I. F. Coordinated scheduling of residential distributed energy resources to optimize smart home energy services. IEEE Transactions on Smart Grid 1, 2 (2010), 134–143.

[145] Pedrasa, M. A. A., Spooner, T. D., and MacGill, I. F. A novel energy service model and optimal scheduling algorithm for residential distributed energy resources. Electric Power Systems Research 81, 12 (2011), 2155–2163.

[146] Peinado, J., and Graeml, A. R. Administração da produção. Operações industriais e de serviços. Unicenp, 2007.

[147] Petrolprices. UK Fuel Prices. accessed Apr. 2018.

[148] Pillai, G. G., Putrus, G. A., Georgitsioti, T., and Pearsall, N. M. Near-term economic benefits from grid-connected residential PV (photovoltaic) systems. Energy 68 (2014), 832–843.

[149] Pipattanasomporn, M., Kuzlu, M., Rahman, S., and Teklu, Y. Load profiles of selected major household appliances and their demand response opportunities. IEEE Transactions on Smart Grid 5, 2 (2014), 742–750.

[150] presse, L. Le gaz naturel. accessed May 2018.

[151] Qian, L. P., Zhang, Y. J. A., Huang, J., and Wu, Y. Demand response management via real-time electricity price control in smart grids. IEEE Journal on Selected Areas in Communications 31, 7 (2013), 1268–1280.

[152] Rahbari-Asr, N., Ojha, U., Zhang, Z., and Chow, M.-Y. Incremental welfare consensus algorithm for cooperative distributed generation/demand response in smart grid. IEEE Transactions on Smart Grid 5, 6 (2014), 2836–2845.

[153] Raisul Islam, M., Sumathy, K., and Ullah Khan, S. Solar water heating systems and their market trends. Renewable and Sustainable Energy Reviews 17 (2013), 1–25.

[154] Rastegar, M., Fotuhi-Firuzabad, M., and Aminifar, F. Load commitment in a smart home. Applied Energy 96 (2012), 45–54.

[155] Renewable Energy Hub. BlueGen - MicroCHP Fuel Cell System. accessed Apr. 2018.

[156] Renewable Energy Hub. How much does a solar thermal system cost? accessed Apr. 2018.

[157] Renewable Energy Hub. How much is a Wind Turbine likely to make me and over what period? accessed Apr. 2018.

[158] Renewable Energy Hub. Solar panels cost. accessed Apr. 2018.

[159] Ressupply.com. Heliodyne-gobi. accessed Apr. 2018.

[160] Rheem. Rheem. accessed Apr. 2018.

[161] Richardson, I., Thomson, M., Infield, D., and Clifford, C. Domestic electricity use: A high-resolution energy demand model. Energy and Buildings 42, 10 (2010), 1878–1887.

[162] Rodrigues, E. M. G., Godina, R., Pouresmaeil, E., Ferreira, J. R., and Catalão, J. P. S. Domestic appliances energy optimization with model predictive control. Energy Conversion and Management 142 (2017), 402–413.

[163] Roh, H.-T., and Lee, J.-W. Residential demand response scheduling with multiclass appliances in the smart grid. IEEE Transactions on Smart Grid 7, 1 (2016), 94–104.

[164] Saad al sumaiti, A., Ahmed, M. H., and Salama, M. M. A. Smart home activities: A literature review. Electric Power Components and Systems 42, 3–4 (2014), 294–305.

[165] Safdarian, A., Fotuhi-Firuzabad, M., and Lehtonen, M. Optimal residential load management in smart grids: A decentralized framework. IEEE Transactions on Smart Grid 7, 4 (2016), 1836–1845.

[166] Salinas, S., Li, M., and Li, P. Multi-objective optimal energy consumption scheduling in smart grids. IEEE Transactions on Smart Grid 4, 1 (2013), 341–348.

[167] Self, S. J., Reddy, B. V., and Rosen, M. A. Geothermal heat pump systems: Status review and comparison with other heating options. Applied Energy 101 (2013), 341–348.

[168] Shafie-Khah, M., and Siano, P. A stochastic home energy management system considering satisfaction cost and response fatigue. IEEE Transactions on Industrial Informatics 14, 2 (2018), 629–638.

[169] Shahidehopour, M., and Yong, F. Benders decomposition: Applying Benders decomposition to power systems. IEEE Power and Energy Magazine 3, 2 (2005), 20–21.

[170] Shakeri, M., Shayestegan, M., Abunima, H., Reza, S. M. S., Akhtaruzzaman, M., Alamoud, A. R. M., Sopian, K., and Amin, N. An intelligent system architecture in home energy management systems (HEMS) for efficient demand response in smart grid. Energy and Buildings 138 (2017), 154–164.

[171] Shakouri G, H., and Kazemi, A. Multi-objective cost-load optimization for demand side management of a residential area in smart grids. Sustainable Cities and Society 32 (2017), 171–180.

[172] Shao, S., Pipattanasomporn, M., and Rahman, S. Development of physical-based demand response-enabled residential load models. IEEE Transactions on Power Systems 28, 2 (2013), 607–614.

[173] Shirazi, E., and Jadid, S. Cost reduction and peak shaving through domestic load shifting and DERs. Energy 124 (2017), 146–159.

[174] Shirazi, E., Zakariazadeh, A., and Jadid, S. Optimal joint scheduling of electrical and thermal appliances in a smart home environment. Energy Conversion and Management 106 (2015), 181–193.

[175] Siano, P. Demand response and smart grids—A survey. Renewable and Sustainable Energy Reviews 30 (2014), 461–478.

[176] Silvente, J., and Papageorgiou, L. G. An MILP formulation for the optimal management of microgrids with task interruptions. Applied Energy 206 (2017), 1131–1146.

[177] Six, D., Vekemans, G., and Dexters, A. Market opportunities for micro-CHP in Flanders (Belgium). 2009 6th International Conference on the European Energy Market (2009), 1–6.

[178] SoltaniNejad Farsangi, A., Hadayeghparast, S., Mehdinejad, M., and Shayanfar, H. A novel stochastic energy management of a microgrid with various types of distributed energy resources in presence of demand response programs. Energy 160 (2018), 257–274.

[179] Sousa, T., Morais, H., Vale, Z., Faria, P., and Soares, J. Intelligent energy resource management considering vehicle-to-grid: A simulated annealing approach. IEEE Transactions on Smart Grid 3, 1 (2012), 535–542.

[180] Stankovic, L., Stankovic, V., Liao, J., and Wilson, C. Measuring the energy intensity of domestic activities from smart meter data. Applied Energy 183 (2016), 1565–1580.

[181] Stull, R. Practical Meteorology: An Algebra Based Survey of Atmospheric Science. BC Campus, 2016.

[182] Sunderland, K. M., Narayana, M., Putrus, G., Conlon, M. F., and McDonald, S. The cost of energy associated with micro wind generation: International case studies of rural and urban installations. Energy 109 (2016), 818–829.

[183] Tan, Z., Yang, P., and Nehorai, A. An optimal and distributed demand response strategy with electric vehicles in the smart grid. IEEE Transactions on Smart Grid 5, 2 (2014), 861–869.

[184] TemperSol. Coupled tempersol. accessed Apr. 2018.

[185] Tesla. Powerwall. accessed Apr. 2018.

[186] Thomas, D., Deblecker, O., and Ioakimidis, C. S. Optimal operation of an energy management system for a grid-connected smart building considering photovoltaics' uncertainty and stochastic electric vehicles' driving schedule. Applied Energy 210 (2018), 1188–1206.

[187] Transition énergétique Québec. Drive Electric Program. accessed May 2018.

[188] Transitionenergetique. Solar Hot Water Heater in Québec. accessed Apr. 2018.

[189] Tsagarakis, G., Collin, A., and Kiprakis, A. A statistical survey of the UK residential sector electrical loads. International Journal of Emerging Electric Power Systems 14, 5 (2013).

[190] UKPower.co.uk. Everything you need to know about Economy 7. accessed Apr. 2018.

[191] UOL. EV cost estimation. accessed Apr. 2018.

[192] van der Stelt, S., AlSkaif, T., and van Sark, W. Techno-economic analysis of household and community energy storage for residential prosumers with smart appliances. Applied Energy 209 (2018), 266–276.

[193] Vardakas, J. S., Zorba, N., and Verikoukis, C. V. A survey on demand response programs in smart grids: Pricing methods and optimization algorithms. IEEE Communications Surveys & Tutorials 17, 1 (2015), 152–178.

[194] Viana, M. S., Manassero, G., and Udaeta, M. E. M. Analysis of demand response and photovoltaic distributed generation as resources for power utility planning. Applied Energy 217 (2018), 456–466.

[195] Villanueva, D., and Feijóo, A. Wind power distributions: A review of their applications. Renewable and Sustainable Energy Reviews 14, 5 (2010), 1490–1495.

[196] Wang, C., Zhou, Y., Jiao, B., Wang, Y., Liu, W., and Wang, D. Robust optimization for load scheduling of a smart home with photovoltaic system. Energy Conversion and Management 102 (2015), 247–257.

[197] Wang, L., Gwilliam, J., and Jones, P. Case study of zero energy house design in UK. Energy and Buildings 41, 11 (2009), 1215–1222.

[198] Wang, Z., and Paranjape, R. Optimal residential demand response for multiple heterogeneous homes with real-time price prediction in a multiagent framework. IEEE Transactions on Smart Grid 8 (2017), 1173–1184.

[199] WeatherOnline. London ground temperature. accessed Apr. 2018.

[200] Weatherspark.com. Average weather. accessed May 2018.

[201] Wei, W., Liu, F., and Mei, S. Energy pricing and dispatch for smart grid retailers under demand response and market price uncertainty. IEEE Transactions on Smart Grid 6, 3 (2015), 1364–1374.

[202] Xie, Y., Gilmour, M. S., Yuan, Y., Jin, H., and Wu, H. A review on house design with energy saving system in the UK. Renewable and Sustainable Energy Reviews 71 (2017), 29–52.

[203] Xu, Z., Guan, X., Jia, Q.-S., Wu, J., Wang, D., and Chen, S. Performance analysis and comparison on energy storage devices for smart building energy management. IEEE Transactions on Smart Grid 3, 4 (2012), 2136–2147.

[204] Yang, X., Zhang, Y., Zhao, B., Huang, F., Chen, Y., and Ren, S. Optimal energy flow control strategy for a residential energy local network combined with demand-side management and real-time pricing. Energy and Buildings 150 (2017), 177–188.

[205] Yang, Z., Long, K., You, P., and Chow, M.-Y. Joint scheduling of large-scale appliances and batteries via distributed mixed optimization. IEEE Transactions on Power Systems 30, 4 (2015), 2031–2040.

[206] Yang, Z., Wu, R., Yang, J., Long, K., and You, P. Economical operation of microgrid with various devices via distributed optimization. IEEE Transactions on Smart Grid (2015), 1–11.

[207] Yao-Jung, W., and Agogino, A. M. Wireless networked lighting systems for optimizing energy savings and user satisfaction. Proceedings of Wireless Hive Networks Conference (2008), 1–7.

[208] Yu, M., and Hong, S. H. A real-time demand-response algorithm for smart grids: A Stackelberg game approach. IEEE Transactions on Smart Grid 7, 2 (2016), 879–888.

[209] Yu, M., and Hong, S. H. Supply–demand balancing for power management in smart grid: A Stackelberg game approach. Applied Energy 164 (2016), 702–710.

[210] Yu, M., and Hong, S. H. Incentive-based demand response considering hierarchical electricity market: A Stackelberg game approach. Applied Energy 203 (2017), 267–279.

[211] Yu, Z., Jia, L., Murphy-Hoye, M. C., Pratt, A., and Tong, L. Modeling and Stochastic Control for Home Energy Management. IEEE Transactions on Smart Grid 4, 4 (2013), 2244–2255.

[212] Yunus, A. C. Heat Transfer: A Practical Approach. McGraw-Hill, New York, 2003.

[213] Zhang, C., Wang, Q., Wang, J., Pinson, P., Morales, J. M., and Ostergaard, J. Real-time procurement strategies of a proactive distribution company with aggregator-based demand response. IEEE Transactions on Smart Grid 9, 2 (2018), 766–776.

[214] Zhang, D., Evangelisti, S., Lettieri, P., and Papageorgiou, L. G. Economic and environmental scheduling of smart homes with microgrid: DER operation and electrical tasks. Energy Conversion and Management 110 (2016), 113–124.

[215] Zhang, H., Chen, H., Liu, H., Huang, J., Guo, X., and Li, M. Design and performance study of a low concentration photovoltaic-thermal module. International Journal of Energy Research 42, 6 (2018), 2199–2212.

[216] Zhou, B., Li, W., Chan, K. W., Cao, Y., Kuang, Y., Liu, X., and Wang, X. Smart home energy management systems: Concept, configurations, and scheduling strategies. Renewable and Sustainable Energy Reviews 61 (2016), 30–40.

[217] Zhou, S., Wu, Z., Li, J., and Zhang, X.-p. Real-time energy control approach for smart home energy management system. Electric Power Components and Systems 42, 3–4 (2014), 315–326.

[218] Zhuang, Z., Won Cheol, L., Yoan, S., and Kyung-Bin, S. An optimal power scheduling method for demand response in home energy management system. IEEE Transactions on Smart Grid 4, 3 (2013), 1391–1400.

[219] Zugno, M., Morales, J. M., Pinson, P., and Madsen, H. A bilevel model for electricity retailers' participation in a demand response market environment. Energy Economics 36 (2013), 182–197.